

O.K. Andersen,
Max-Planck Institute for Solid-State Research, Stuttgart:

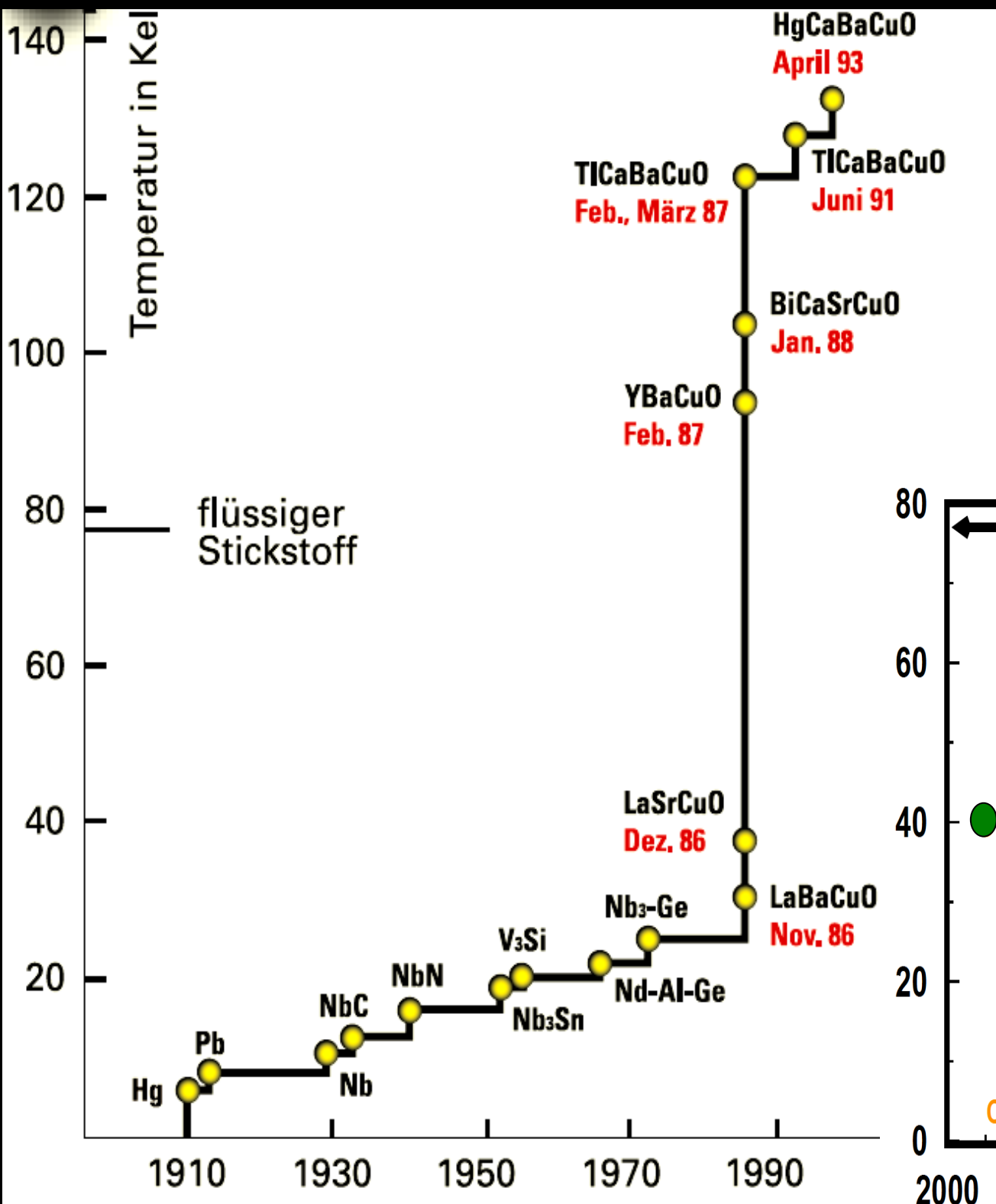
Band structures of known families of HTSC cuprates;

Ove Jepsen, S. Lichtenstein, I. Mazin, I. Dasgupta, E. Pavarini,
T. Saha-Dasgupta.

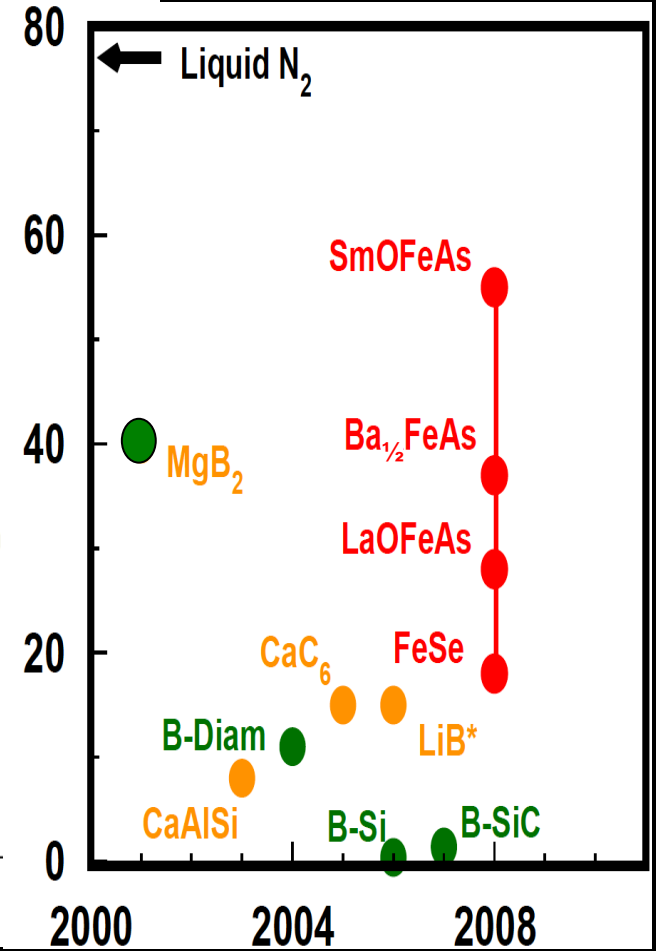
can we engineer them to
get further?

Xiaoping Yang, P. Hansmann, A. Toschi, G. Khaliullin, K. Held

The crackpot contribution at the end of an otherwise serious school



The quest for high-temperature superconductivity



In order to get better superconductors,
do we need to understand the
mechanism?

and if we do,
does it help?

What can be learned about high T_c from the LDA?

- 1988 Physica C **153-155**; Zaanen, Jepsen, Gunnarsson, Paxton, Andersen, Svane.
- 1988 - Presumably nothing, because strong electronic correlations in HTSCs.**
- 1988 - 91 LDA+U calculations for undoped compounds. Parameters of the 3-band Hubbard model supporting the Emery and t-J models.
- 1988 - 92 Fermi surfaces for many cuprates. Agreement with positron annihilation and early ARPES.
YBa₂Cu₃O₇:
Interband transitions. Agreement with optical spectra for $\omega > 2\text{eV}$.
Phonon frequencies and linewidths at high symmetry \mathbf{q} 's. Consistent with Raman data.
Raman intensities for the various polarizations. Consistent with exp.
- 1994 - 95 Extract low-energy TB models explaining the "chemistry". Predict t'/t , bi-layer splitting $t_{\text{perp}}(\mathbf{k}_x, \mathbf{k}_y) \propto (\cos k_x - \cos k_y)^2$ and interplane exch-coupling $J_{\text{perp}} \propto \int t_{\text{perp}}(\mathbf{k}) t_{\text{perp}}(\mathbf{k} + \mathbf{Q}) d\mathbf{k} / U$
- 1995 - 96 Phonon frequencies and linewidths for all \mathbf{q} 's in s - and d -wave channels. Analytical $g(\mathbf{k}, \mathbf{k}')$
- 2000- Who cares! ARPES sees the FS and the dressed band structure!**
- We do, because ARPES from overdoped systems do confirm the LDA FS predictions.
- 2001 t'/t for 15-20 families of HTSC; correlation with $T_{c, \text{max}}$
- 2003- Numerically exact Wannier functions, 1- and 3-band Hubbard Hamiltonians. DMFT, DCA and other many-body calculations.
- 2009- **After 23 years, the mechanism of HTSC remains an unsolved problem**

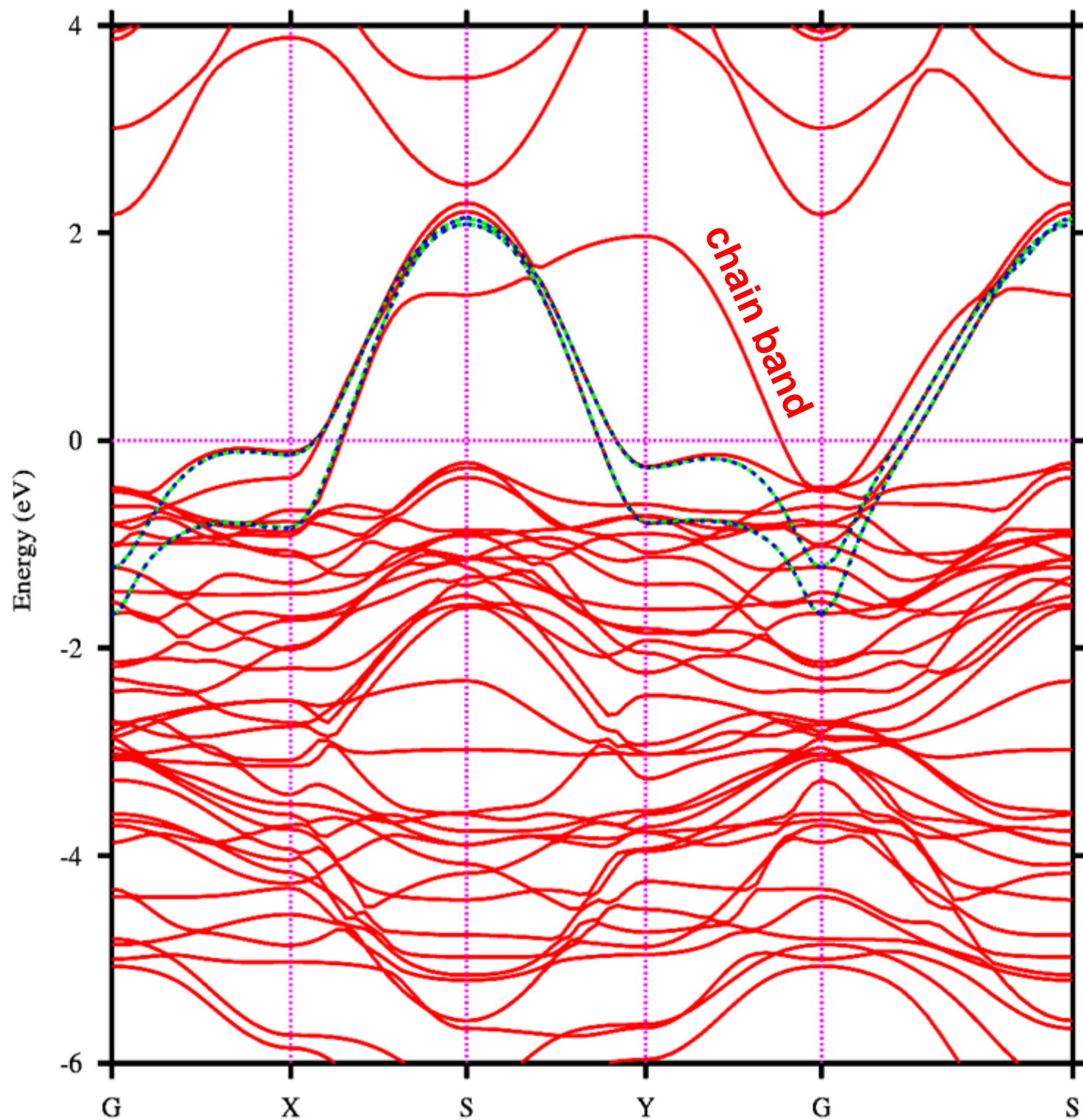




Stoichiometric at optimal doping

LDA

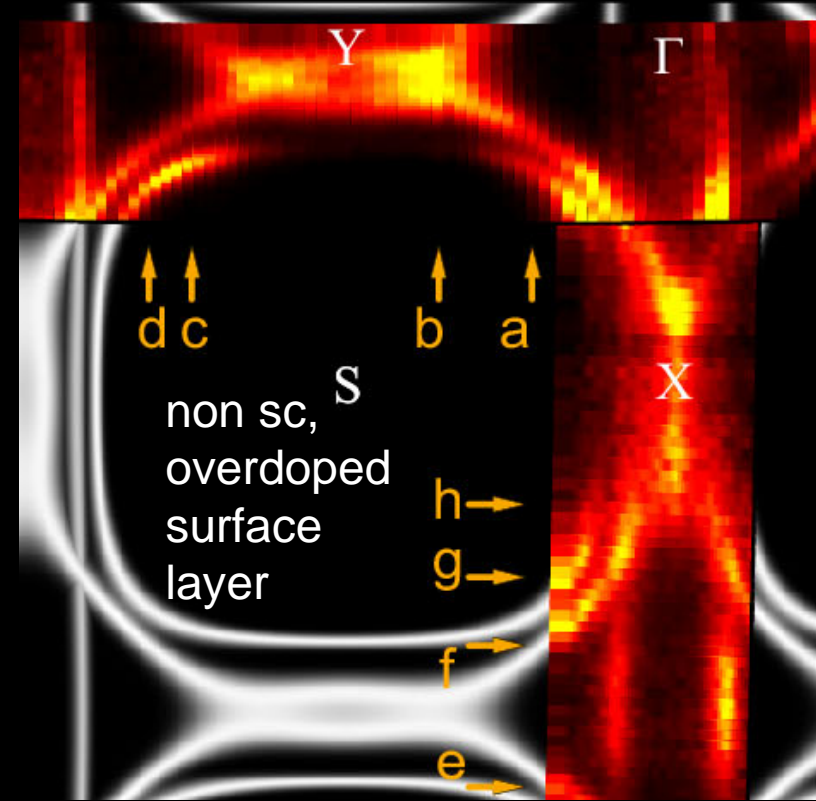
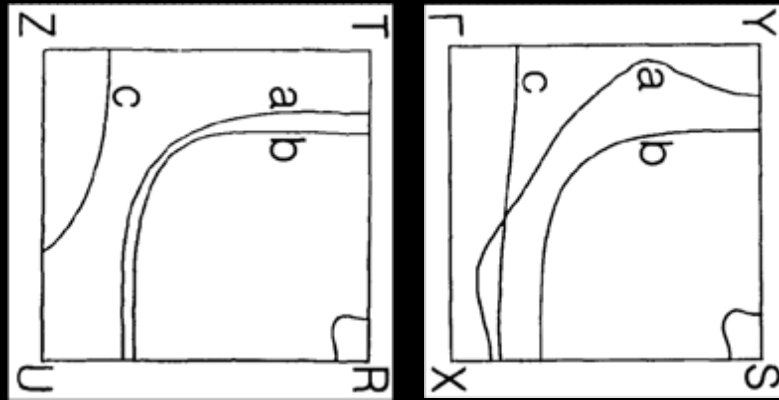
Bi-layer splitting:



LDA

$\text{YBa}_2\text{Cu}_3\text{O}_7$

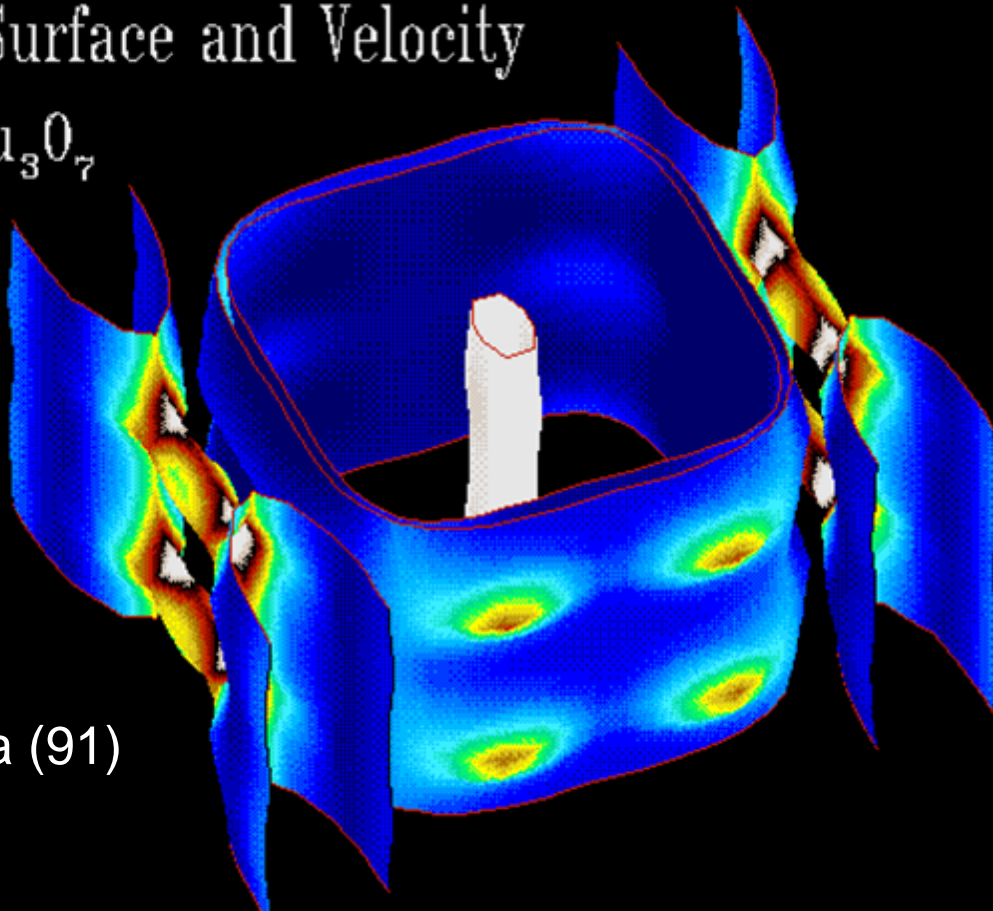
ARPES



Andersen,
Liechtenstein,...
JPhysChemSolids
(95)

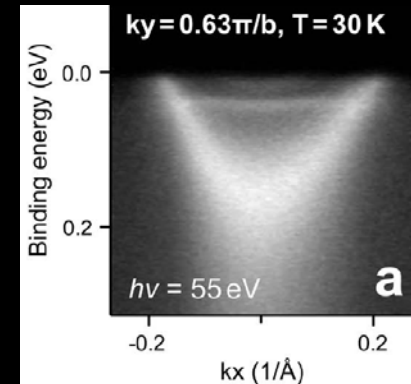
Fermi Surface and Velocity

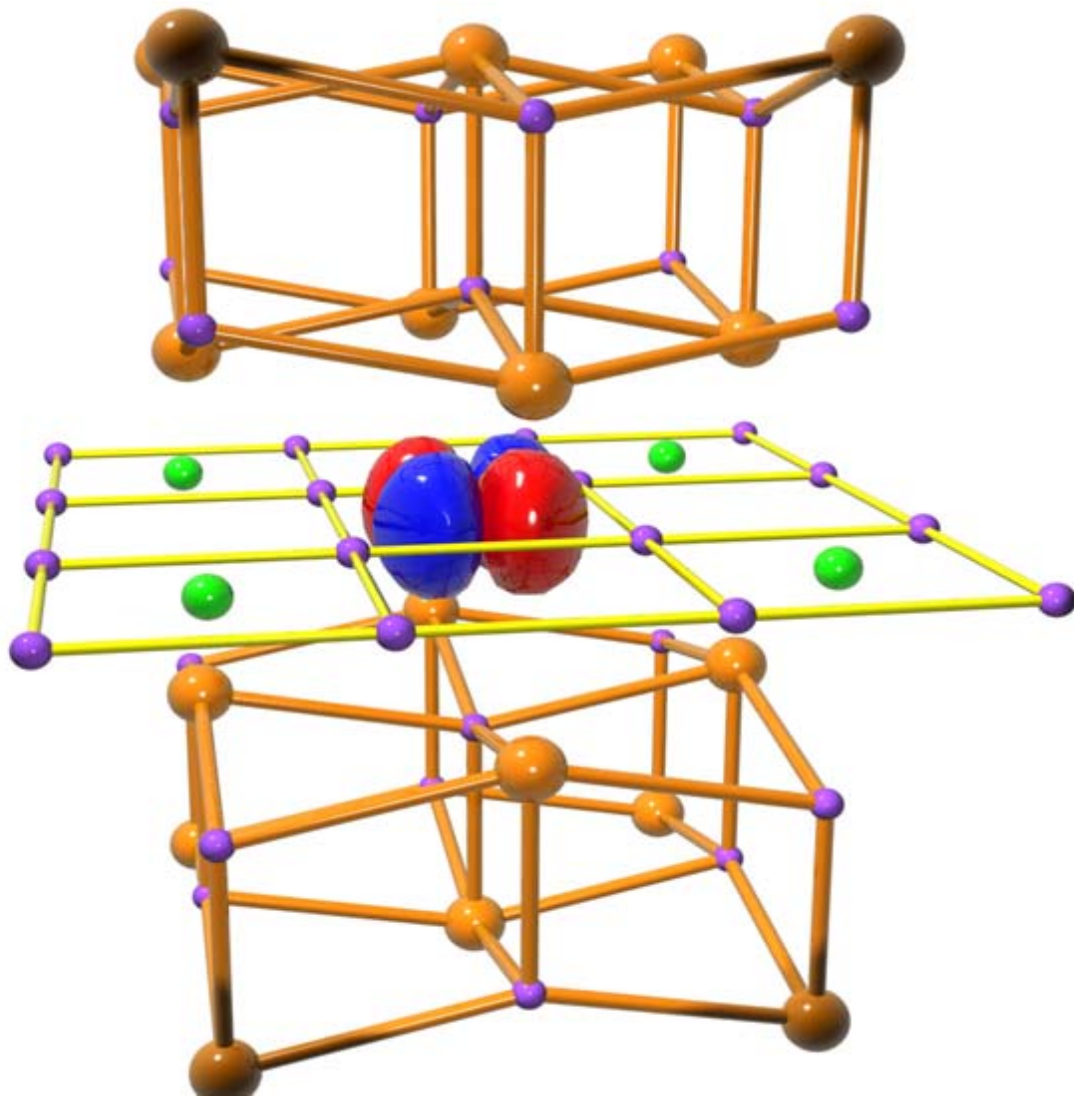
$\text{YBa}_2\text{Cu}_3\text{O}_7$



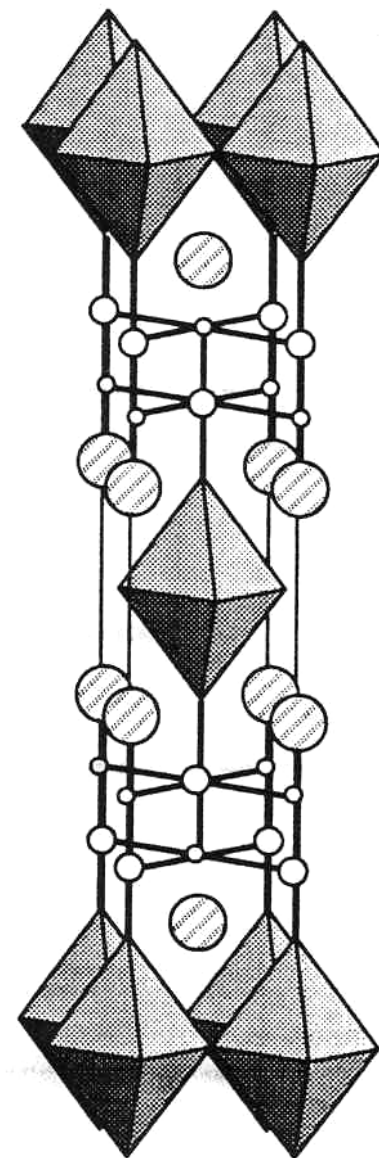
Physica (91)

Zabolotnyy,
Borisenko,...
PR (07)



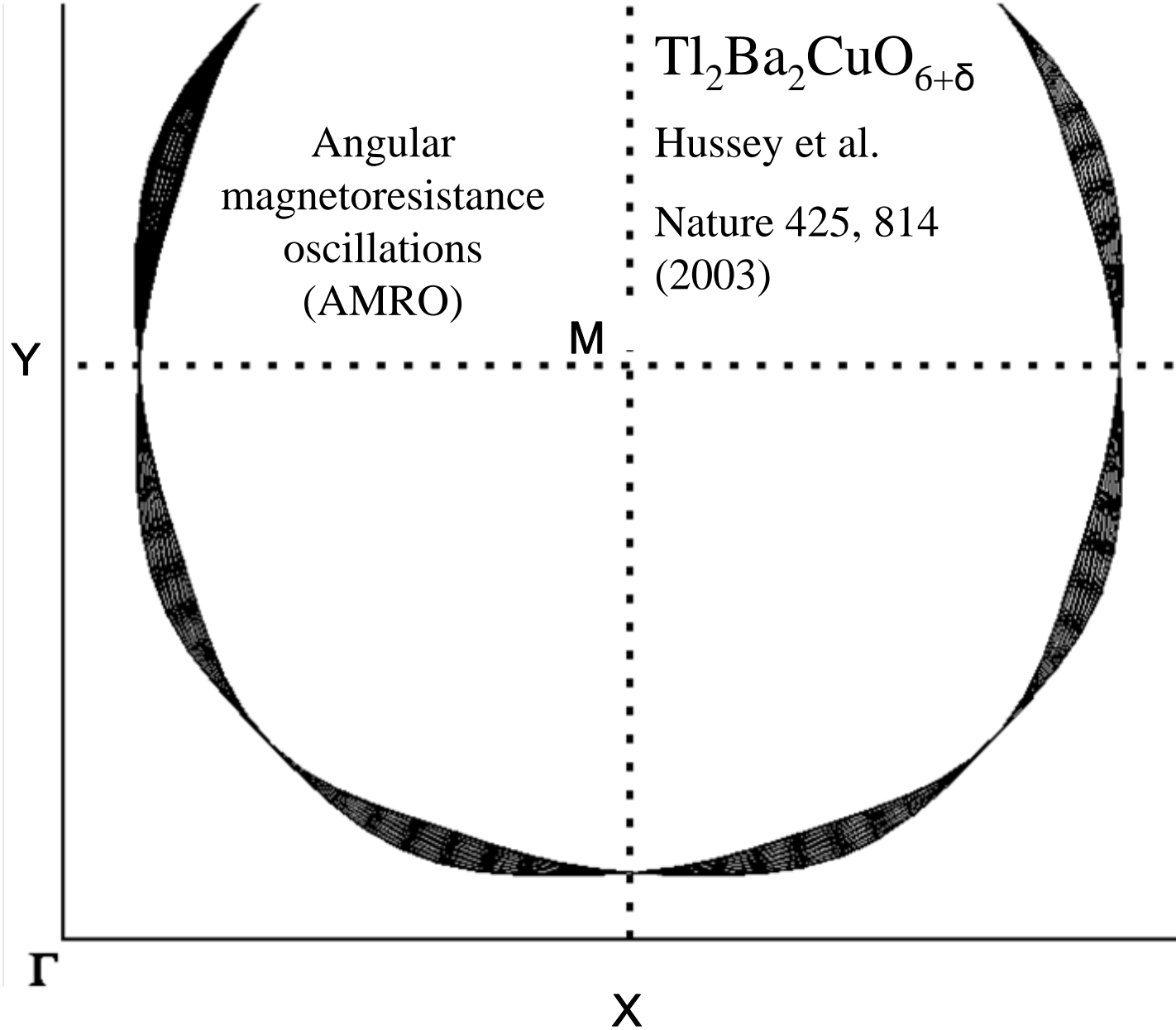


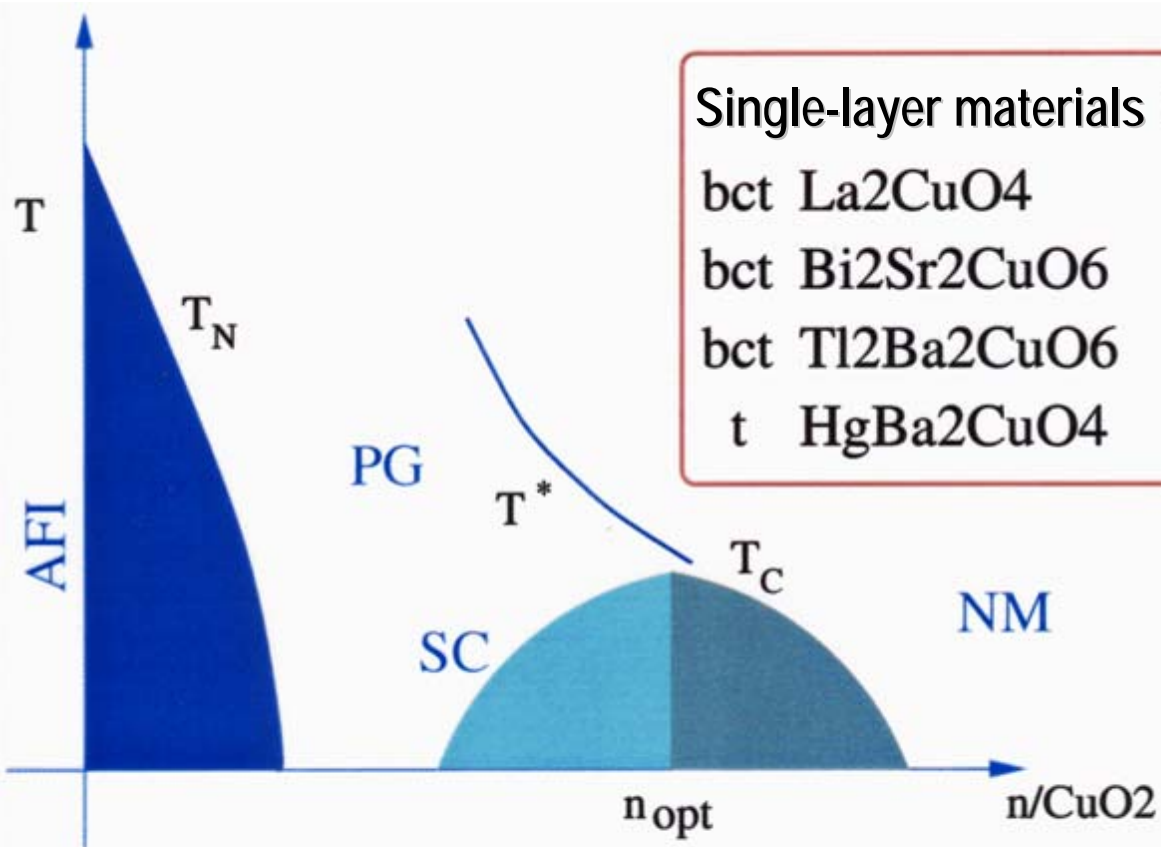
Electron count: $+3 \times 2 - n + 11 - 2 \times 4 = 9 - n \rightarrow \text{Cu } d^{9-n}$



$n=1$

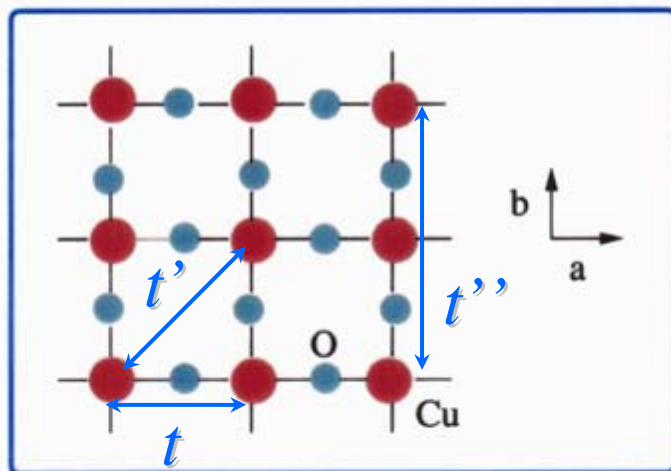
- Tl, Bi
- ⊙ Ba, Sr
- Ca





Single-layer materials max T_C

bct	La ₂ CuO ₄	40 K
bct	Bi ₂ Sr ₂ CuO ₆	40 K
bct	Tl ₂ Ba ₂ CuO ₆	90 K
t	HgBa ₂ CuO ₄	90 K



Electronic structure $\rightarrow H = \sum t_{ij} c_i^\dagger c_j + U \sum_i n_{i\uparrow} n_{i\downarrow}$

Where does this materials dependence come from?

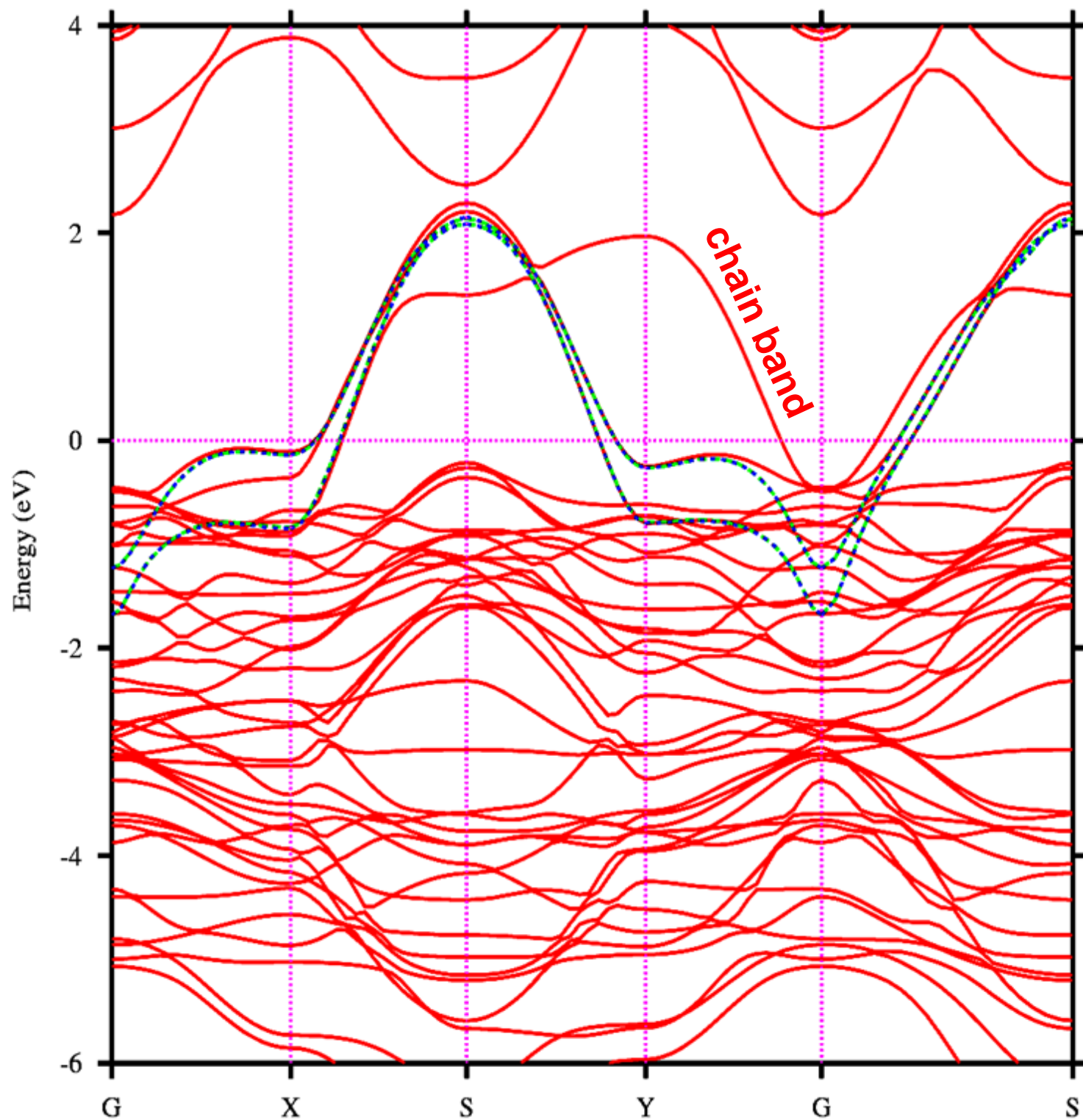
There is presently no accepted theory of high-temperature superconductivity in the cuprates



Stoichiometric at optimal doping

LDA

Bi-layer splitting:

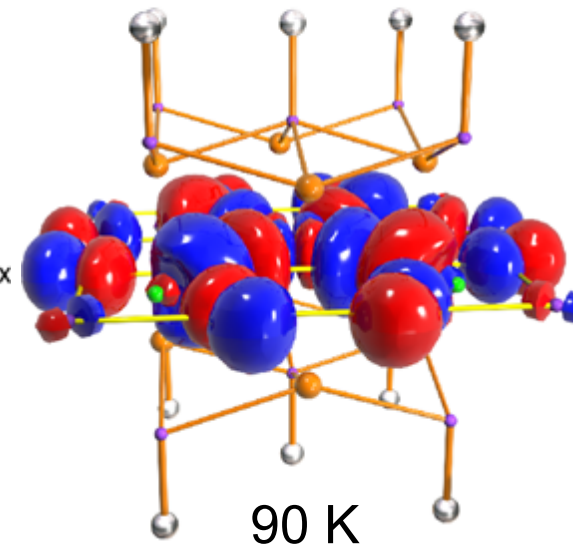
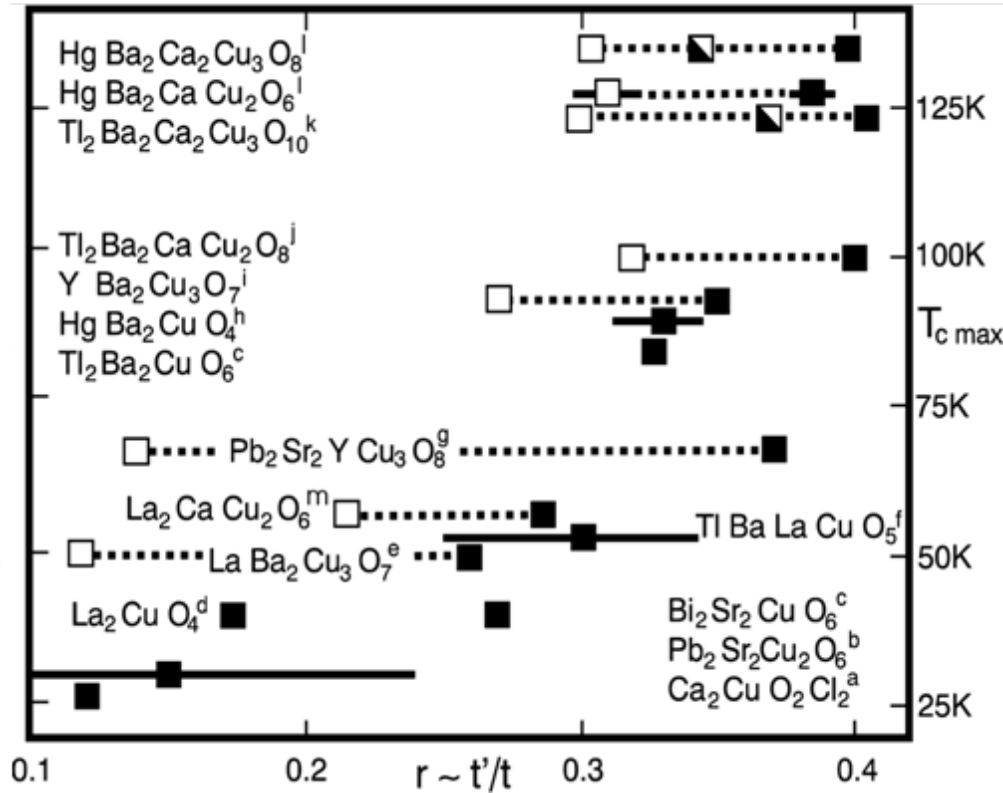
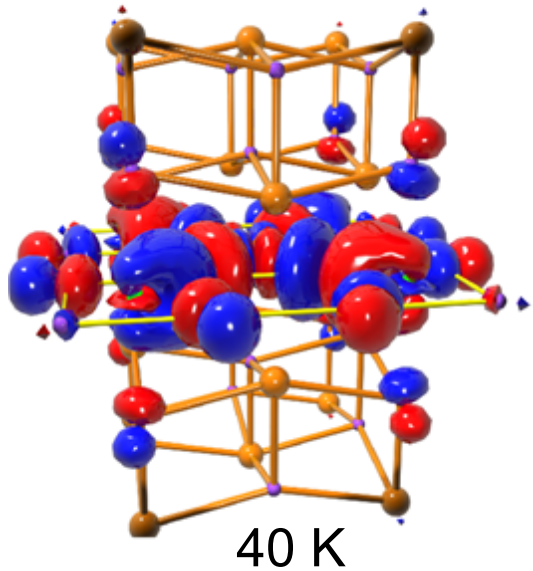


Cuprates $3d^{9-x}$
 $= 3d_{x^2-y^2}^{1-x}$

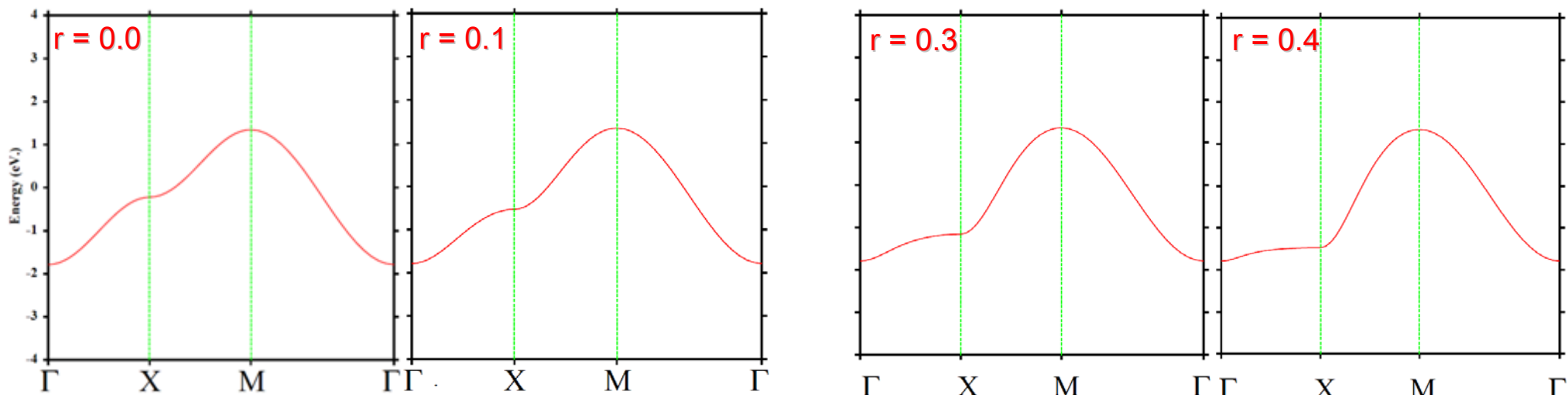
The Materials Trend, PRL 87, 047003 (2001)

HgBa₂CuO₄

La₂CuO₄

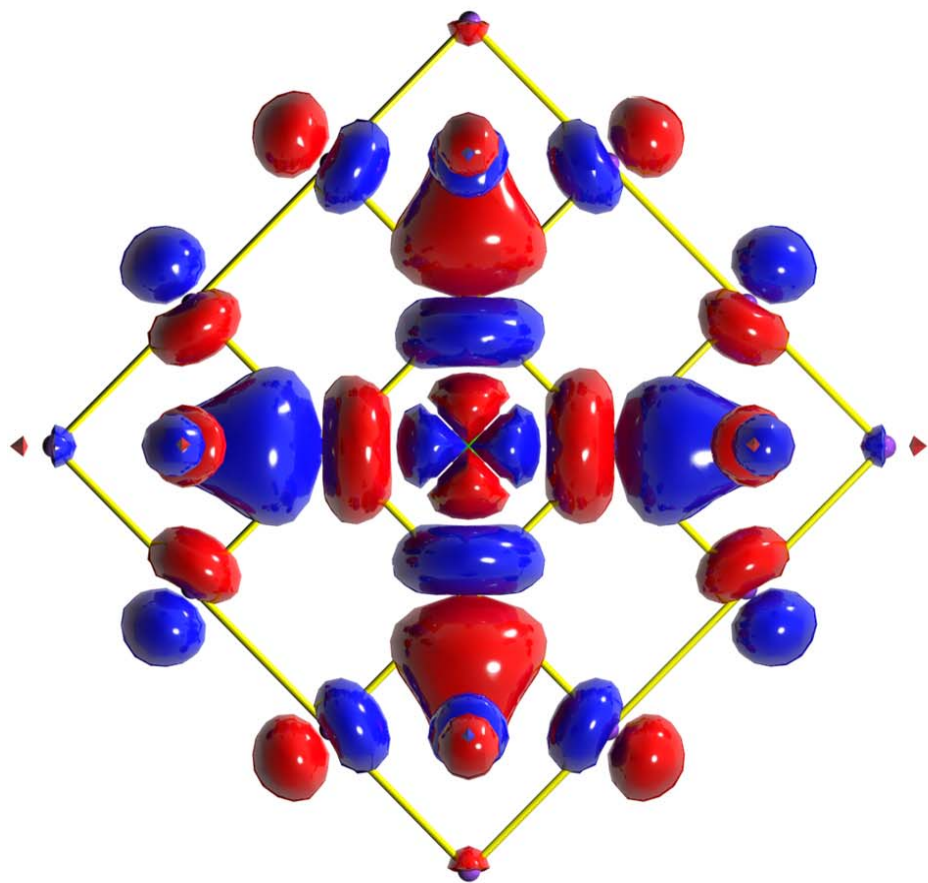


LDA conduction-band (x^2-y^2) shapes and ARPES Fermi surfaces for overdoped HTSCs

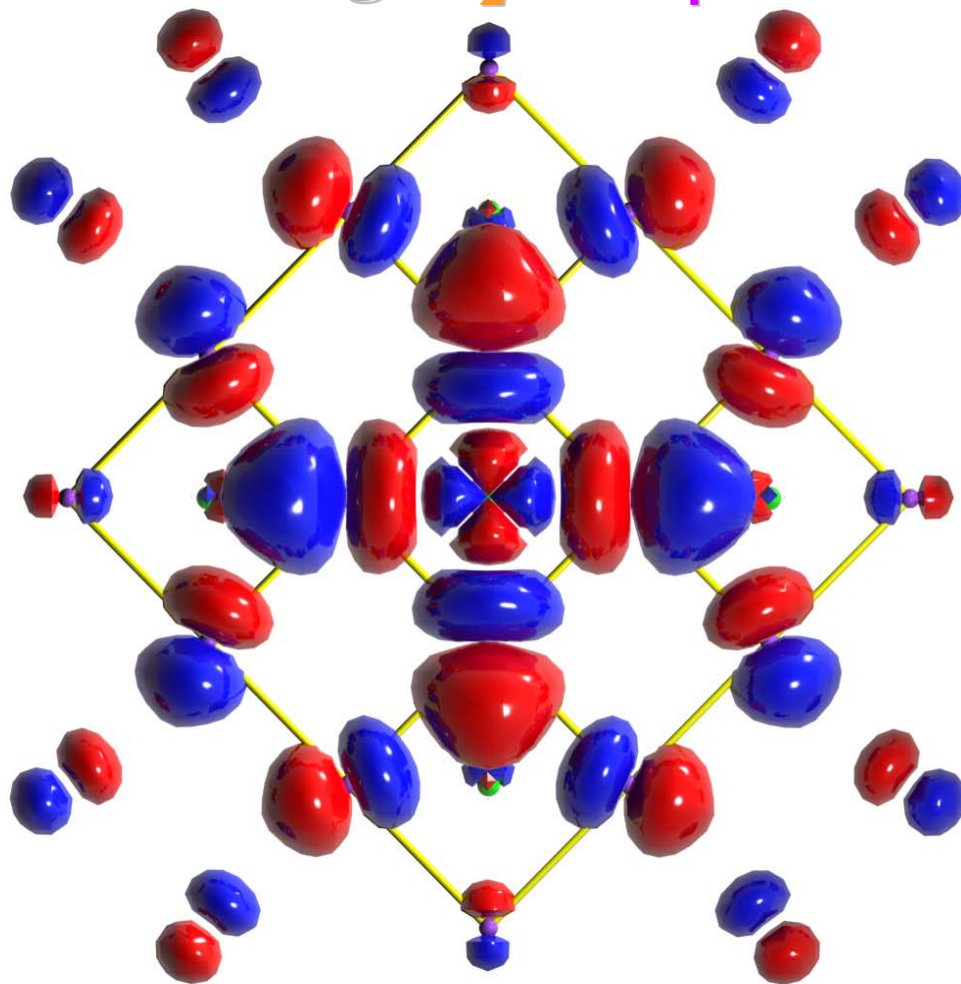


**Which structural
elements determine r ?**

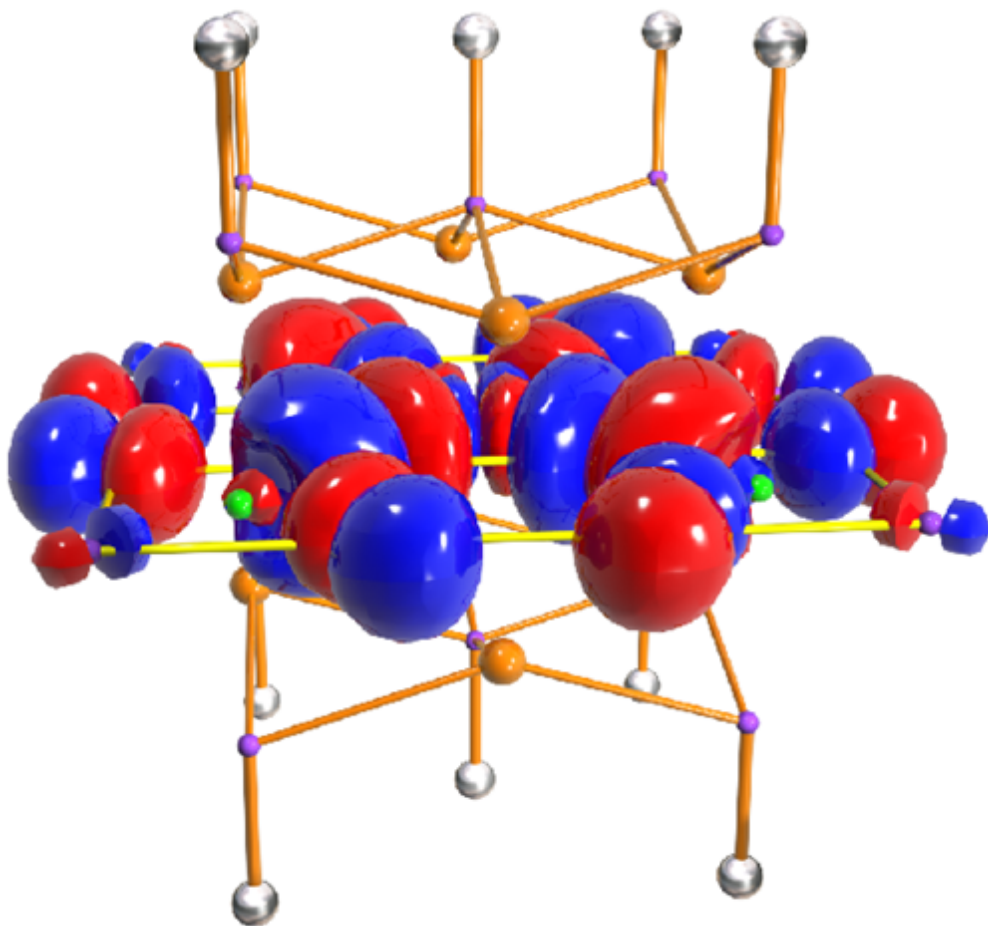
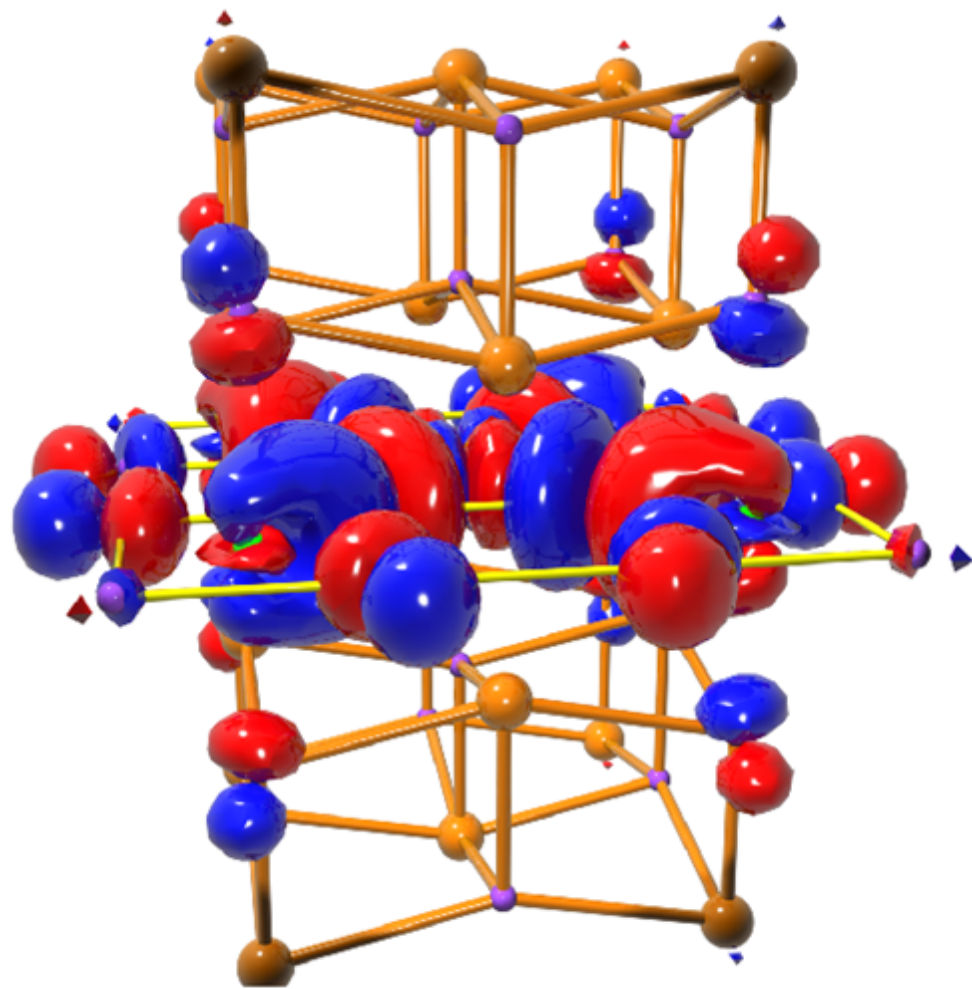
One-orbital LDA Wannier-like function



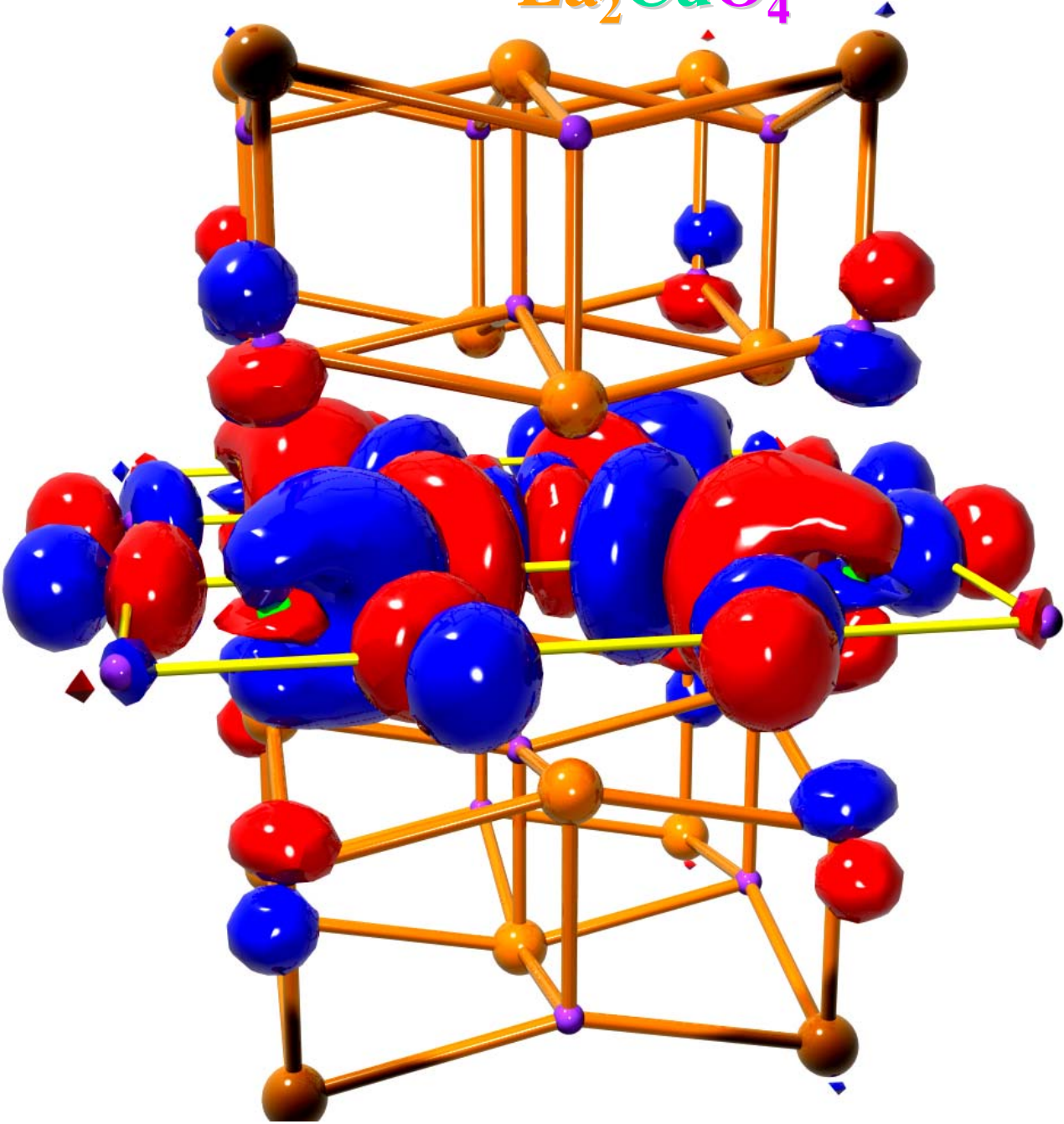
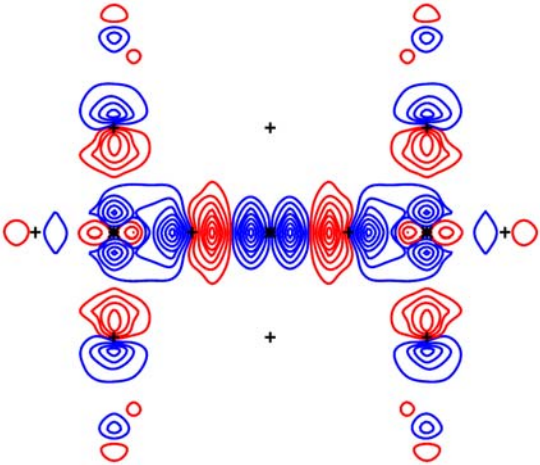
$T_c = 40 \text{ K}, r=0.17$



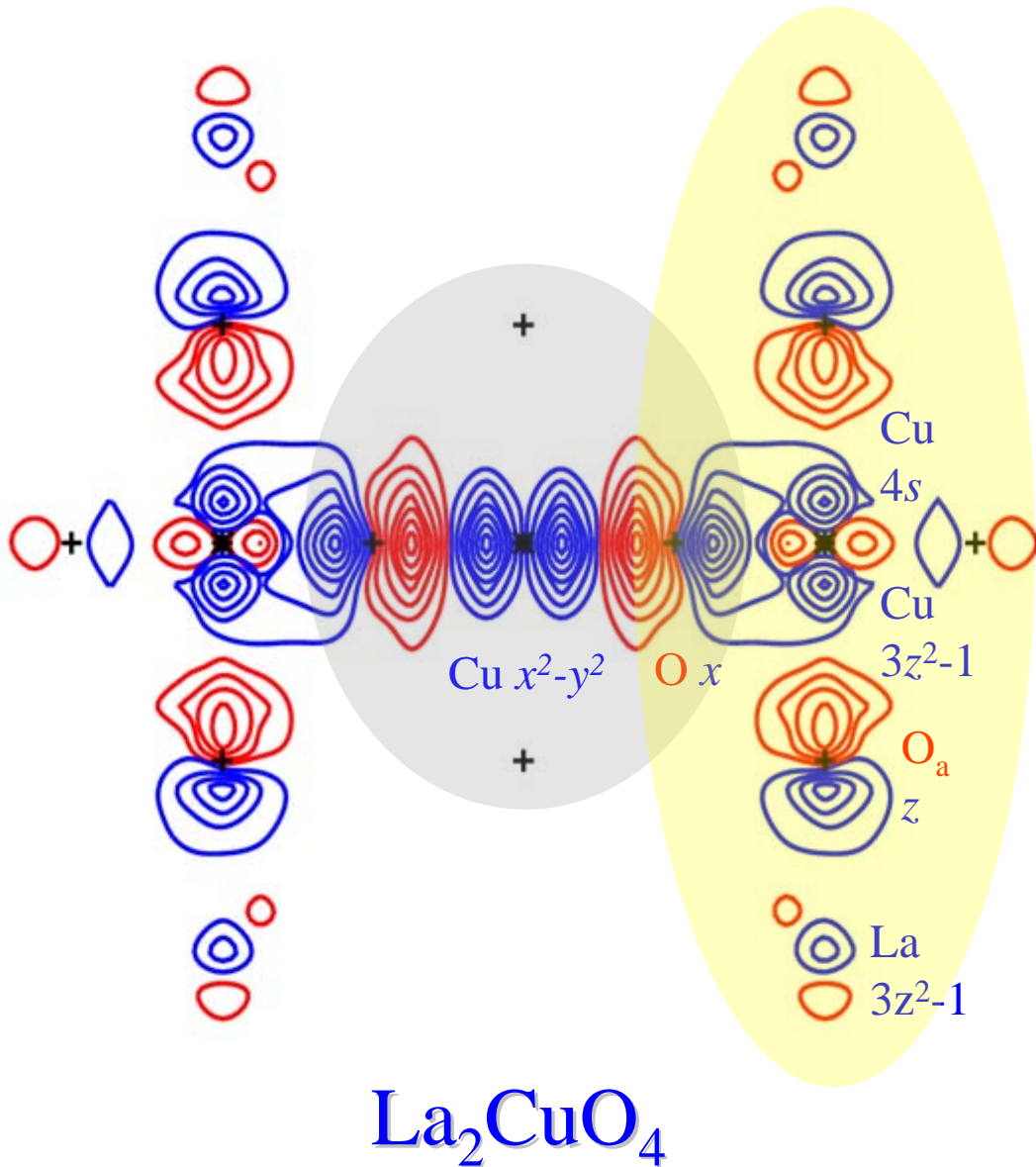
$T_c = 90 \text{ K}, r=0.33$



One-orbital LDA Wannier-like function



Wannier function for the cuprate conduction band



The materials trend is best understood in terms of a tight-binding model with two orbitals:

$$d = \text{Cu } x^2-y^2$$

dressed with

$$O p$$

and

$$s = \text{axial orbital} = \text{Cu } 4s$$

dressed with

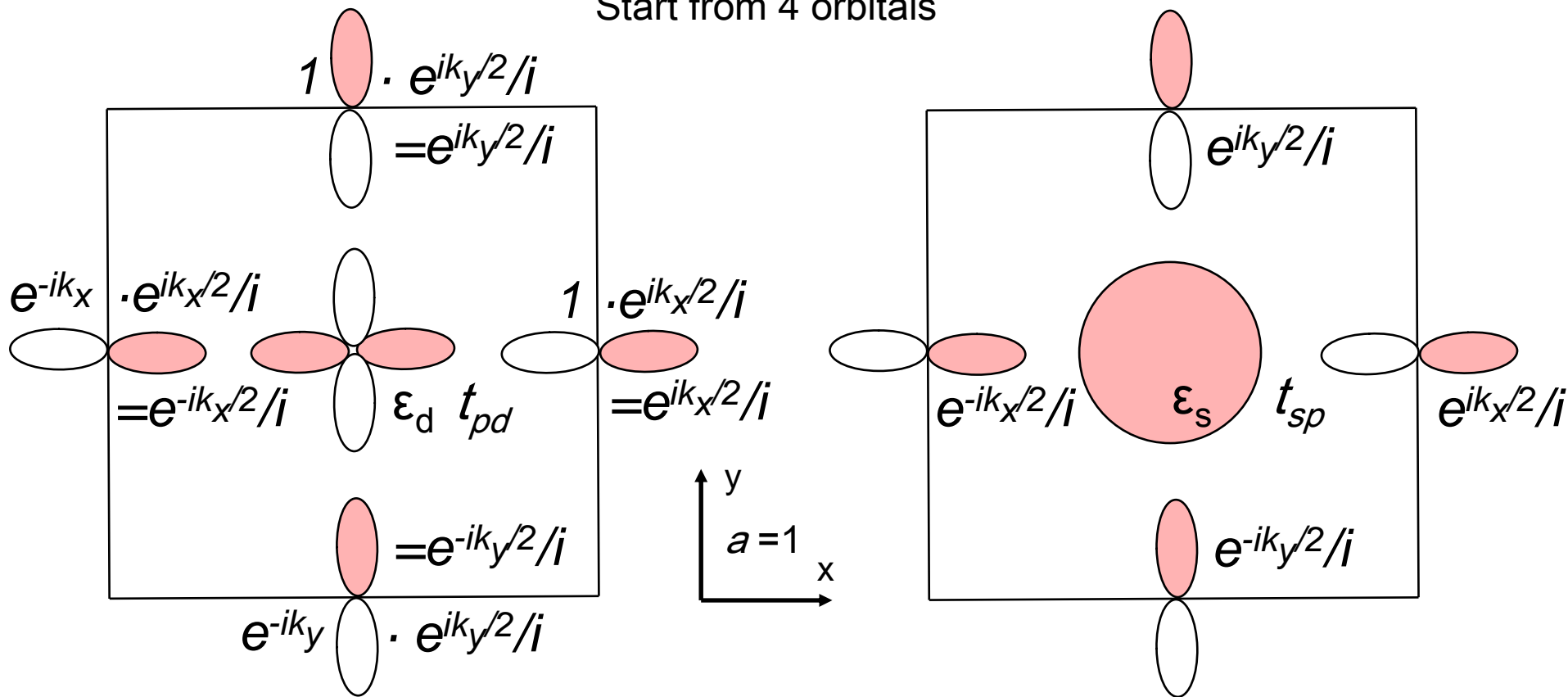
$$\text{Cu } 3z^2-1,$$

$$O_a z,$$

$$\text{La } 3z^2-1, \text{ a.s.o.}$$

The material-dependent parameter is $\epsilon_s - \epsilon_F (> 0)$. The smaller it is, the larger is $r \sim t'/t$.

Start from 4 orbitals



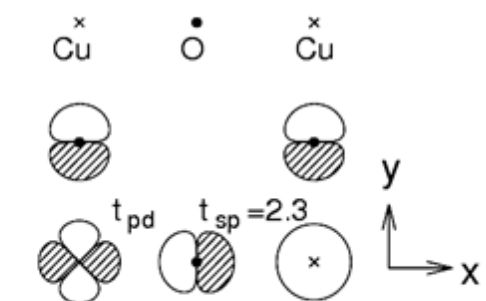
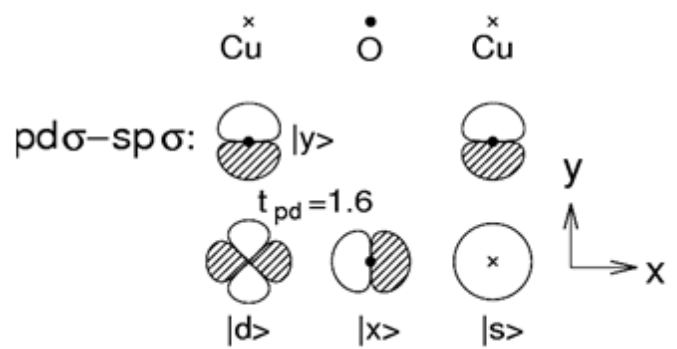
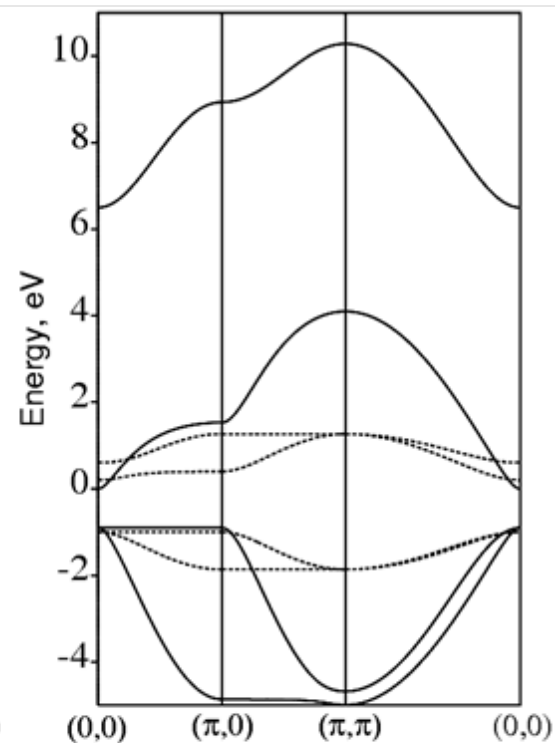
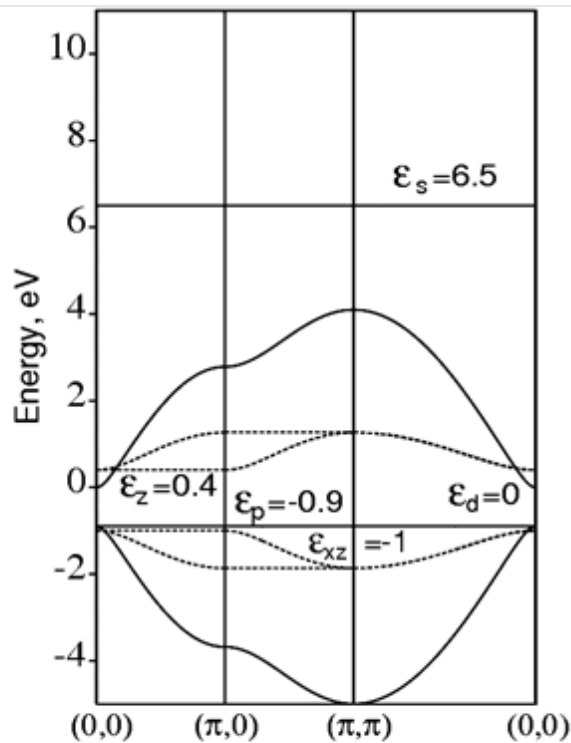
$H4$	$ d, \mathbf{k}\rangle$	$ s, \mathbf{k}\rangle$	$ x, \mathbf{k}\rangle$	$ y, \mathbf{k}\rangle$
$\langle d, \mathbf{k} $	ϵ_d	0	$2t_{pd} \sin \frac{k_x}{2}$	$-2t_{pd} \sin \frac{k_y}{2}$
$\langle s, \mathbf{k} $	0	ϵ_s	$2t_{sp} \sin \frac{k_x}{2}$	$2t_{sp} \sin \frac{k_y}{2}$
$\langle x, \mathbf{k} $	$2t_{pd} \sin \frac{k_x}{2}$	$2t_{sp} \sin \frac{k_x}{2}$	ϵ_p	0
$\langle y, \mathbf{k} $	$-2t_{pd} \sin \frac{k_y}{2}$	$2t_{sp} \sin \frac{k_y}{2}$	0	ϵ_p

Löwdin downfolding to 2 orbitals:

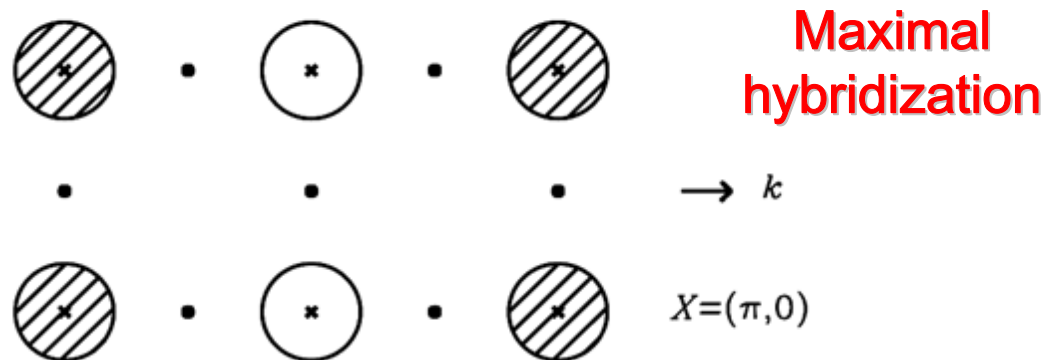
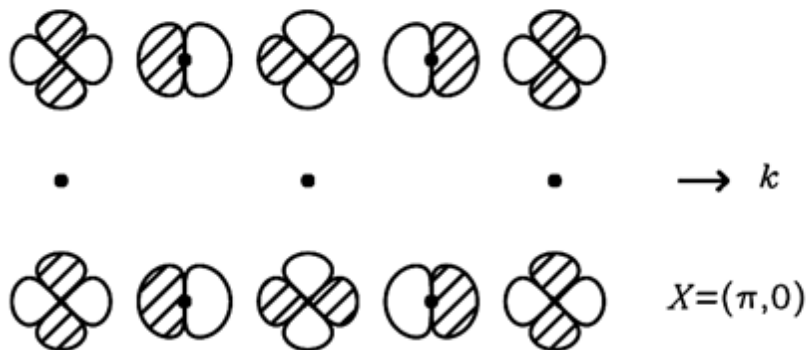
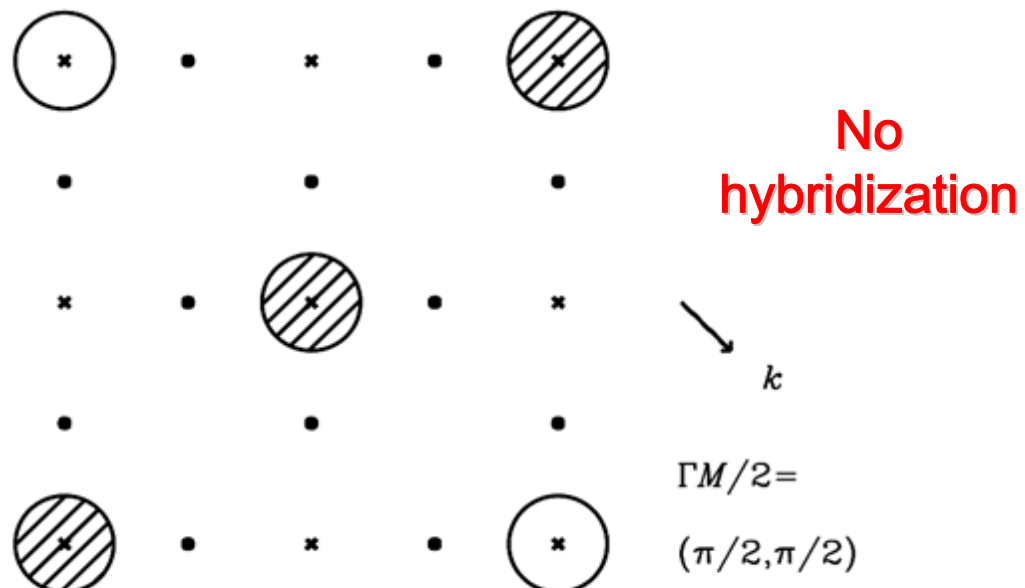
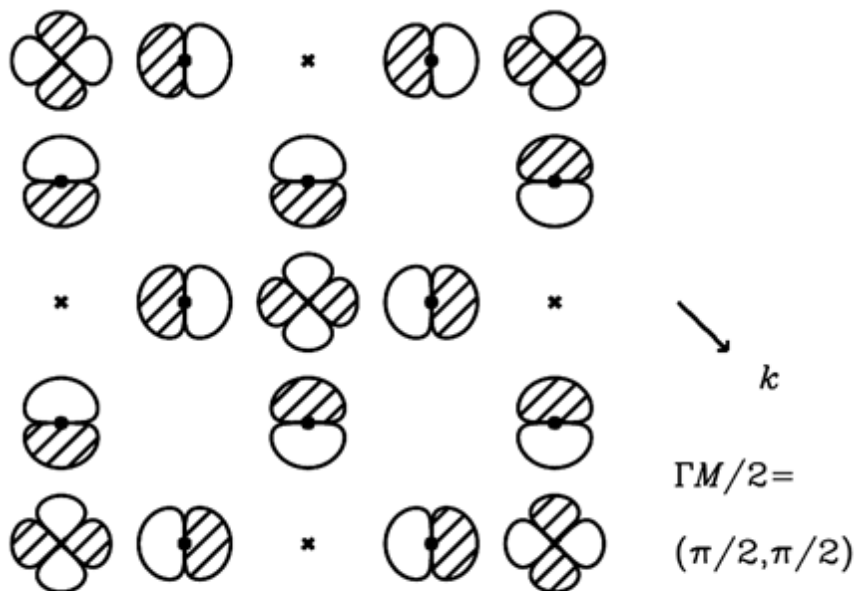
$H4$	$ d, \mathbf{k}\rangle$	$ s, \mathbf{k}\rangle$	$ x, \mathbf{k}\rangle$	$ y, \mathbf{k}\rangle$
$\langle d, \mathbf{k} $	ϵ_d	0	$2t_{pd} \sin \frac{k_x}{2}$	$-2t_{pd} \sin \frac{k_y}{2}$
$\langle s, \mathbf{k} $	0	ϵ_s	$2t_{sp} \sin \frac{k_x}{2}$	$2t_{sp} \sin \frac{k_y}{2}$
$\langle x, \mathbf{k} $	$2t_{pd} \sin \frac{k_x}{2}$	$2t_{sp} \sin \frac{k_x}{2}$	ϵ_p	0
$\langle y, \mathbf{k} $	$-2t_{pd} \sin \frac{k_y}{2}$	$2t_{sp} \sin \frac{k_y}{2}$	0	ϵ_p

→

$H2(\epsilon)$	$ d, \epsilon, \mathbf{k}\rangle$	$ s, \epsilon, \mathbf{k}\rangle$
$\langle d, \epsilon, \mathbf{k} $	$\epsilon_d + \frac{4t_{pd}^2}{\epsilon - \epsilon_p} \left(\sin^2 \frac{k_x}{2} + \sin^2 \frac{k_y}{2} \right)$	$\frac{4t_{sp}t_{pd}}{\epsilon - \epsilon_p} \left(\sin^2 \frac{k_x}{2} - \sin^2 \frac{k_y}{2} \right)$
$\langle s, \epsilon, \mathbf{k} $	$\frac{4t_{sp}t_{pd}}{\epsilon - \epsilon_p} \left(\sin^2 \frac{k_x}{2} - \sin^2 \frac{k_y}{2} \right)$	$\epsilon_s + \frac{4t_{pd}^2}{\epsilon - \epsilon_p} \left(\sin^2 \frac{k_x}{2} + \sin^2 \frac{k_y}{2} \right)$



Hybridization between x^2-y^2 and axial orbital Cu $4s$, apical O $2p_z$, etc.



Hybridization $\sim (\cos k_x - \cos k_y)^2$

$H2(\varepsilon)$	$ d, \varepsilon, \mathbf{k}\rangle$	$ s, \varepsilon, \mathbf{k}\rangle$
$\langle d, \varepsilon, \mathbf{k} $	$\varepsilon_d + \frac{4t_{pd}^2}{\varepsilon - \varepsilon_p} \left(1 - \frac{\cos k_x + \cos k_y}{2}\right)$	$-\frac{4t_{sp}t_{pd}}{\varepsilon - \varepsilon_p} \frac{\cos k_x - \cos k_y}{2}$
$\langle s, \varepsilon, \mathbf{k} $	$-\frac{4t_{sp}t_{pd}}{\varepsilon - \varepsilon_p} \frac{\cos k_x - \cos k_y}{2}$	$\varepsilon_s + \frac{4t_{sp}^2}{\varepsilon - \varepsilon_p} \left(1 - \frac{\cos k_x + \cos k_y}{2}\right)$

Downfolding to 1 orbital:

$$H1(\varepsilon) = \langle \tilde{d}, \varepsilon, \mathbf{k} | H | \tilde{d}, \varepsilon, \mathbf{k} \rangle =$$

$$= \varepsilon_d + \frac{4t_{pd}^2}{\varepsilon - \varepsilon_p} \left(1 - \frac{\cos k_x + \cos k_y}{2} + \frac{\frac{4t_{sp}^2}{\varepsilon - \varepsilon_p} \left(\frac{\cos k_x - \cos k_y}{2} \right)^2}{\varepsilon - \varepsilon_s - \frac{4t_{sp}^2}{\varepsilon - \varepsilon_p} \left(1 - \frac{\cos k_x + \cos k_y}{2} \right)} \right)$$

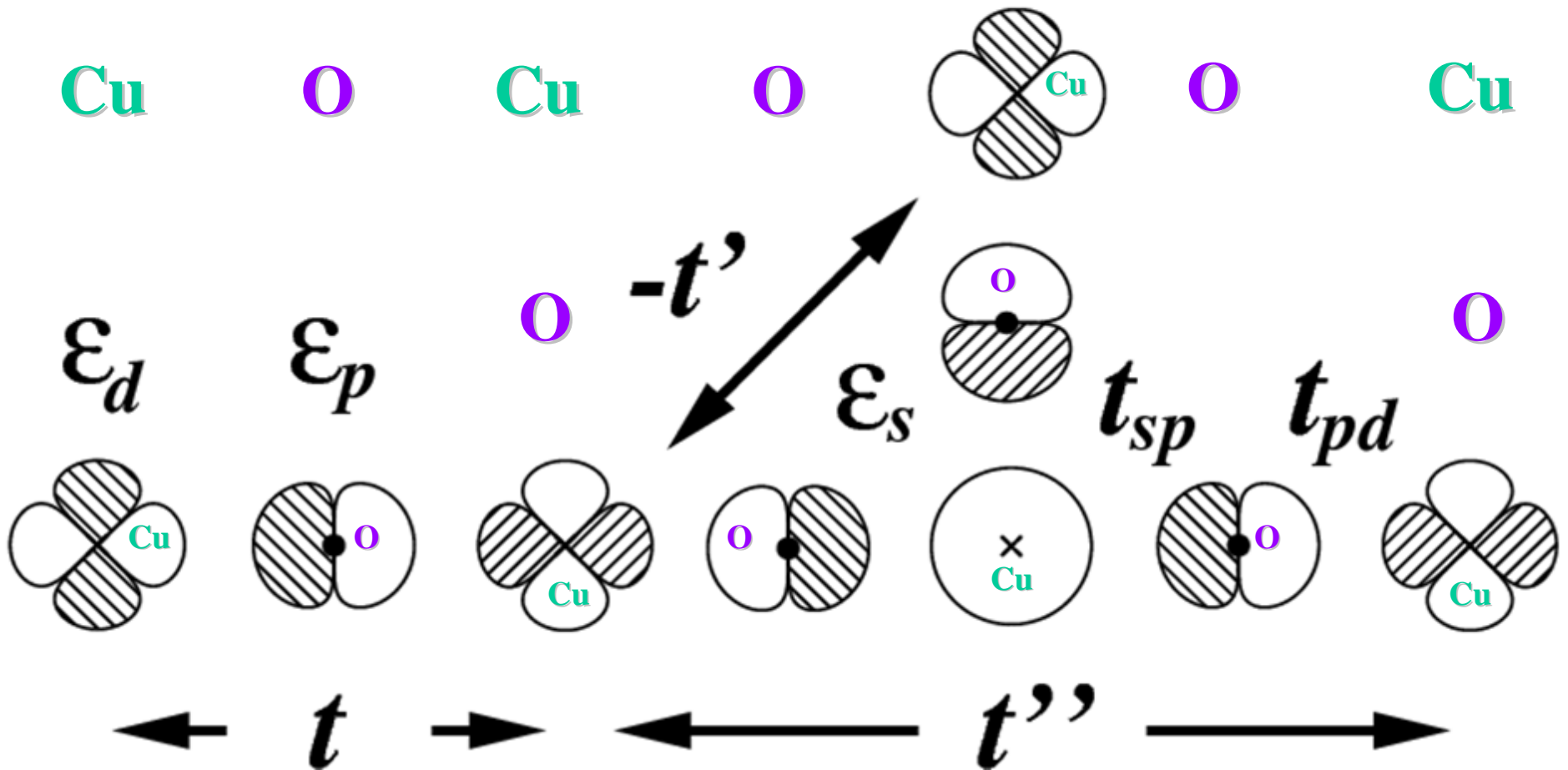
$$= \varepsilon_d + \frac{4t_{pd}^2}{\varepsilon - \varepsilon_p} \left(1 - \frac{\cos k_x + \cos k_y}{2} + \frac{\frac{t_{sp}^2}{\varepsilon - \varepsilon_p} \left(1 - 2 \cos k_x \cos k_y + \frac{\cos 2k_x + \cos 2k_y}{2} \right)}{\varepsilon - \varepsilon_s - \frac{4t_{sp}^2}{\varepsilon - \varepsilon_p} \left(1 - \frac{\cos k_x + \cos k_y}{2} \right)} \right)$$

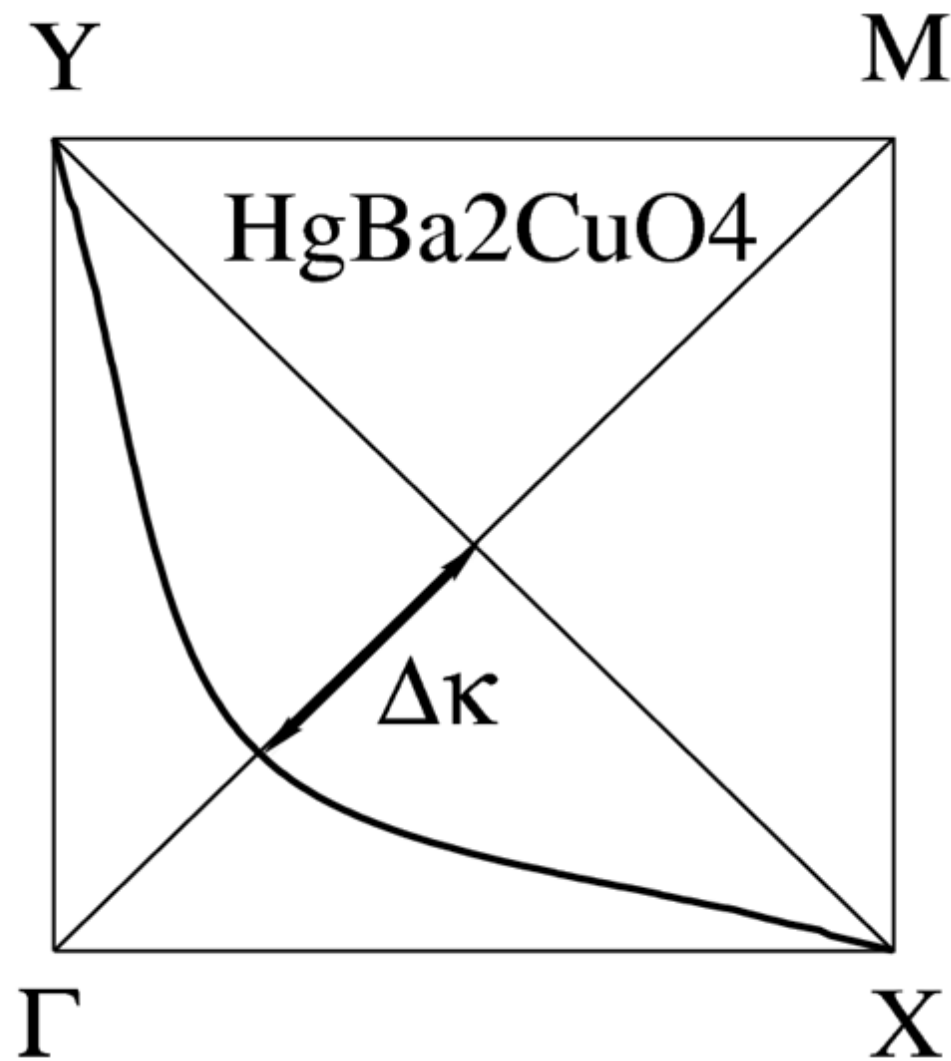
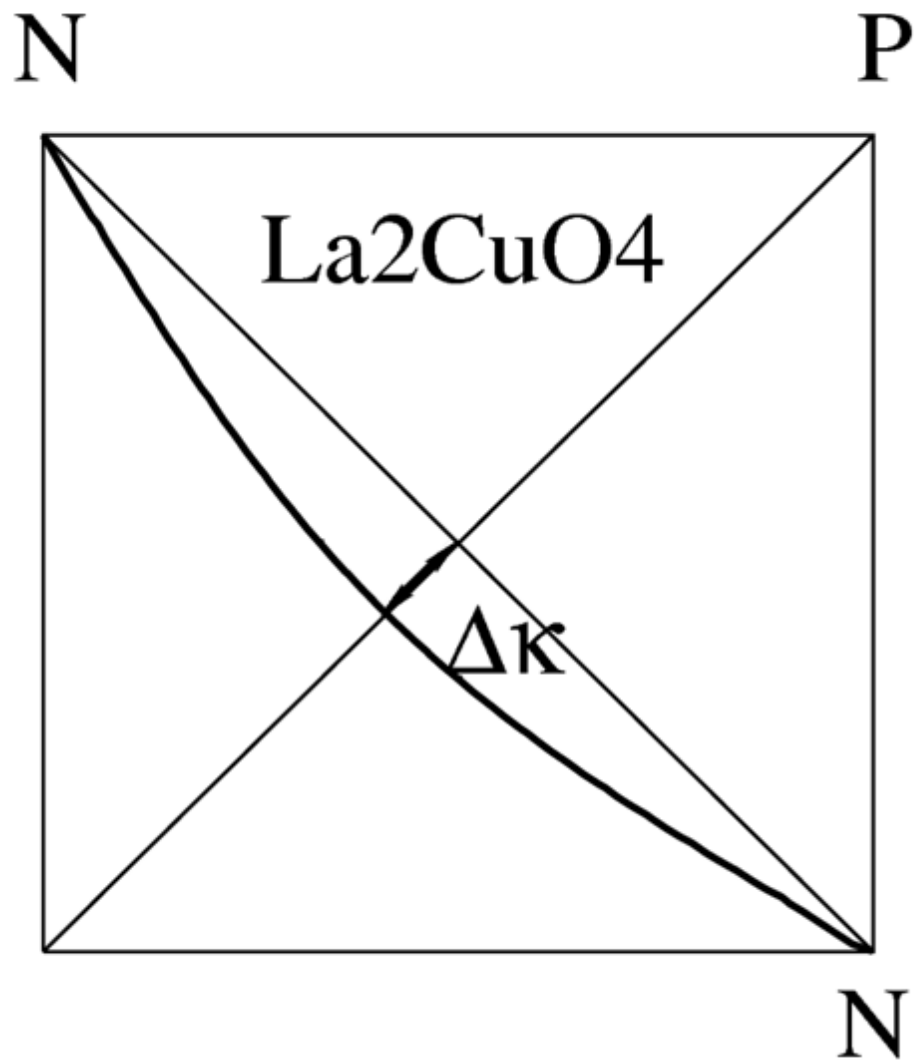
$$\equiv \varepsilon_0 - 2t (\cos k_x + \cos k_y) + 4t' \cos k_x \cos k_y - 2t'' (\cos 2k_x + \cos 2k_y) + \dots$$

$$t = \frac{t_{pd}^2}{\varepsilon - \varepsilon_p}, \quad t'/t \approx \frac{\frac{2t_{sp}^2}{\varepsilon - \varepsilon_p}}{\varepsilon_s - \varepsilon + \frac{4t_{sp}^2}{\varepsilon - \varepsilon_p}} \equiv r(\varepsilon), \quad t''/t' = \frac{1}{2}$$

From the nearest-neighbor 4-orbital model ($\epsilon_p, \epsilon_d, \epsilon_s, t_{pd}, t_{sp}$)

to the longer-ranged 1-orbital model (t, t', t'', \dots)

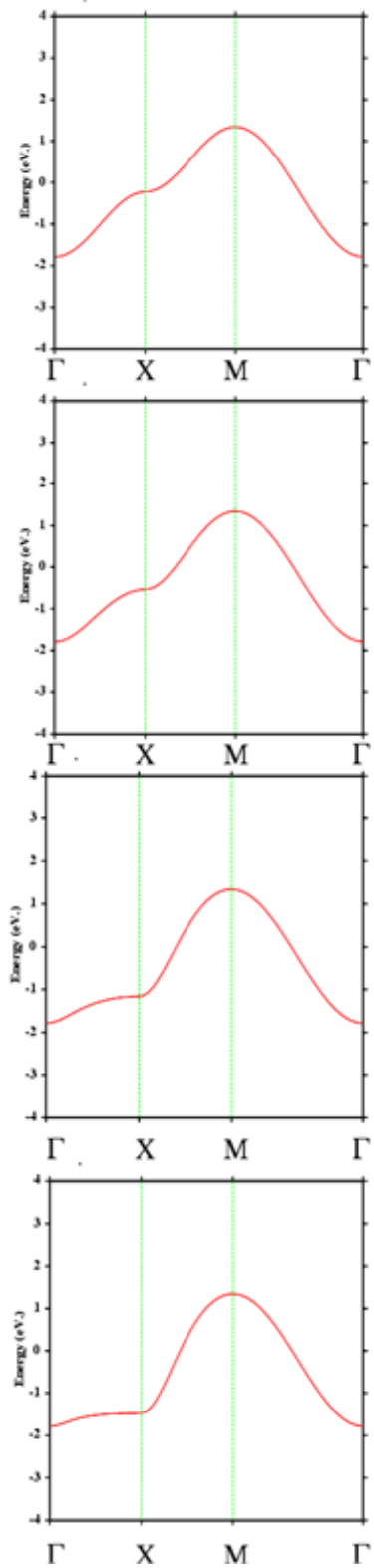




$$T_{c \max} = 40\text{K}, \quad r = 0.17$$

$$T_{c \max} = 90\text{K}, \quad r = 0.33$$

$$r = \frac{1}{2} \sin(\pi \Delta\kappa)$$

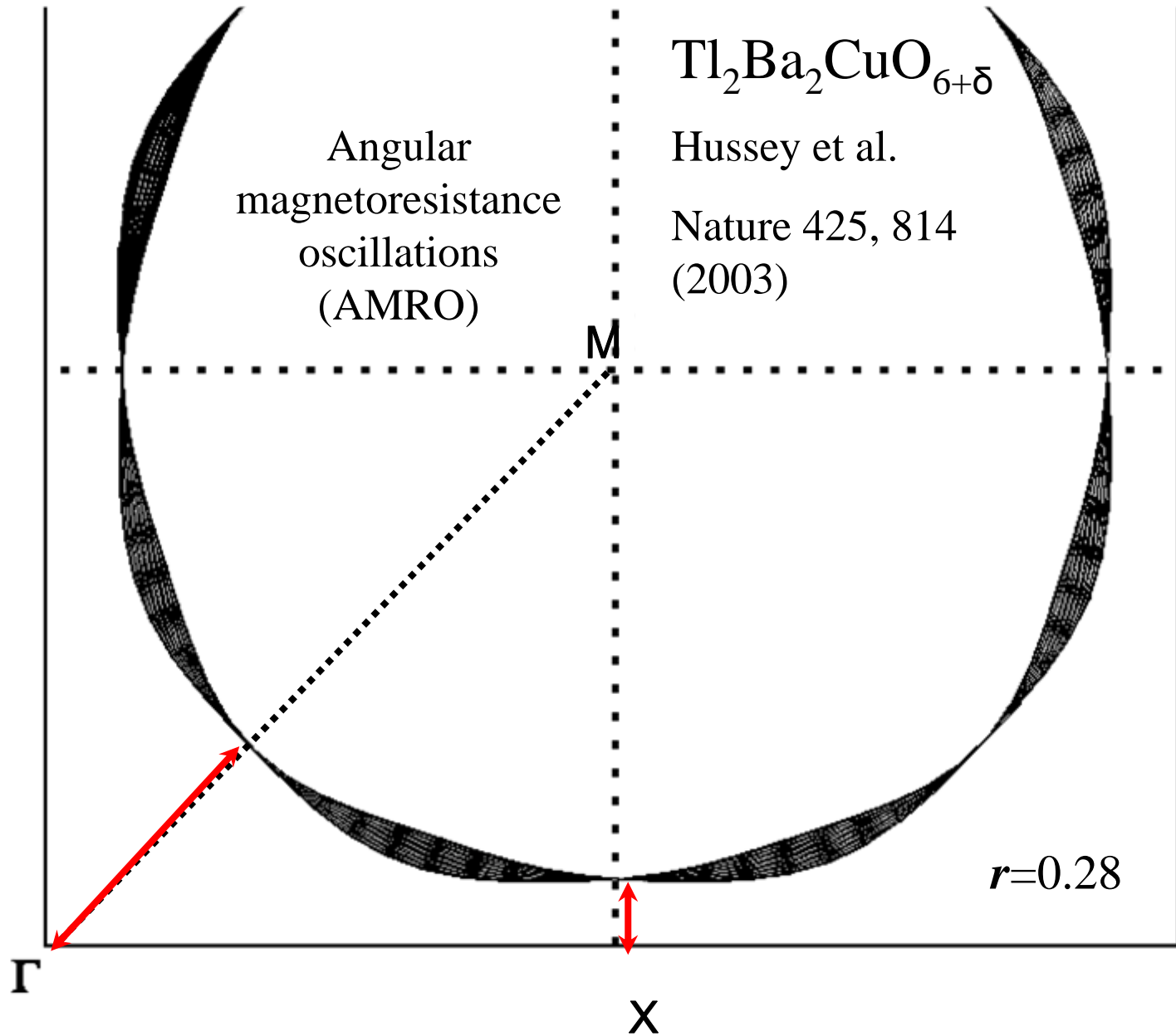


$r=0.$

$r=0.1$

$r=0.3$

$r=0.4$



$\text{Tl}_2\text{Ba}_2\text{CuO}_{6+\delta}$

Hussey et al.

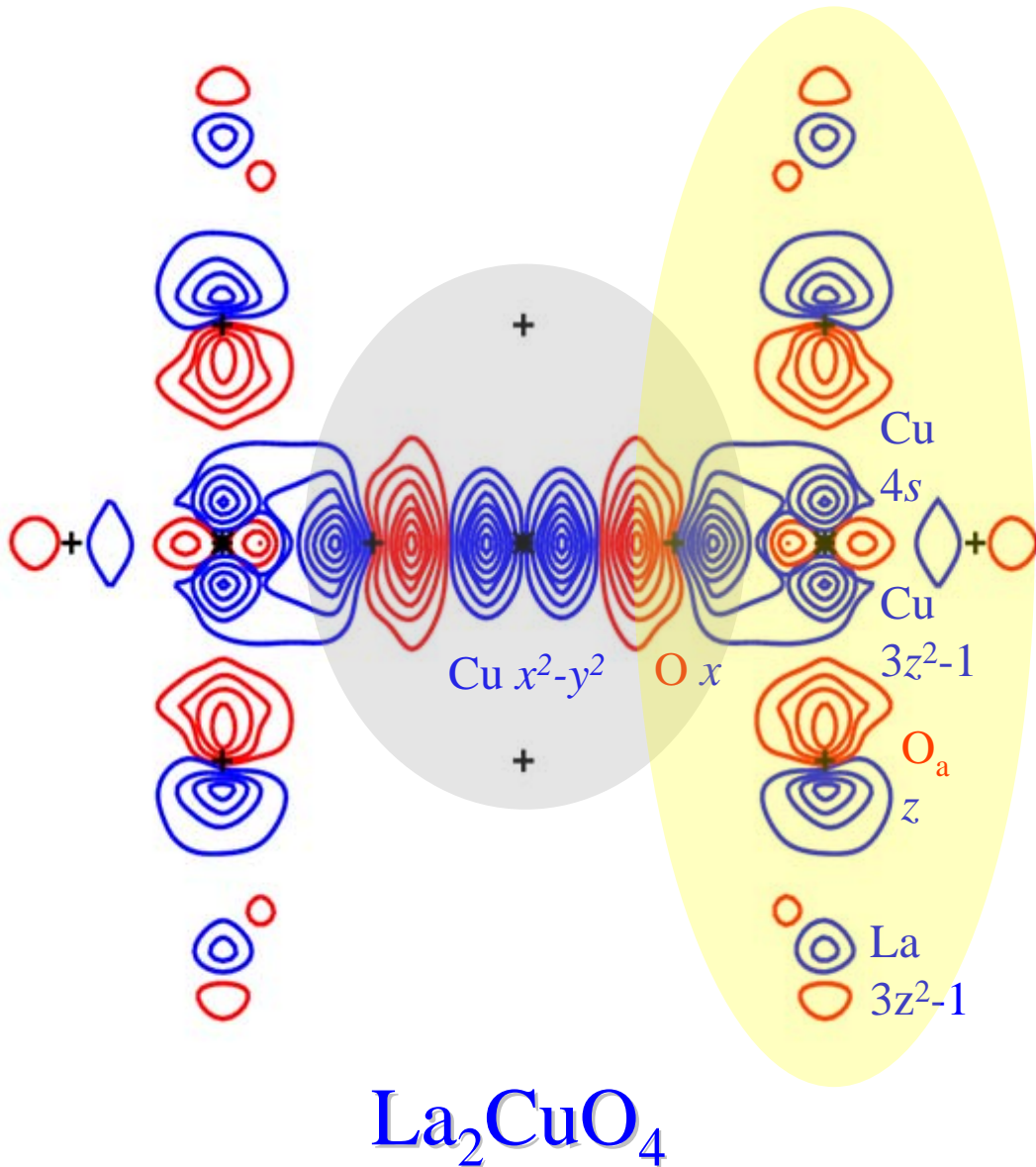
Nature 425, 814
(2003)

Angular
magnetoresistance
oscillations
(AMRO)

$r=0.28$

$$r = \frac{1}{2} \frac{\cos(\pi k_{\Gamma M}/\Gamma M) + \sin^2\left(\frac{\pi}{2} k_{\chi M}/\chi M\right)}{1 - \sin^2\left(\frac{\pi}{2} k_{\chi M}/\chi M\right) [2 + \cos(\pi k_{\Gamma M}/\Gamma M)]}$$

Wannier function for the cuprate conduction band



The materials trend is best understood in terms of a tight-binding model with two orbitals:

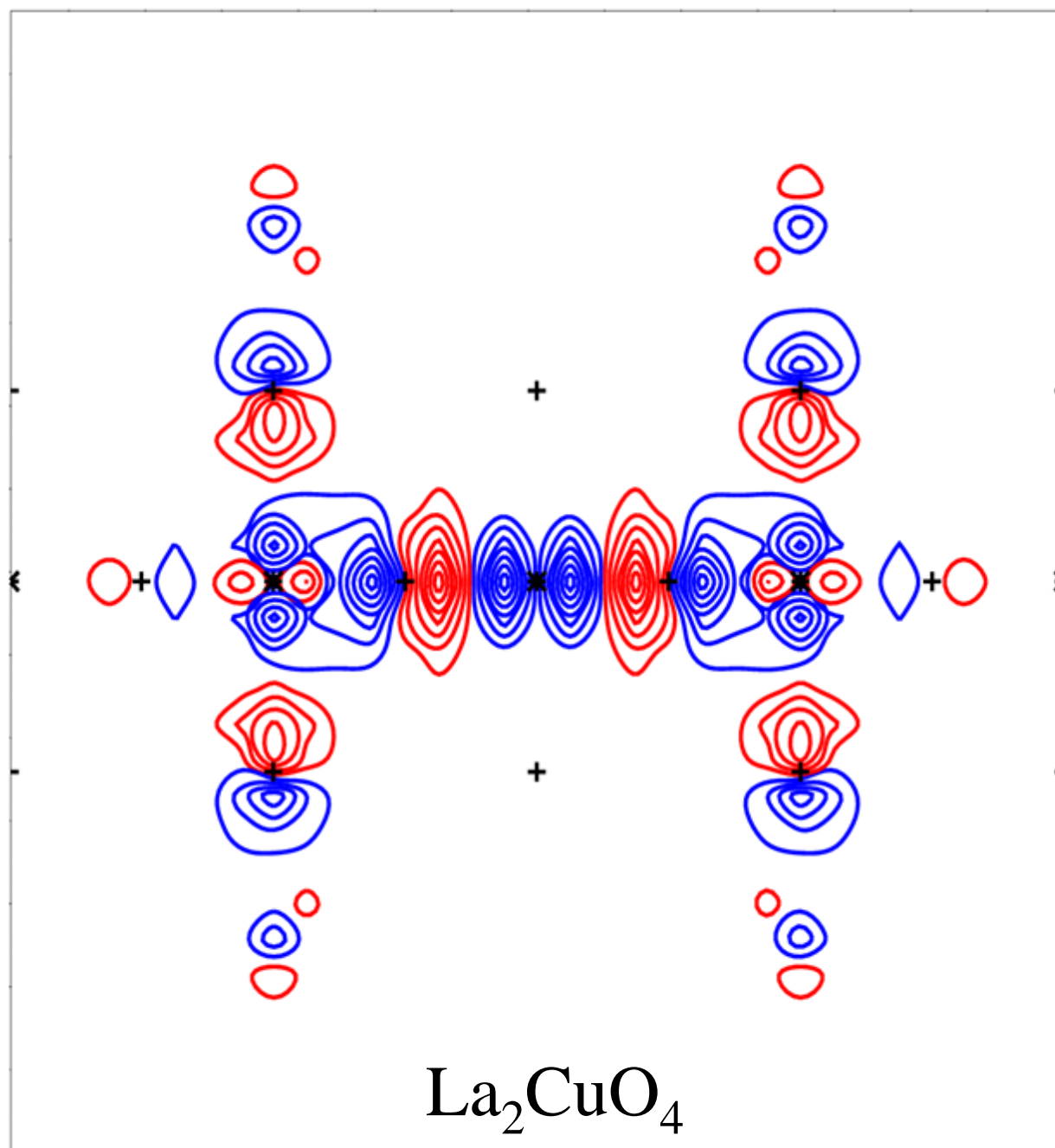
$d = \text{Cu } x^2-y^2$
dressed with
 $O p$

and

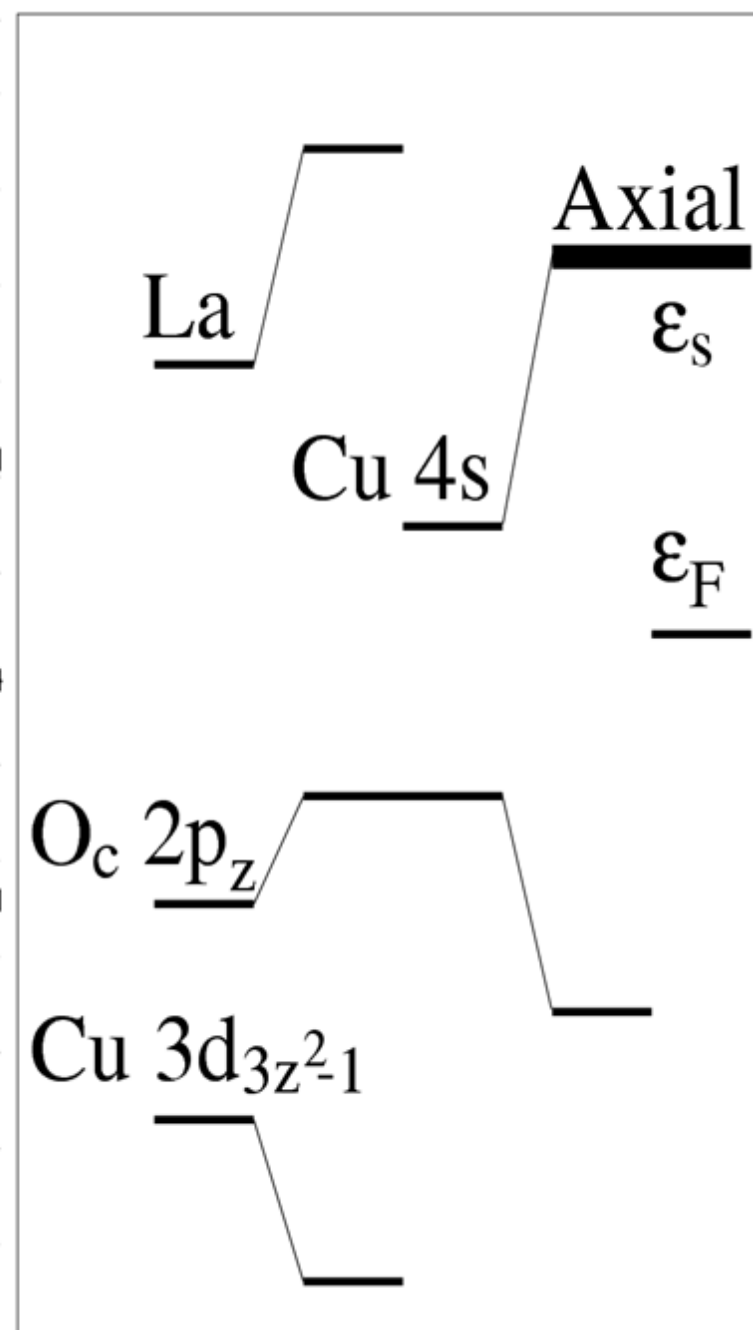
$s = \text{axial orbital} = \text{Cu } 4s$
dressed with
 $\text{Cu } 3z^2-1,$
 $O_a z,$
 $\text{La } 3z^2-1, \text{ a.s.o.}$

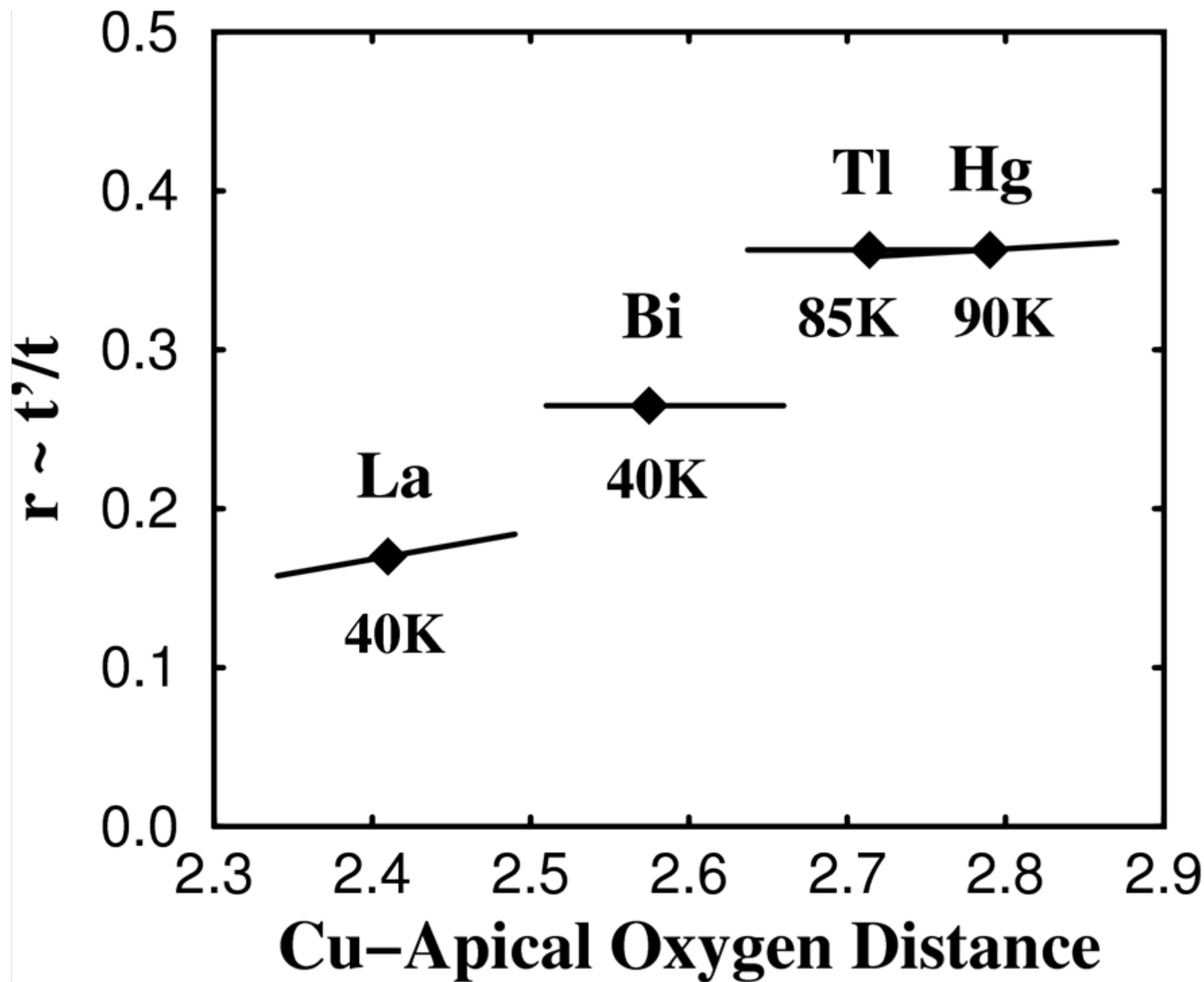
The material-dependent parameter is $\epsilon_s - \epsilon_F (> 0)$. The smaller it is, the larger is $r \sim t'/t$.

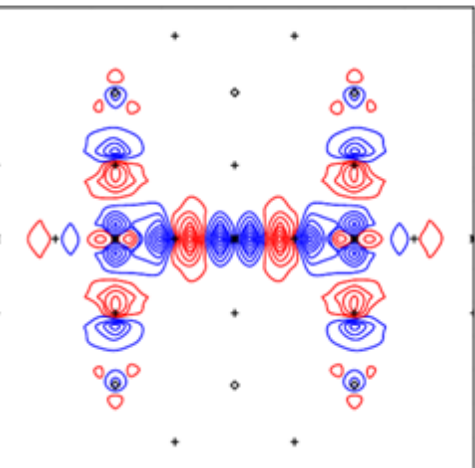
One-orbital LDA Wannier-like function



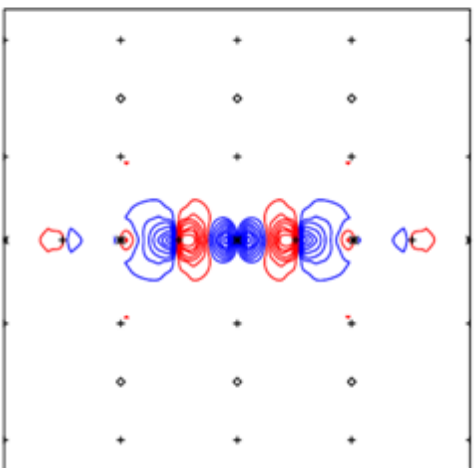
Four-orbital model



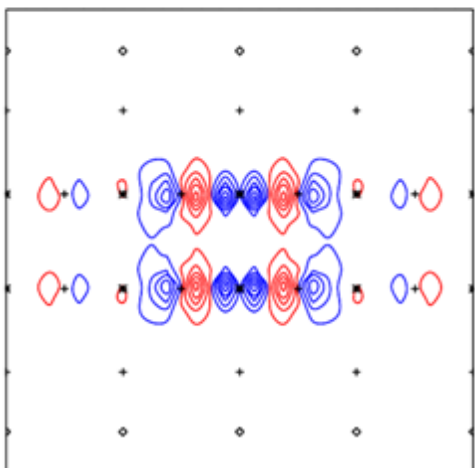




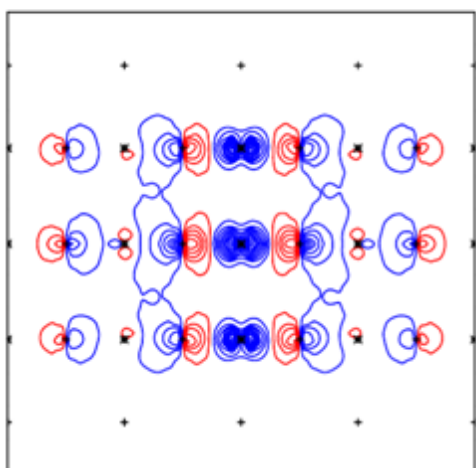
La_2CuO_4



$\text{HgBa}_2\text{CuO}_4$



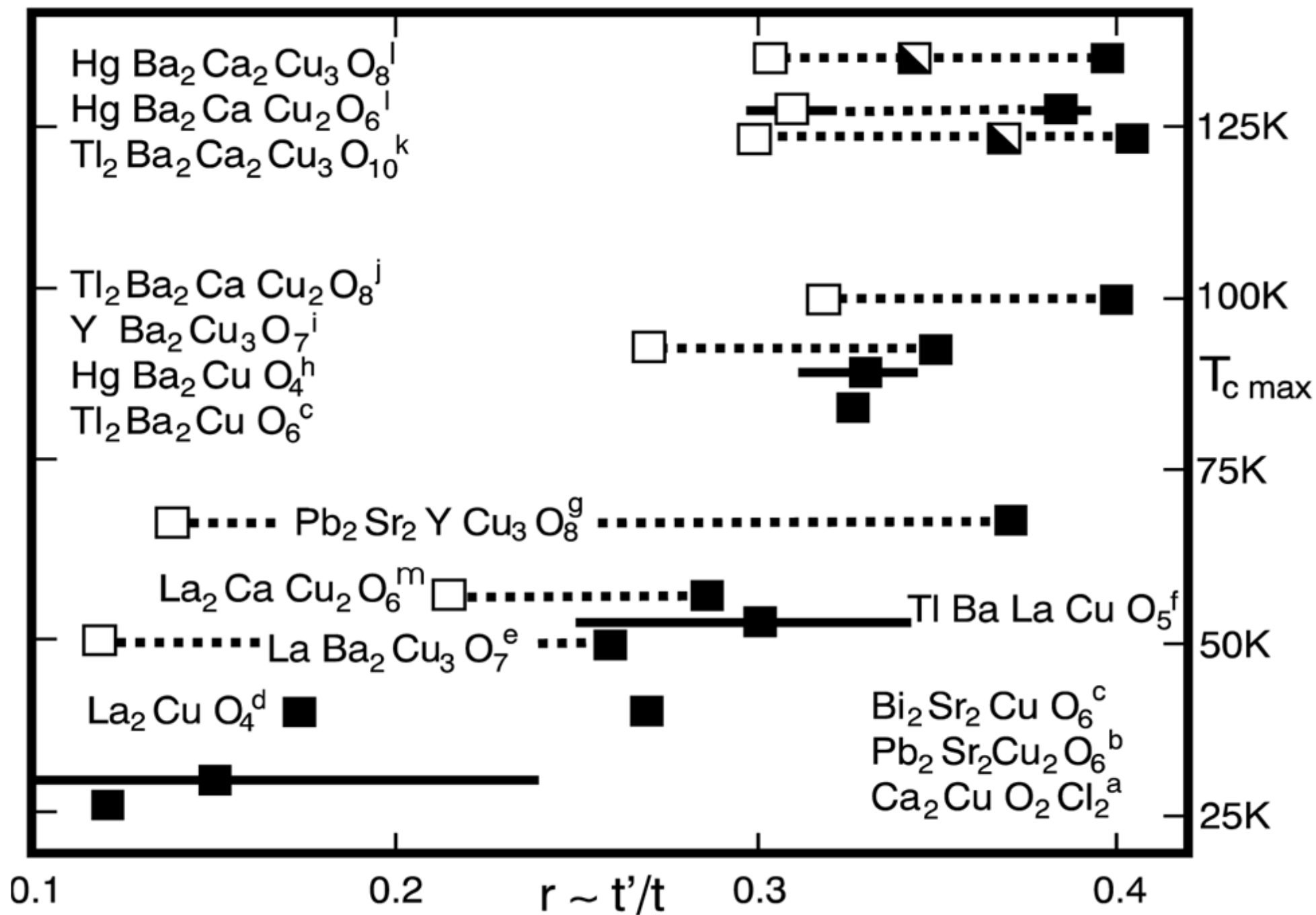
$\text{HgBa}_2\text{CaCu}_2\text{O}_6$



$\text{HgBa}_2\text{Ca}_2\text{Cu}_3\text{O}_8$

One-orbital LDA Wannier-like function

The Materials Trend, PRL **87**, 047003 (2001)



That the axial orbital is the channel for coupling the CuO_2 layer to its surroundings is supported by the experimental observations that c -axis transport is strongly suppressed by the opening of a pseudogap with a $(\cos k_x - \cos k_y)^2$ -dependence and that the scattering in the normal state has a similar k_{\parallel} -dependence.

At the same time, the axial orbital is the vehicle for coupling *between* neighboring oxygens *inside* the layer. It therefore seems plausible that contraction of the axial orbital around the CuO_2 -layer, away from the non-stoichiometric layers, will strengthen the phase coherence and thus increase $T_{c \text{ max}}$.

It was completely unexpected that for multi-layer materials, the $T_{c \text{ max}}$ trend is followed the Fermi-surface sheet with the largest r -value, i.e. with the lowest ϵ_{axial} and, hence, with the smallest hole volume.

How r determines $T_{c \text{ max}}$ remains to be understood.

Computations for **materials** with strong electronic correlations:

Current approximations to ab initio Density-Functional Theory (LDA) are insufficient for conduction bands with strong electronic correlations, e.g. they do not account for the Mott metal-insulator transition.

On the other hand, LDA Fermi surfaces are accurate for **most metals**, including overdoped high-temperature superconductors.

Presently, we therefore start with the **LDA**.

For the few correlated bands, we then construct **localized Wannier orbitals** and a corresponding **low-energy Hubbard Hamiltonian**.

The latter is solved in the Dynamical Mean-Field Approximation.

Low-energy multiband Hubbard Hamiltonian

$$\hat{H} = \sum_{im\sigma, i'm'\sigma'} \delta_{\sigma, \sigma'} h_{im, i'm'} c_{im\sigma}^\dagger c_{i'm'\sigma'} + \frac{1}{2} \delta_{i, i'} \sum'_{imm'\sigma\sigma'} U_{imm'} \hat{n}_{im\sigma} \hat{n}_{im'\sigma'} - d.c.$$

$h_{im, i'm'}$ is the LDA one-electron part. For the two-electron, on- d -site term, we use:

$$\frac{1}{2} \sum_{m=1} \sum_{m'=1} \sum_{\sigma} \sum_{\sigma'} U_{imm'} \hat{n}_{im\sigma} \hat{n}_{im'\sigma'} \approx$$

$$U_i \sum_m \hat{n}_{im\uparrow} \hat{n}_{im\downarrow} +$$

$$(U_i - 2J_i) \sum_m \sum_{m' \neq m} \hat{n}_{im\uparrow} \hat{n}_{im'\downarrow} +$$

$$(U_i - 3J_i) \sum_m \sum_{m' > m} \left(\hat{n}_{im\uparrow} \hat{n}_{im'\uparrow} + \hat{n}_{im\downarrow} \hat{n}_{im'\downarrow} \right)$$

for two electrons in
same orbital

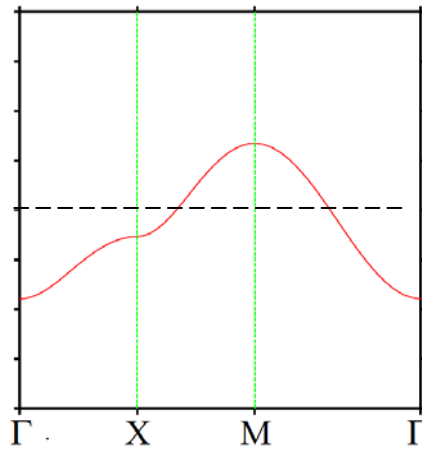
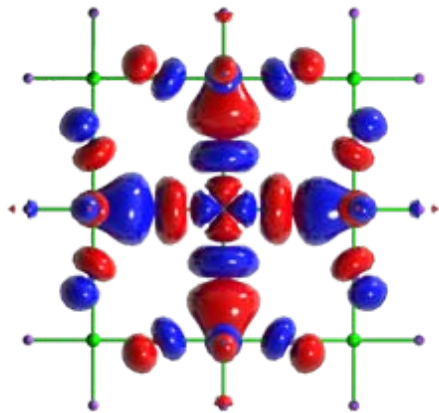
different orbitals and spins

same spin

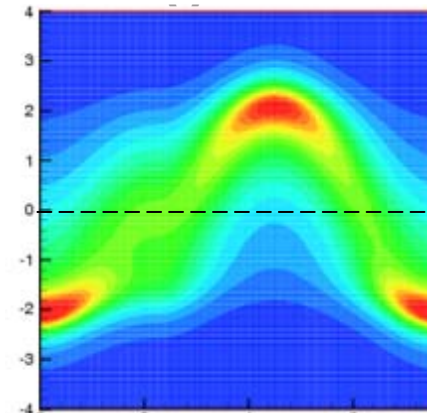
Mott transition in cuprate HTSCs

Wannier orbitals and
conduction band, LDA

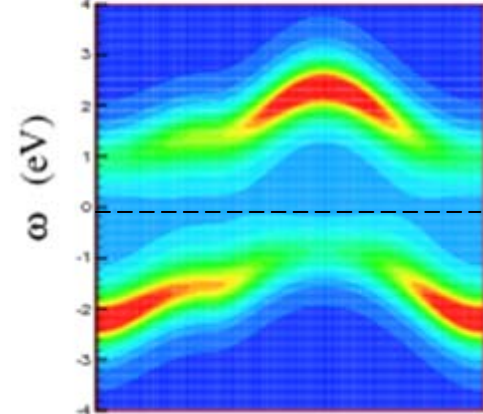
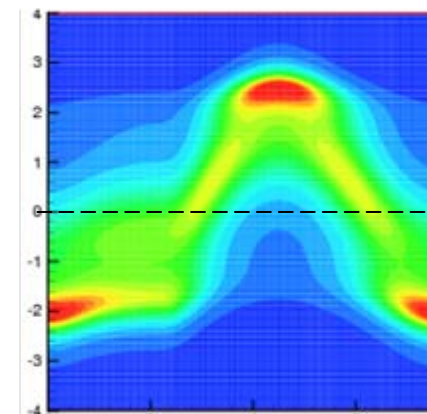
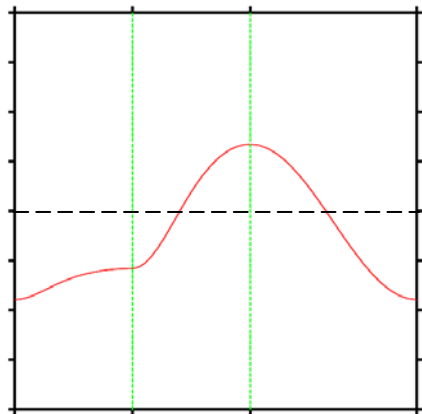
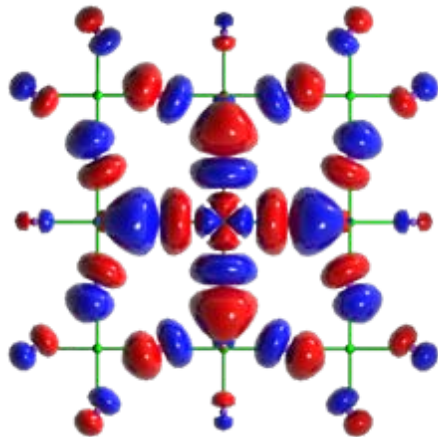
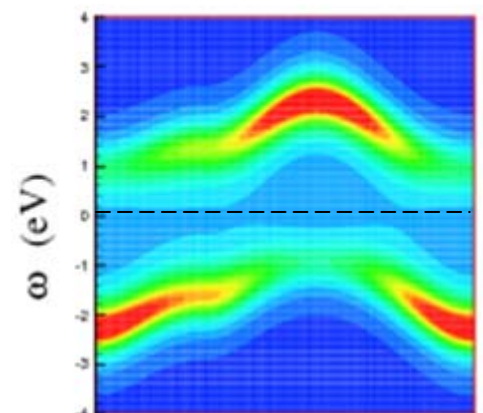
Hubbard model, LDA+DMFT
 $T=2000\text{K}$, undoped



$U = 2.1$

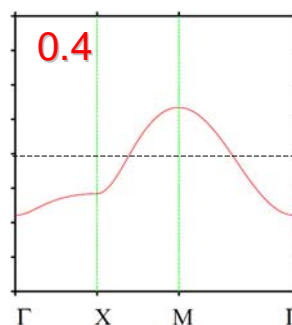
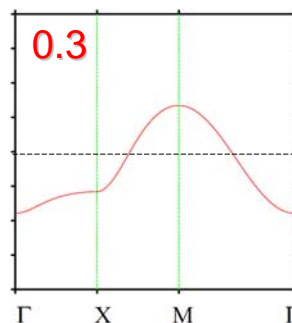
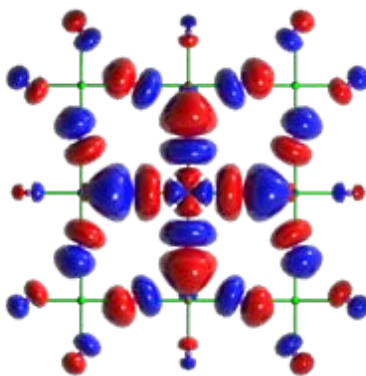
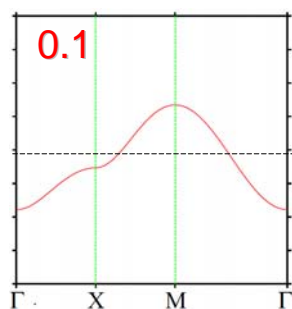
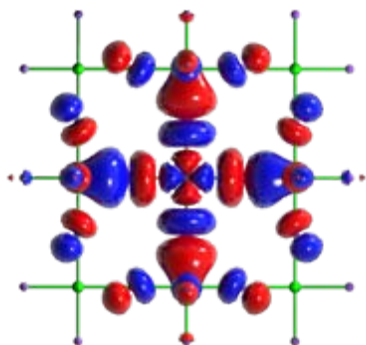
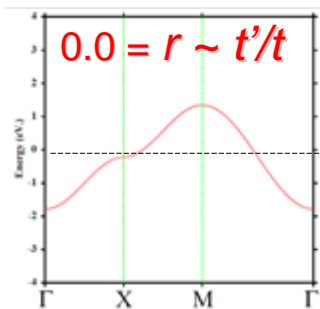


$U = 3.0 \text{ eV}$



Cuprates $3d^{9-x} = 3d_{x^2-y^2}^{1-x}$

Conduction band LDA



T. Saha-Dasgupta
and OKA 2002

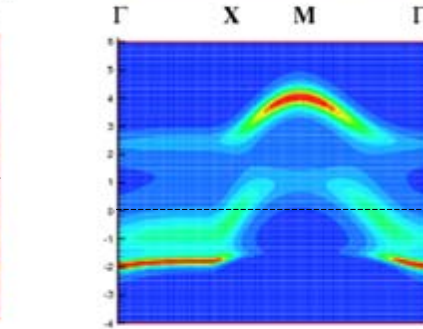
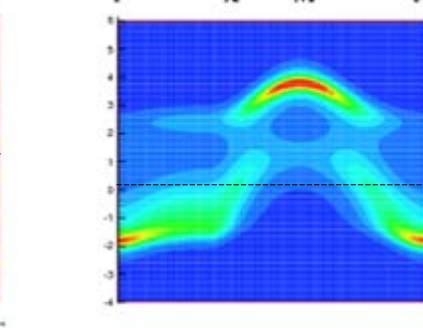
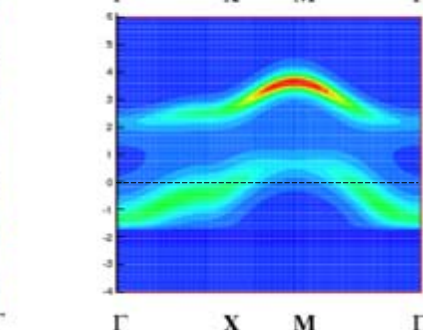
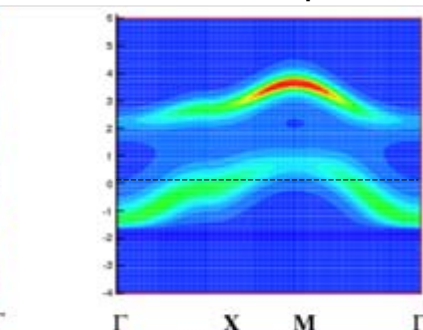
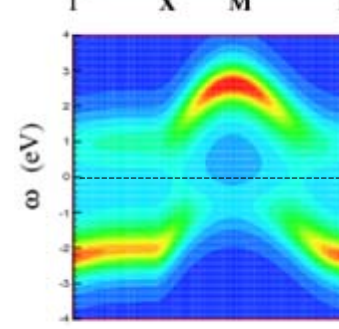
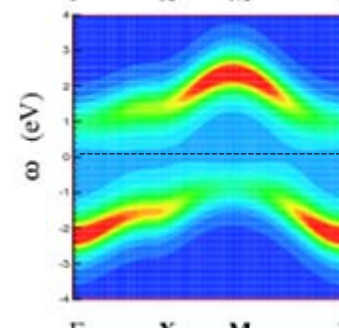
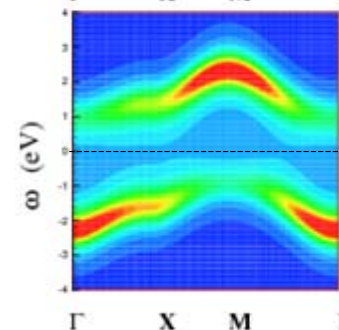
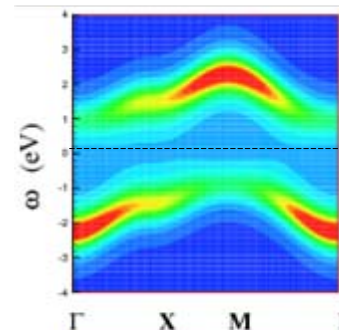
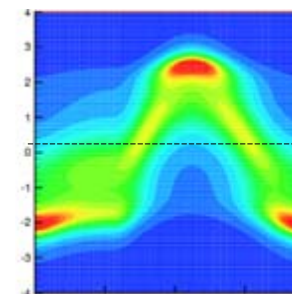
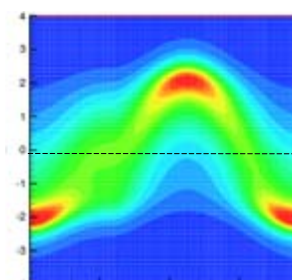
One-band Hubbard model LDA+DMFT

$U = 2.1$ eV
undoped

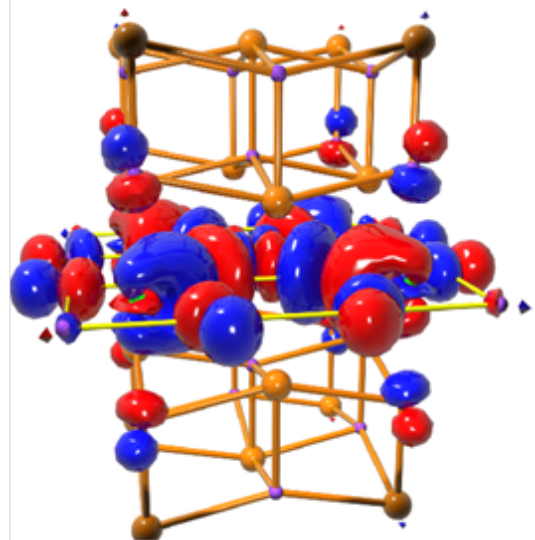
$U = 3.0$ eV

undoped

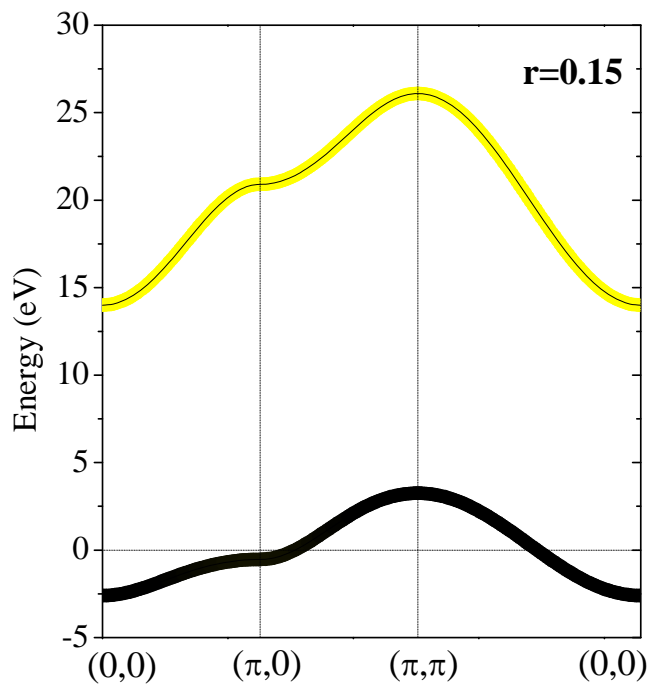
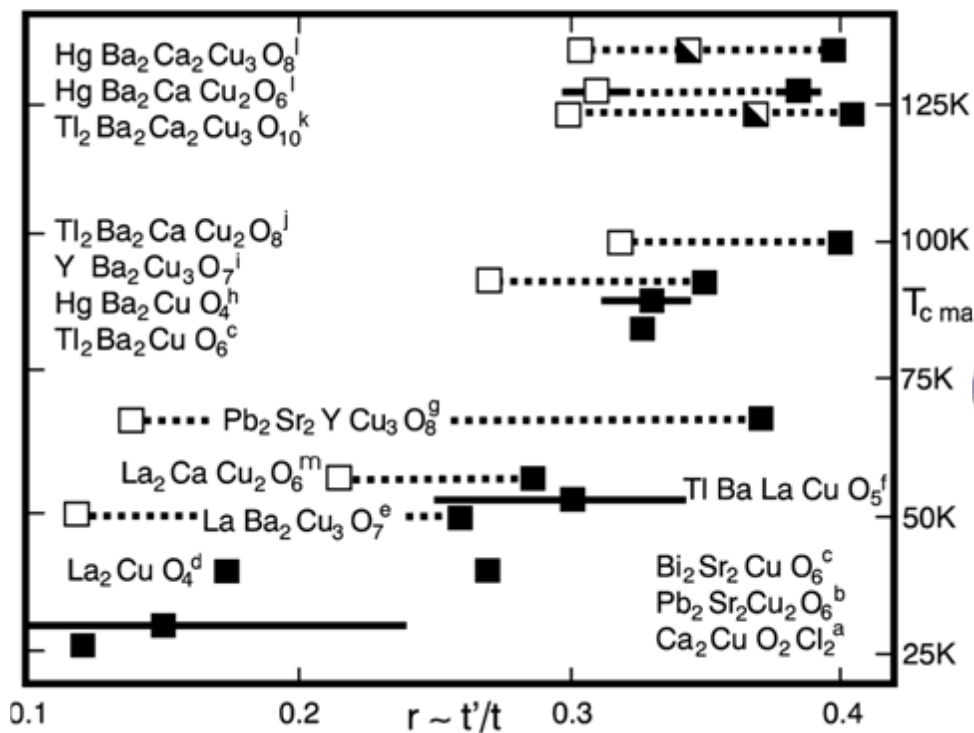
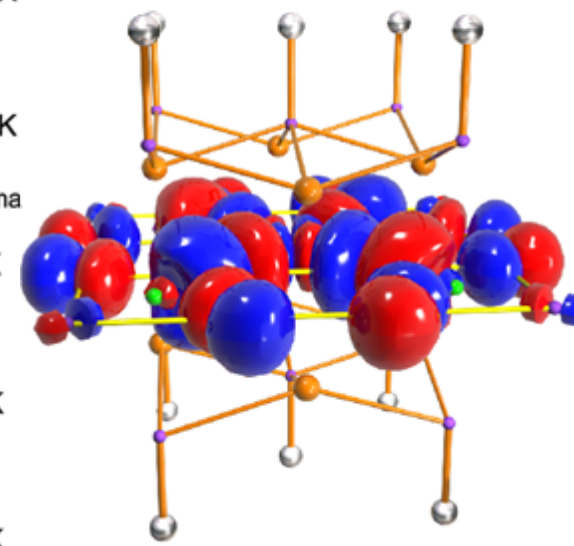
10% doped



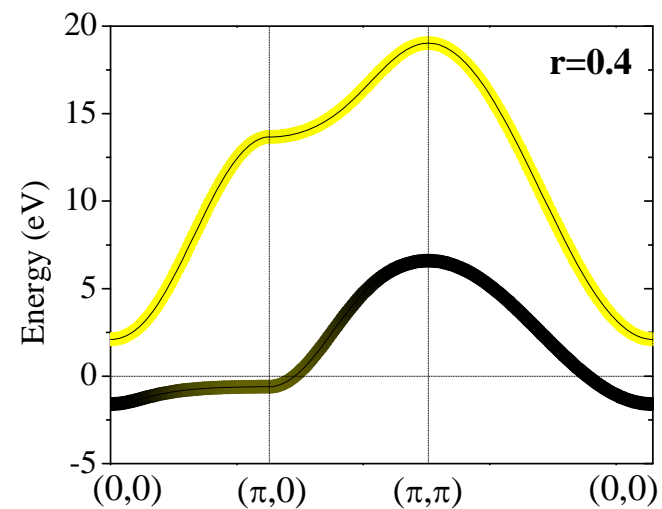
La₂CuO₄



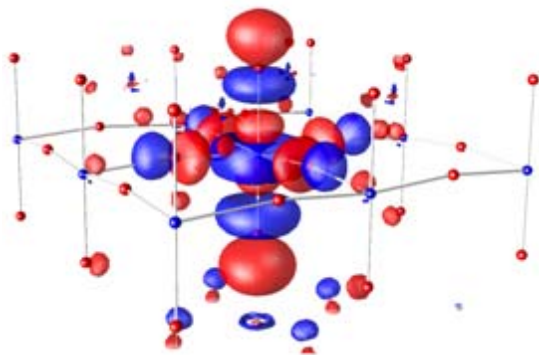
HgBa₂CuO₄



**Axial 4s-like orbital
and x^2-y^2**



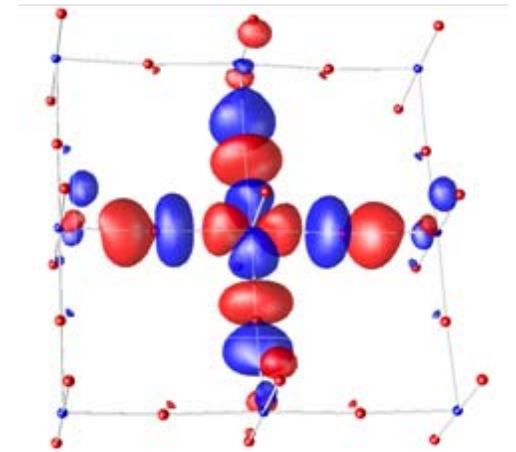
How to make a cuprate Fermi surface out of a nickelate heterostructure, in theory



$3z^2-1$

$3d^7 (e_g^1)$

x^2-y^2



**X. Yang¹, P. Hansmann²,
A. Toschi², K. Held²,
G. Khaliullin¹, O.K. Andersen¹**

¹ Max-Planck-Institut für Festkörperforschung, Stuttgart

² Institute for Solid State Physics, Vienna University of
Technology

Khaliullin's idea:

Make $\text{Ni}^{3+}(\text{d}^7)$ -based HTSCs by sandwiching hole doped LaO-NiO_2 layers between insulating layers through heterostructuring (orbital engineering)

- The confinement together with the electronic correlations should make it possible to localize or empty the $3z^2-1$ band thus leaving the conduction electron in the x^2-y^2 band
- If the $3z^2-1$ orbital can be manipulated to lie *above* x^2-y^2 , it might play the role of the axial orbital in the cuprate d^9 HTSCs
- Charge disproportionation (d^6+d^8) must be avoided

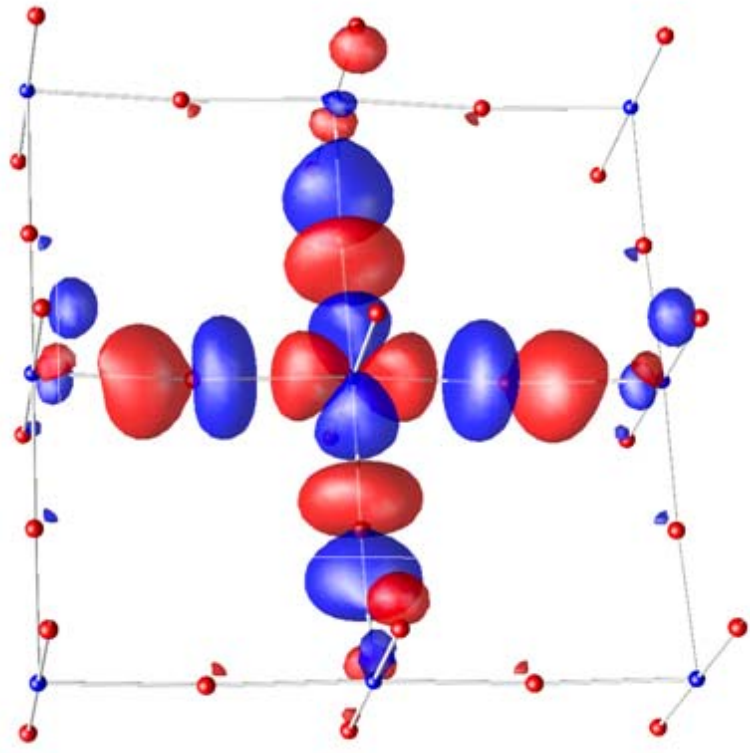
J. Chaloupka and G. Khaliullin, PRL 100, 016404 (2008).

P. Hansmann, Xiaoping Yang, A. Toschi, G. Khaliullin, O.K. Andersen, and K. Held, PRL 103, 016401 (2009).

Nickellate

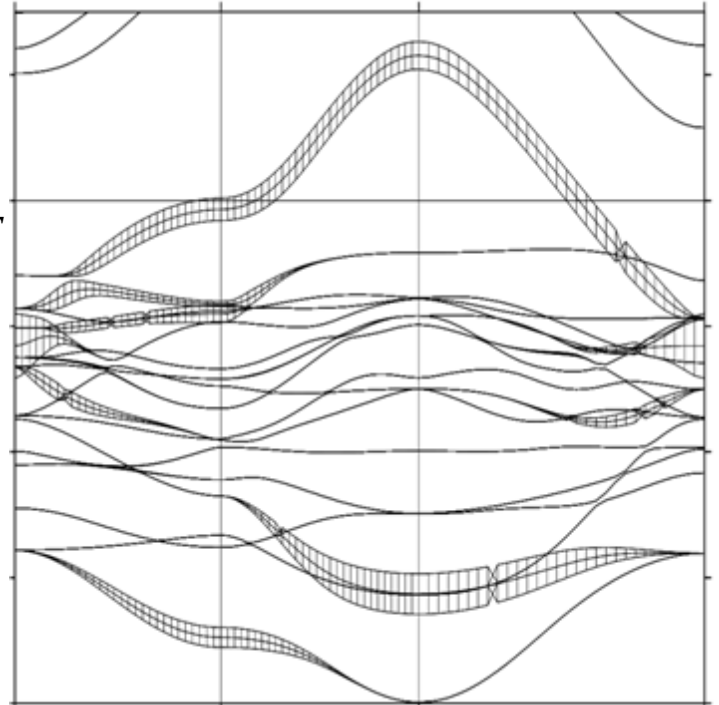
e_g orbitals

La_2CuO_4

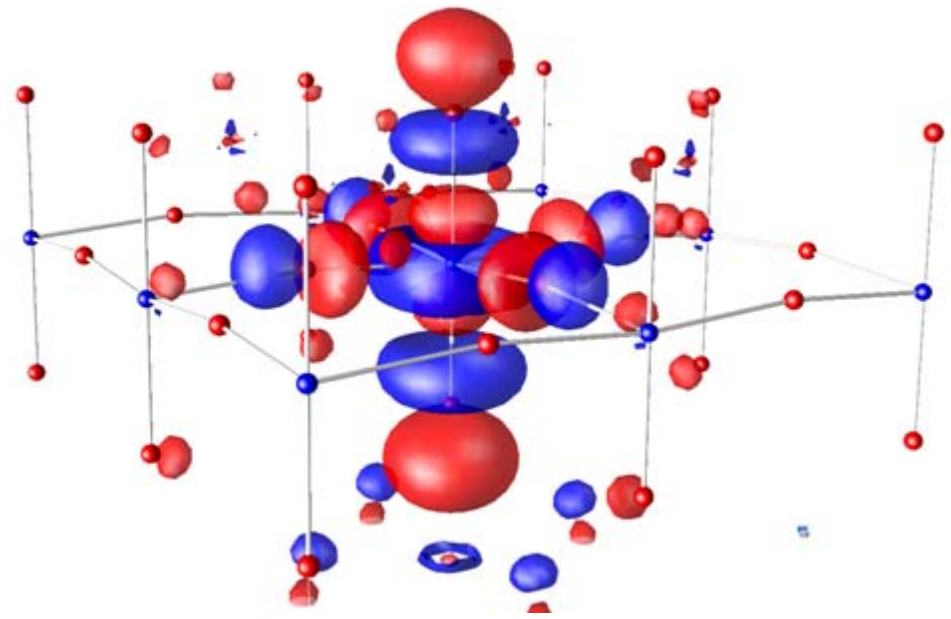


x^2-y^2

ϵ_F

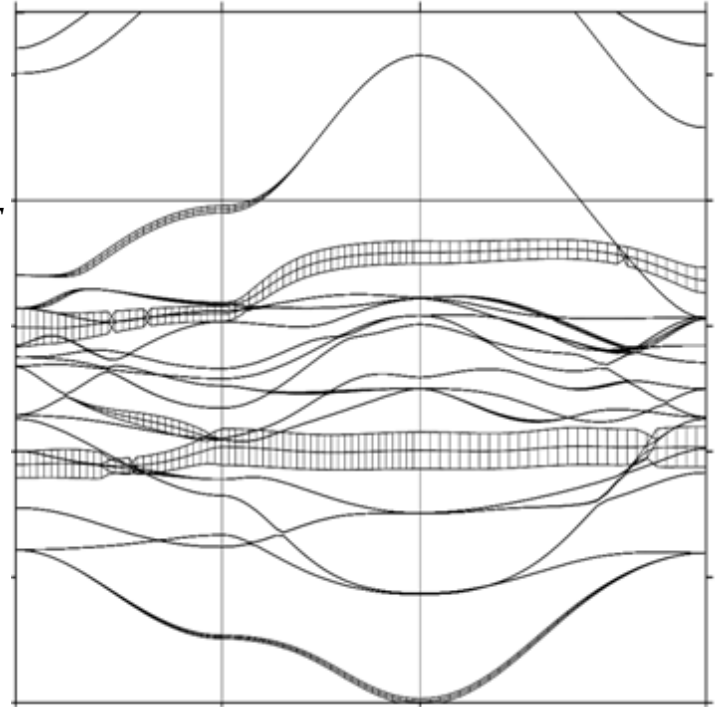


10 eV

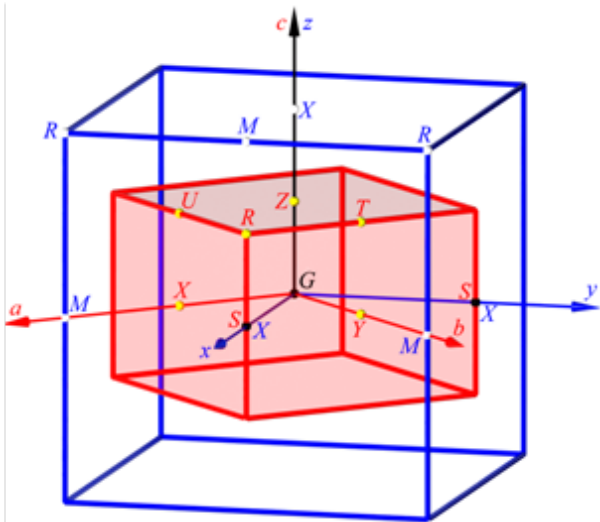


$3z^2-1$

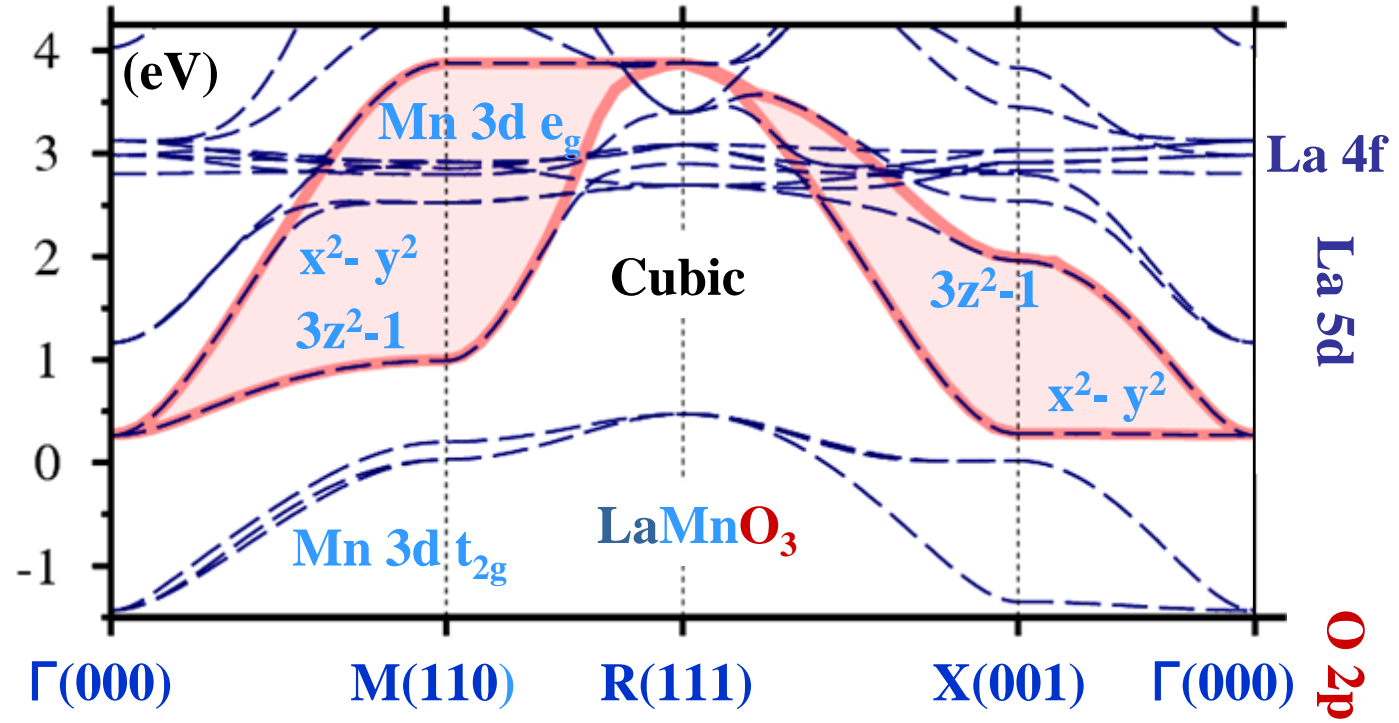
ϵ_F



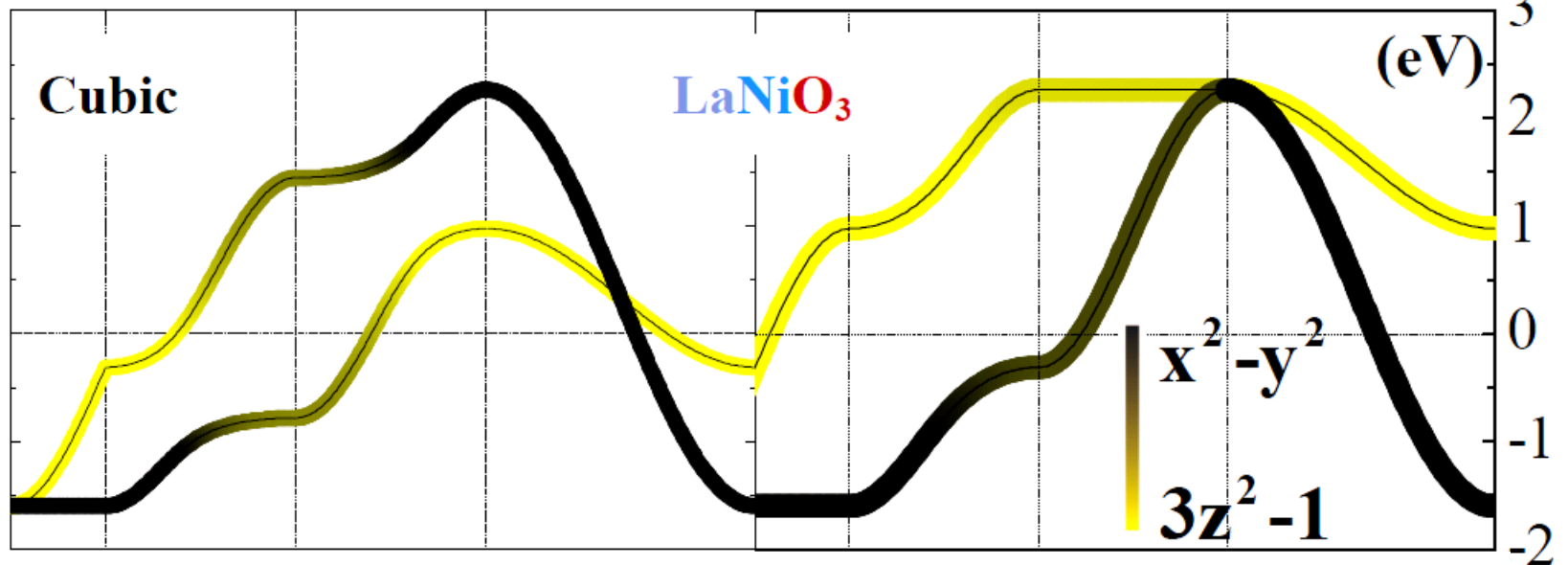
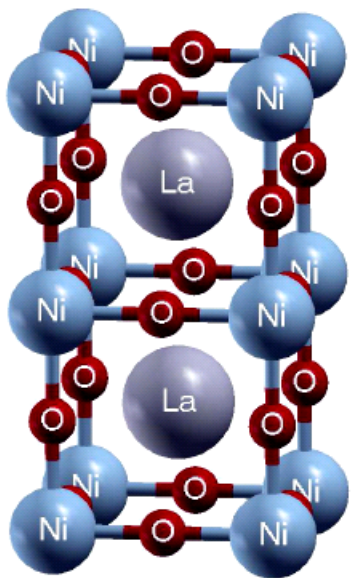
Confinement:



Paramagnetic LDA bands in (1 -1 0) plane

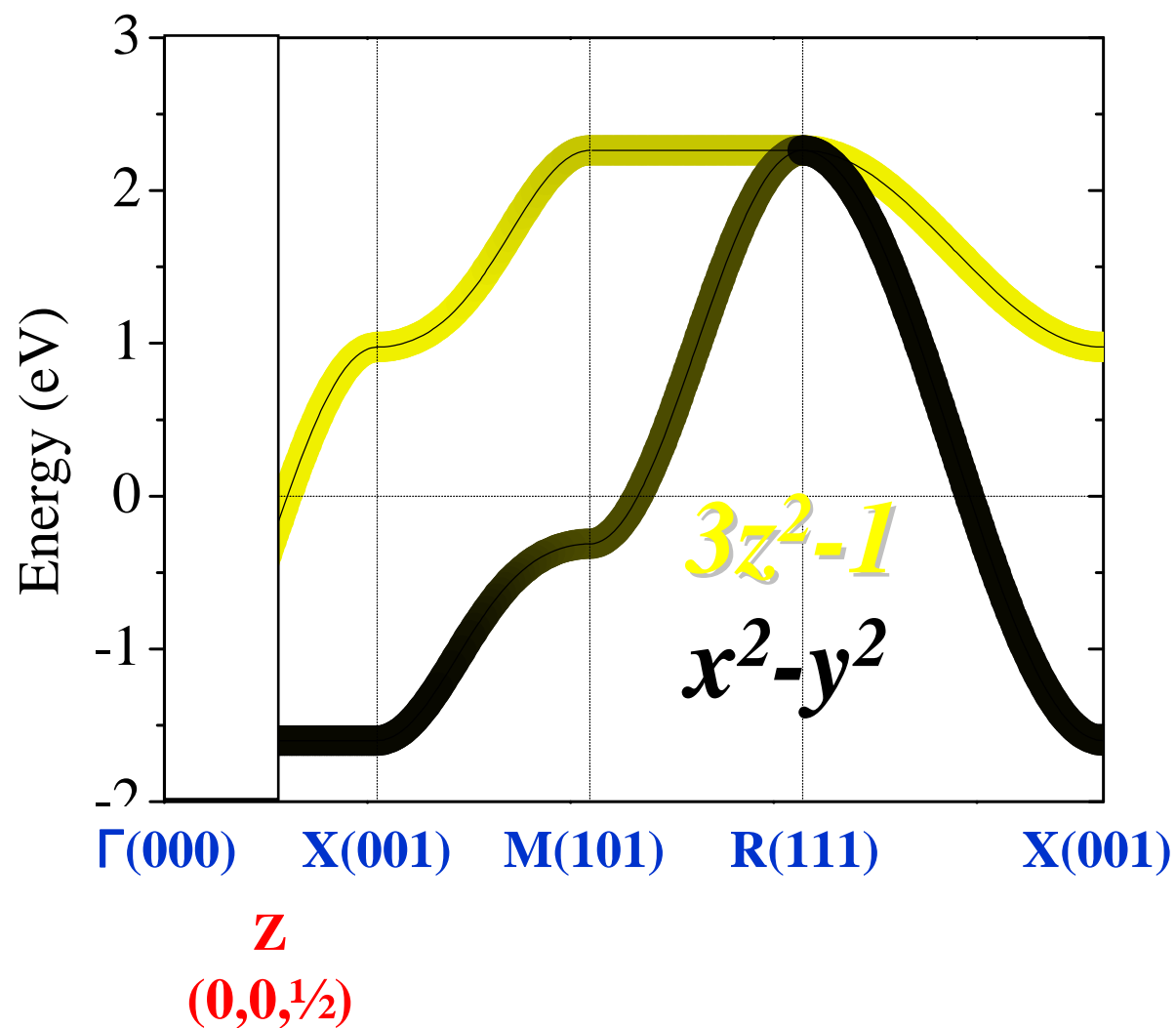
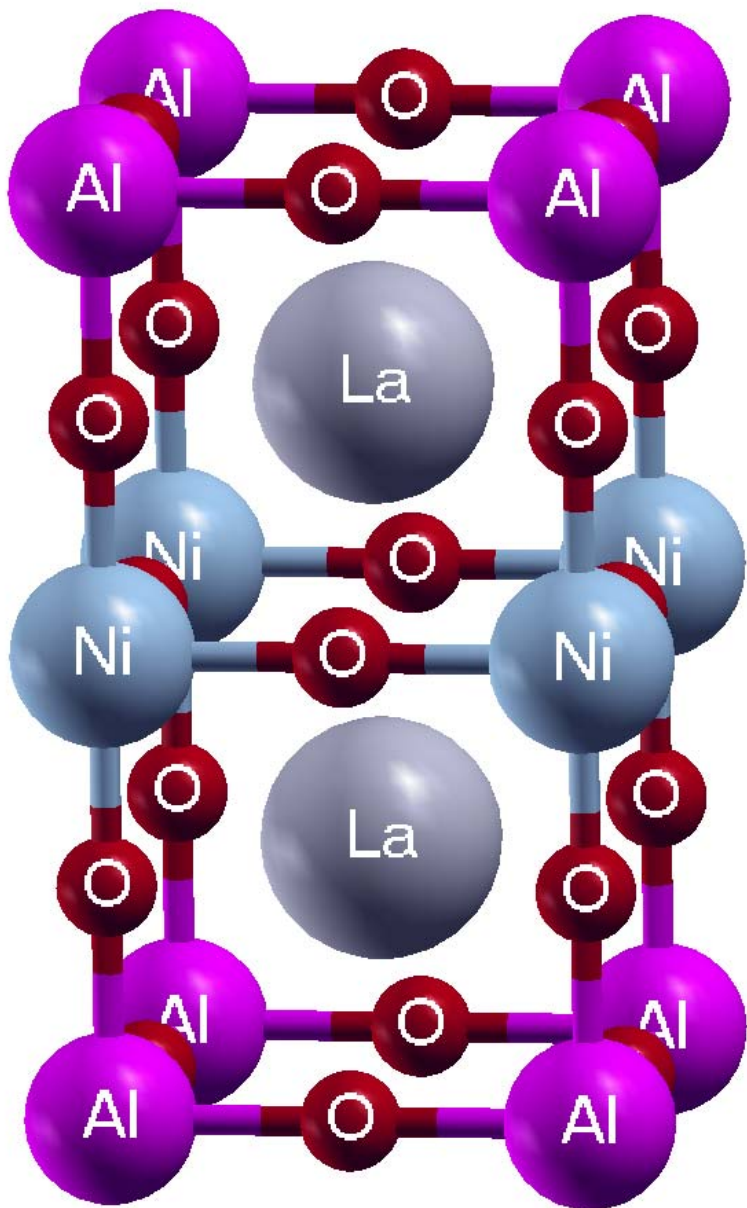


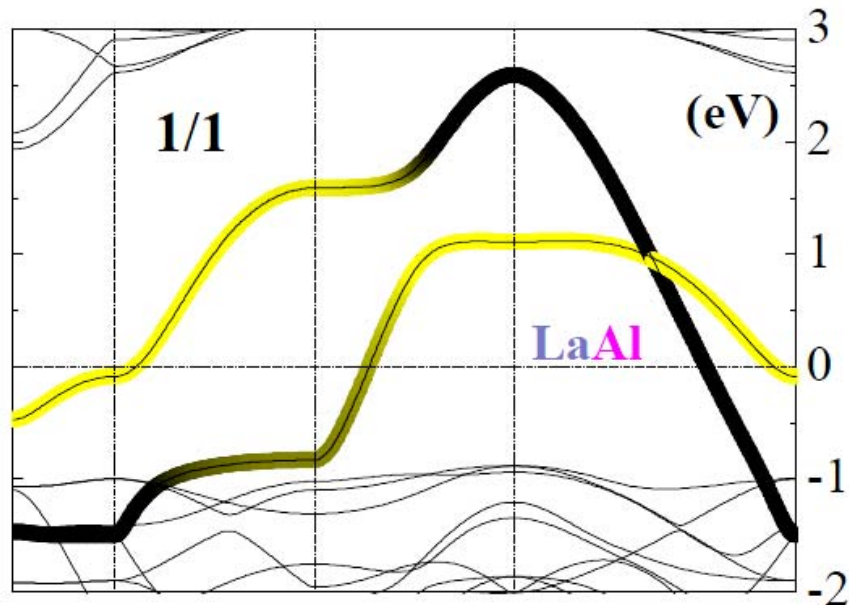
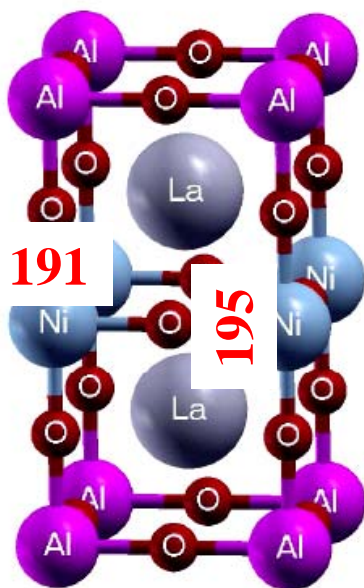
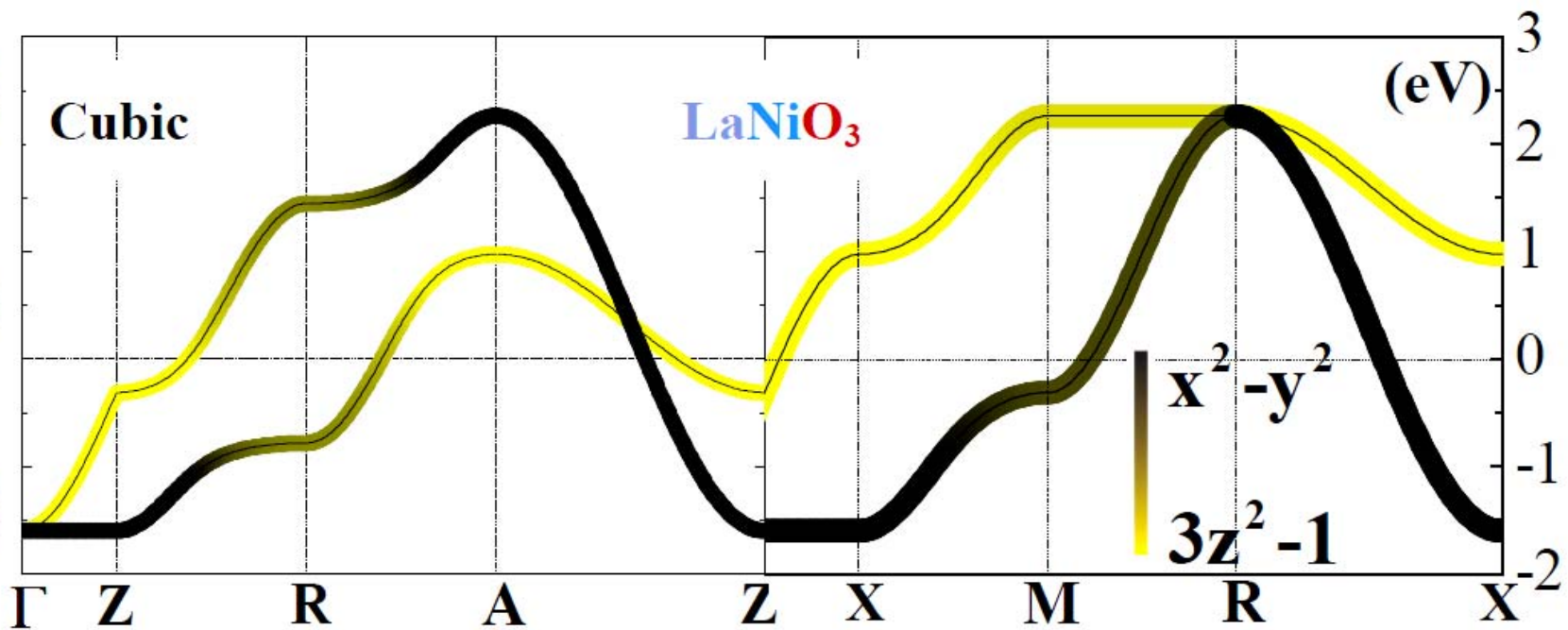
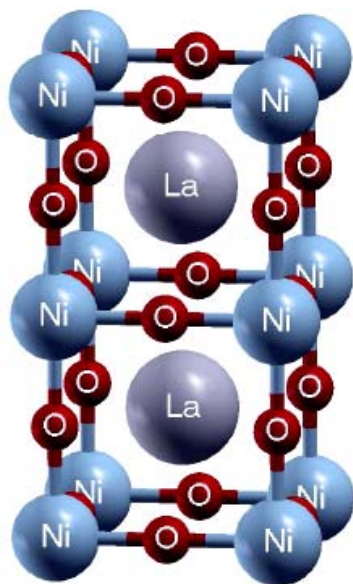
$\Gamma(000)$ $Z(00\frac{1}{2})$ $R(10\frac{1}{2})$ $A(11\frac{1}{2})$ $Z(00\frac{1}{2})$ $X(001)$ $M(101)$ $R(111)$ $X(001)$



d^7 nickelates

Simplified e_g conduction-band structure in 2D square lattice:





Ni 4s, La 5d, Al 3p

Ni t_{2g} , O 2p, Al 3s

LDA

LDA+DMFT

Undoped

$U = 6.7$ eV

$J = 0.7$ eV,

$T = 1100$ K.

$0 < U < 6.4$ eV

two FS sheets.

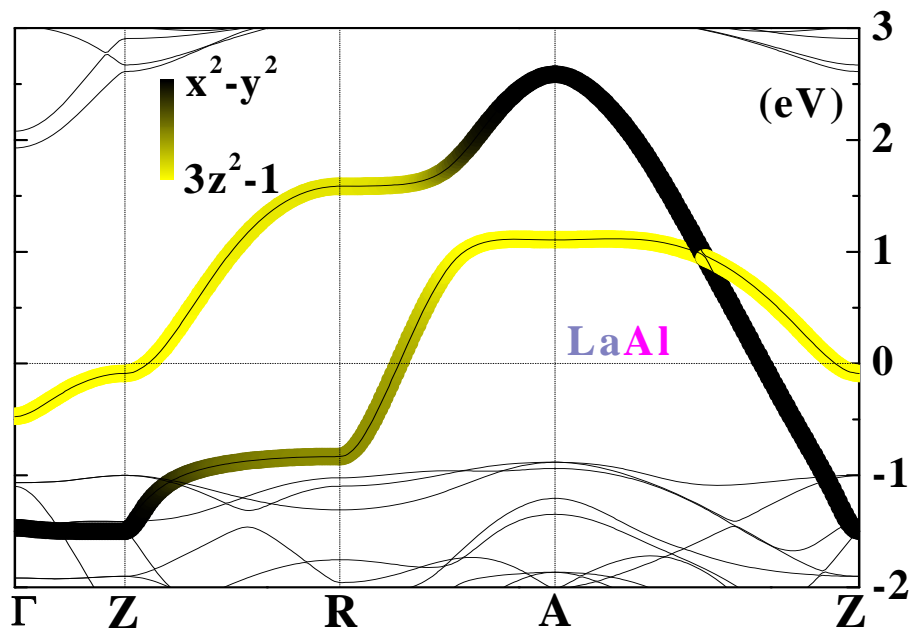
$6.4 < U < 7.4$

one FS sheet.

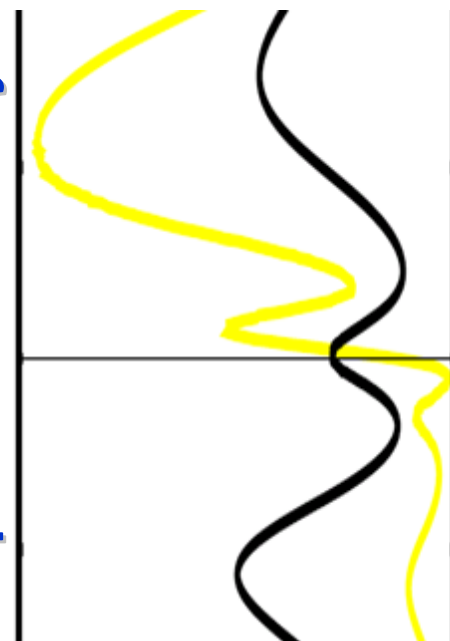
$7.4 < U$

no FS; Mott ins.

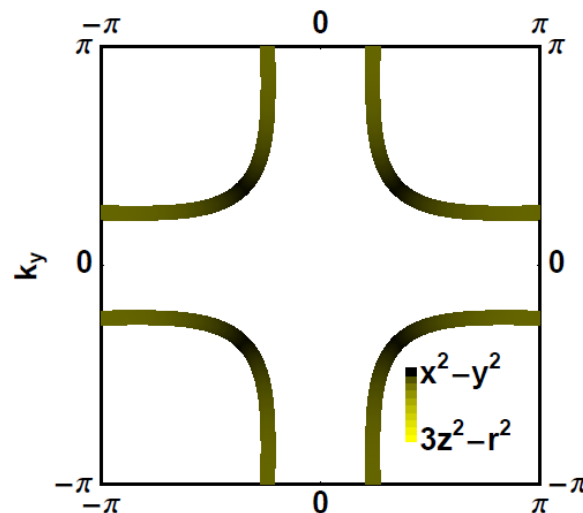
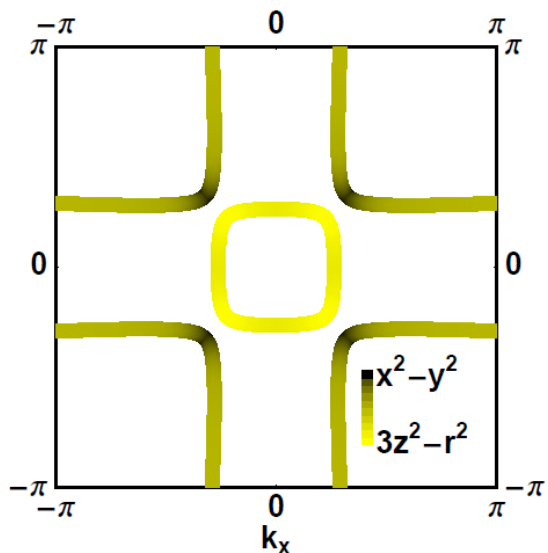
Band structure



Spectral-density



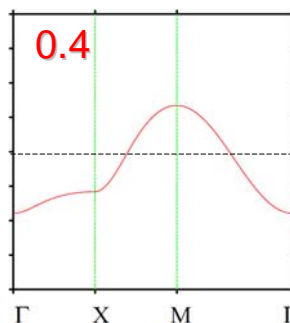
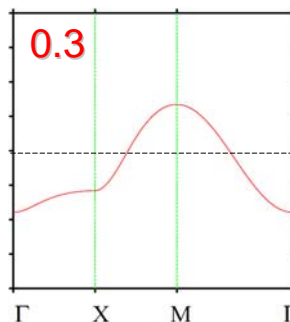
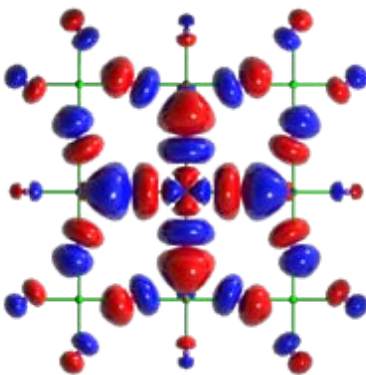
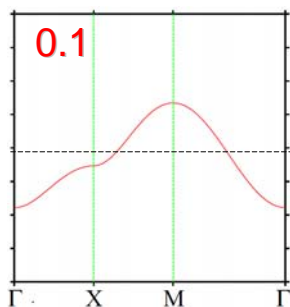
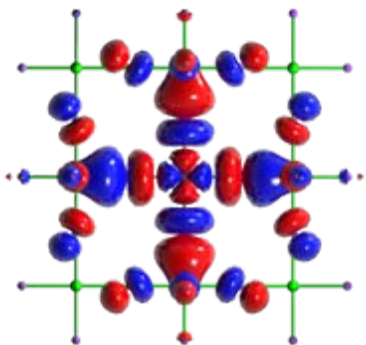
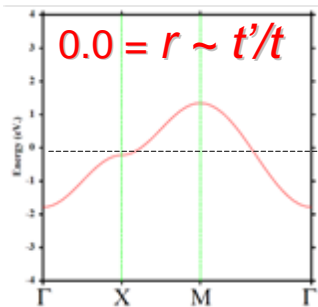
Fermi surface



The Coulomb correlations enhance the crystal-field splitting and simplifies the Fermi surface to **one** sheet when $\epsilon_{3z^2-1}(\Gamma) > \epsilon_F$, i.e. with a shape ($r \sim 1/2$), like that in the cuprates with the highest T_{cmax}

Cuprates $3d^{9-x} = 3d_{x^2-y^2}^{1-x}$

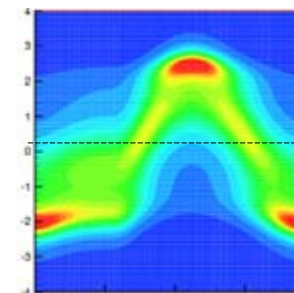
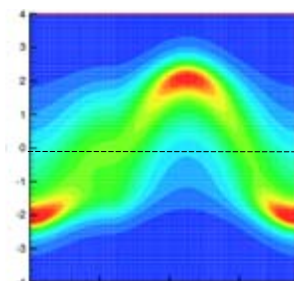
Conduction band LDA



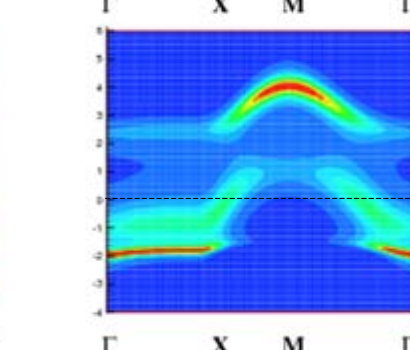
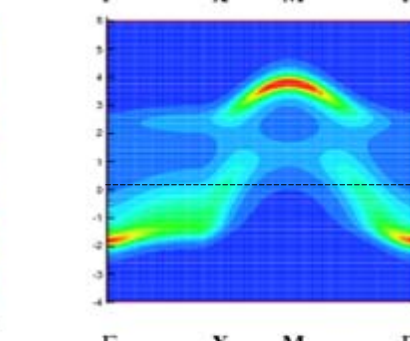
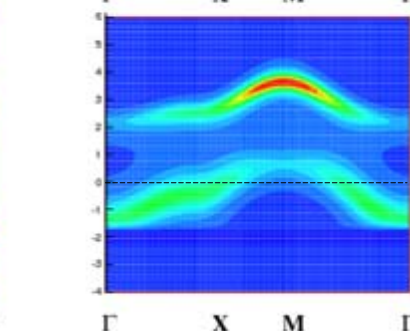
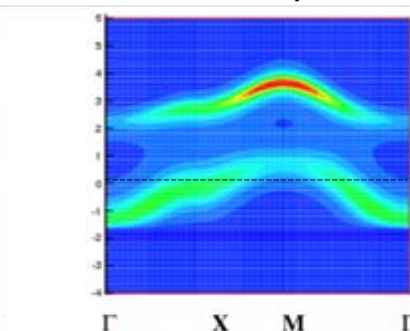
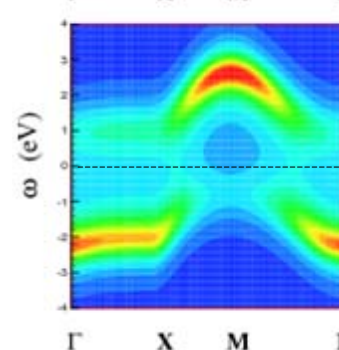
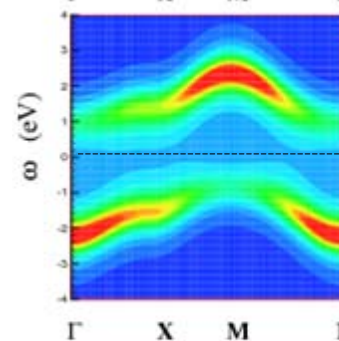
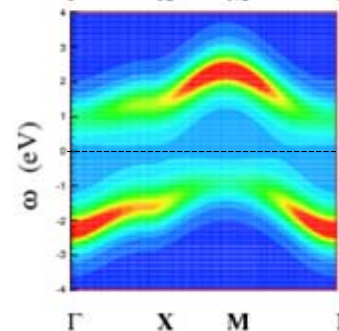
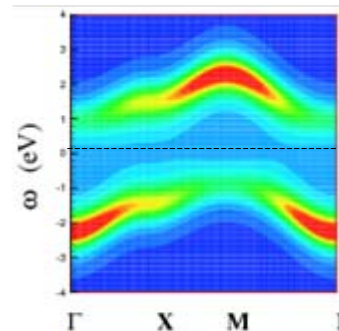
T. Saha-Dasgupta
and OKA 2002

One-band Hubbard model LDA+DMFT

$U = 2.1$ eV
undoped



$U = 3.0$ eV
undoped 10% doped



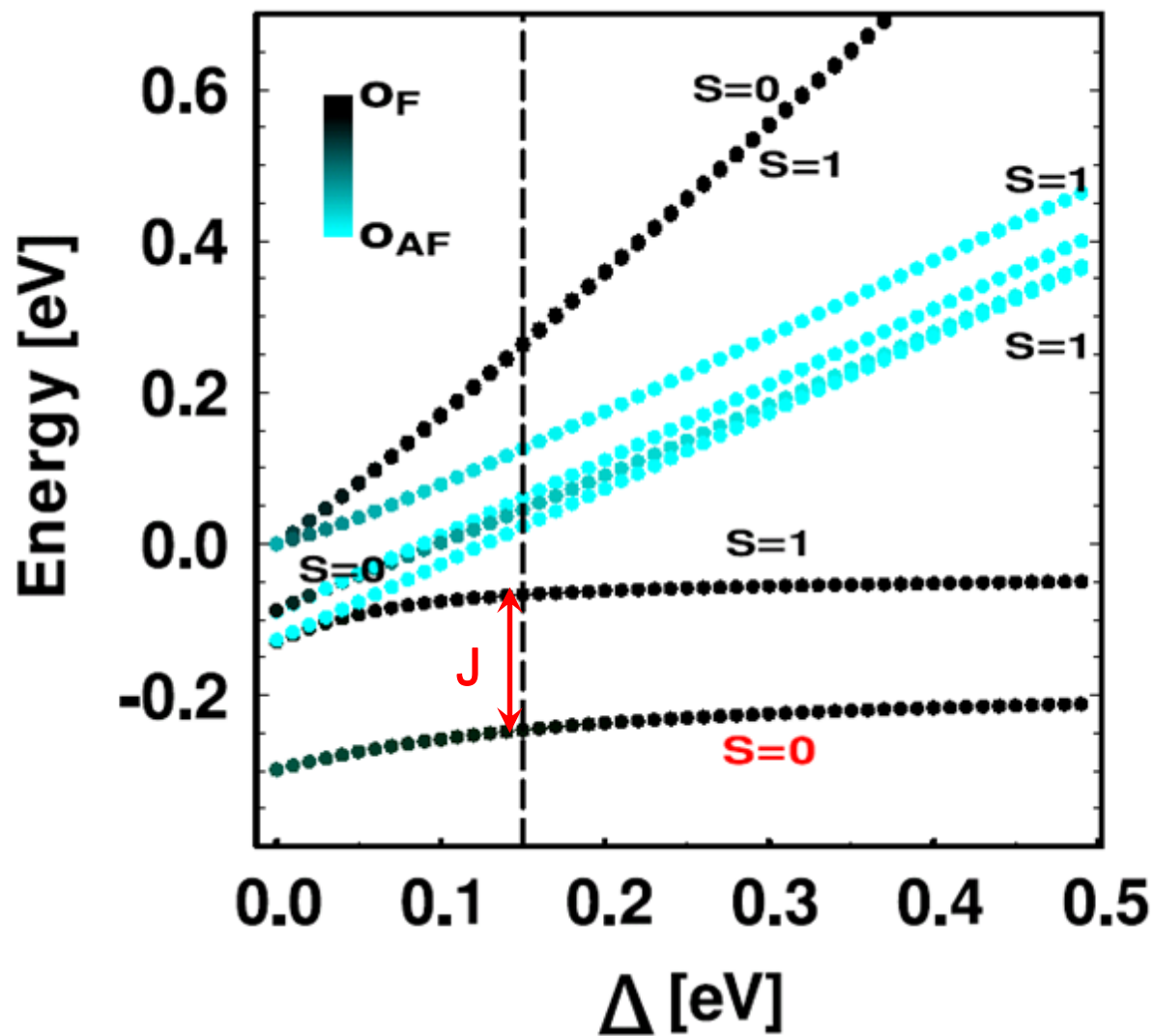
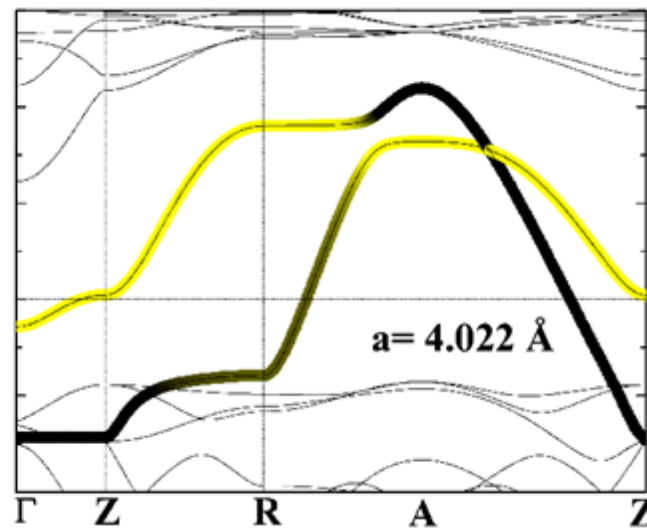
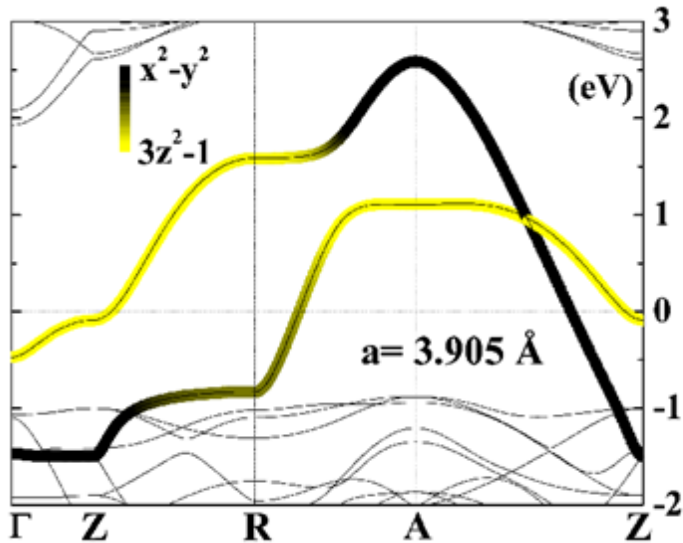
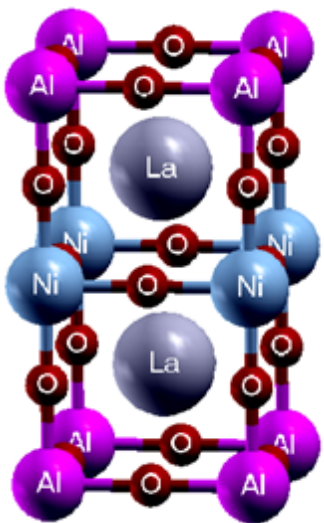
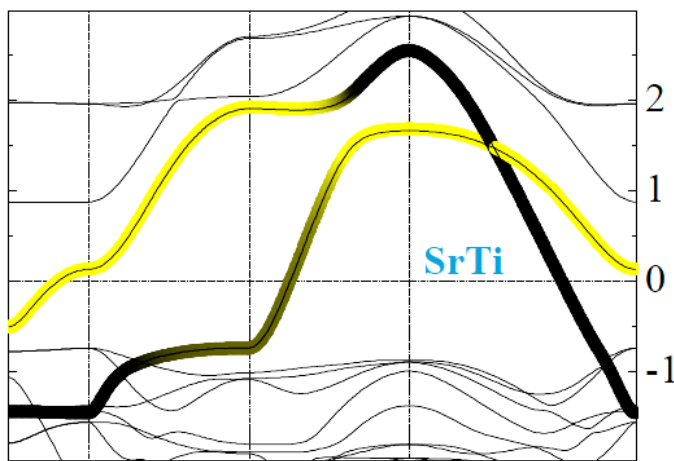
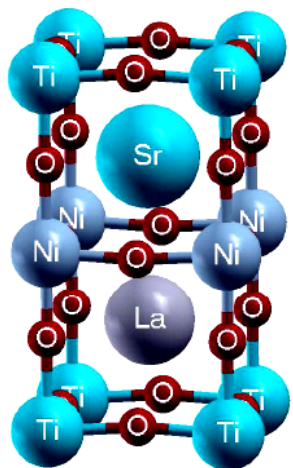


FIG. 3 (color online). Energy levels for the unstrained two-site model with $U = 6.4$ eV as a function of the splitting Δ between the energies of the $3z^2 - 1$ and $x^2 - y^2$ Wannier orbitals. The LDA value of Δ is indicated by the dashed line. O_F (O_{AF}) denotes a configuration with the same (different) orbital(s) on the two sites.

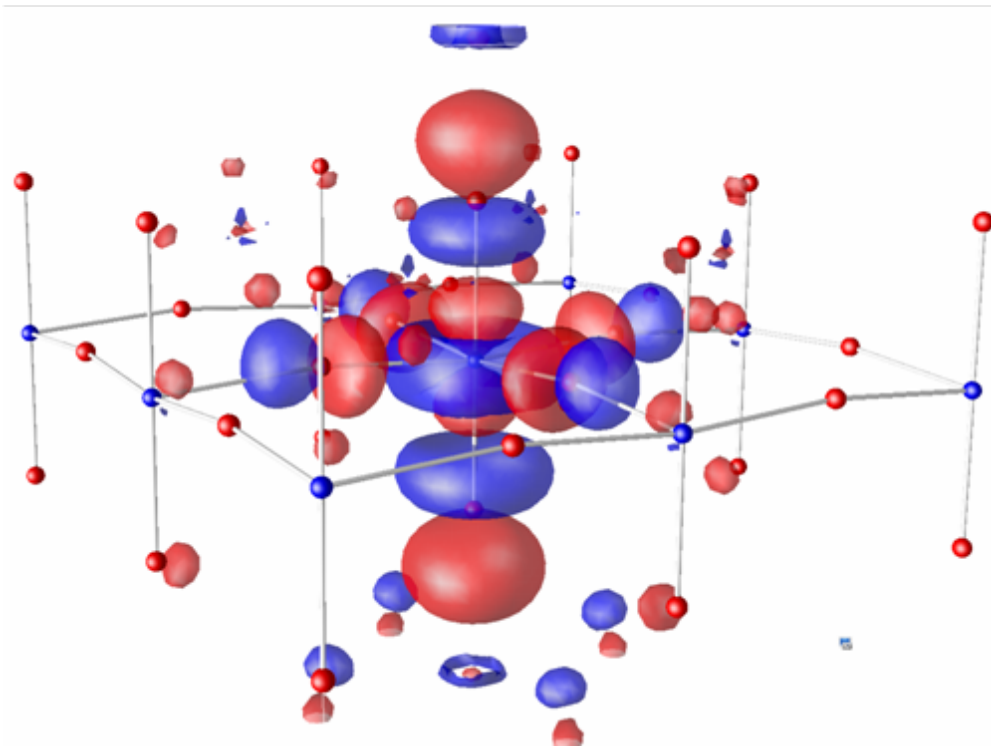
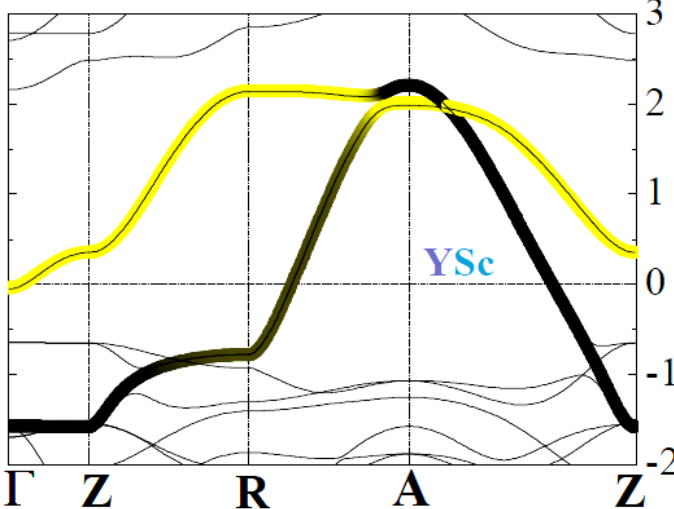
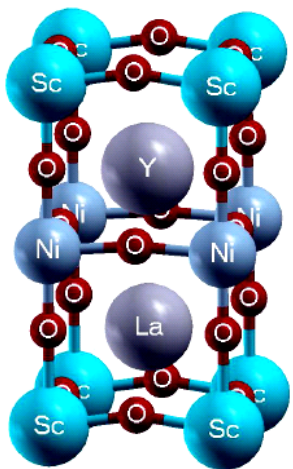


Control by lattice constant of the substrate

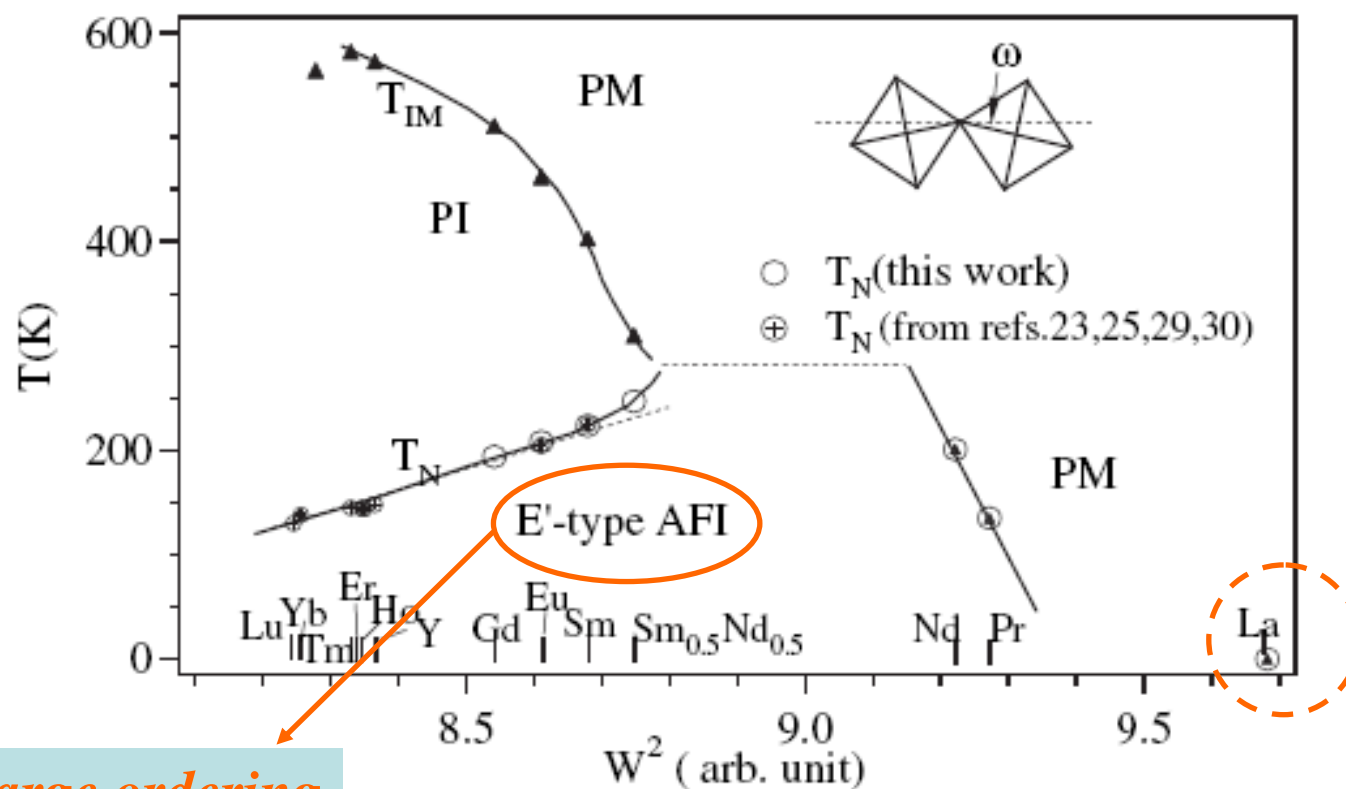
1-sheet FS:
 $5.7 < U < 6.5 \text{ eV}$



Control by the chemistry (Al, Ti, Sc) of the insulating layers



Phase diagram of **3D** RNiO₃ perovskites

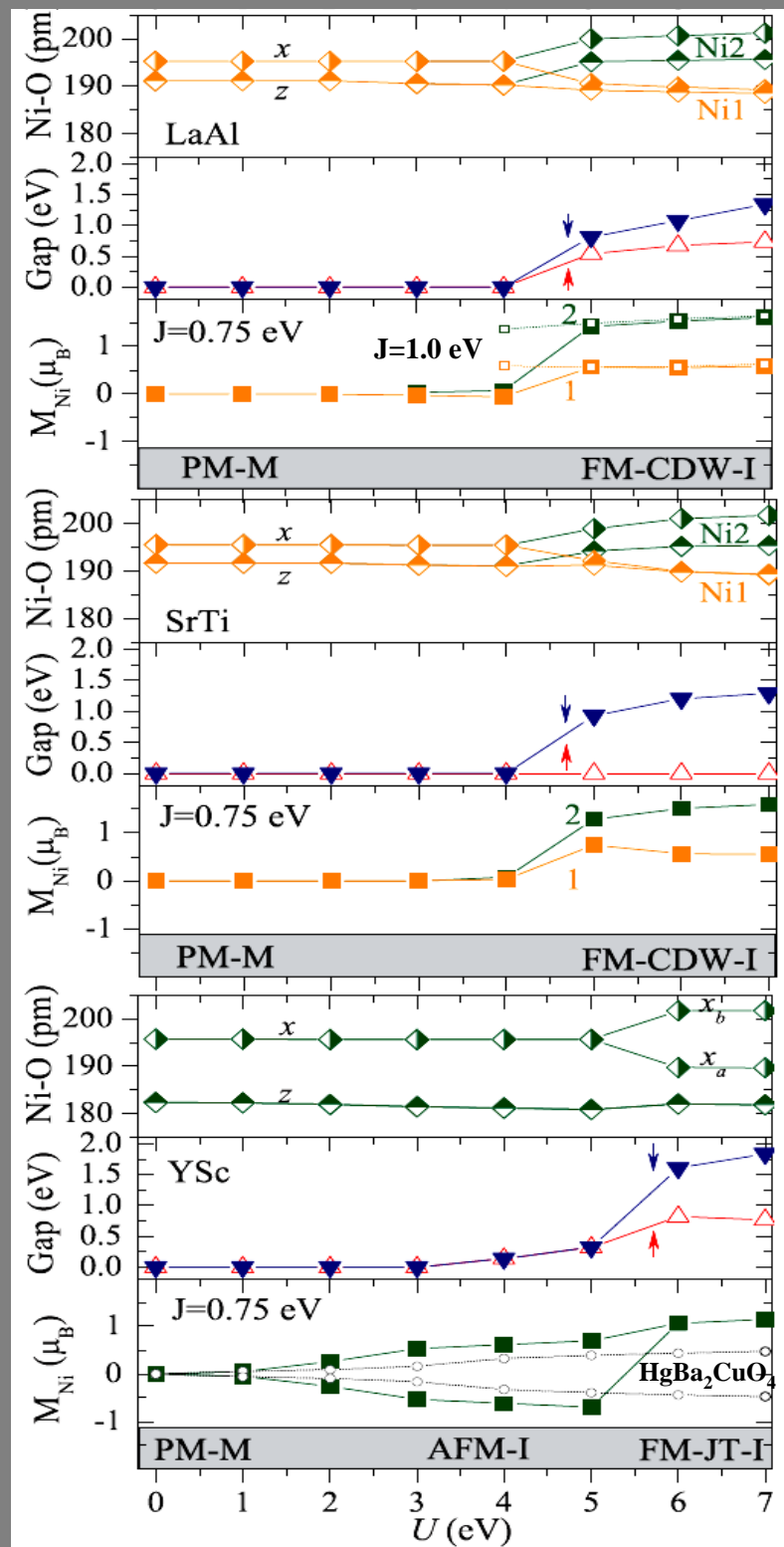
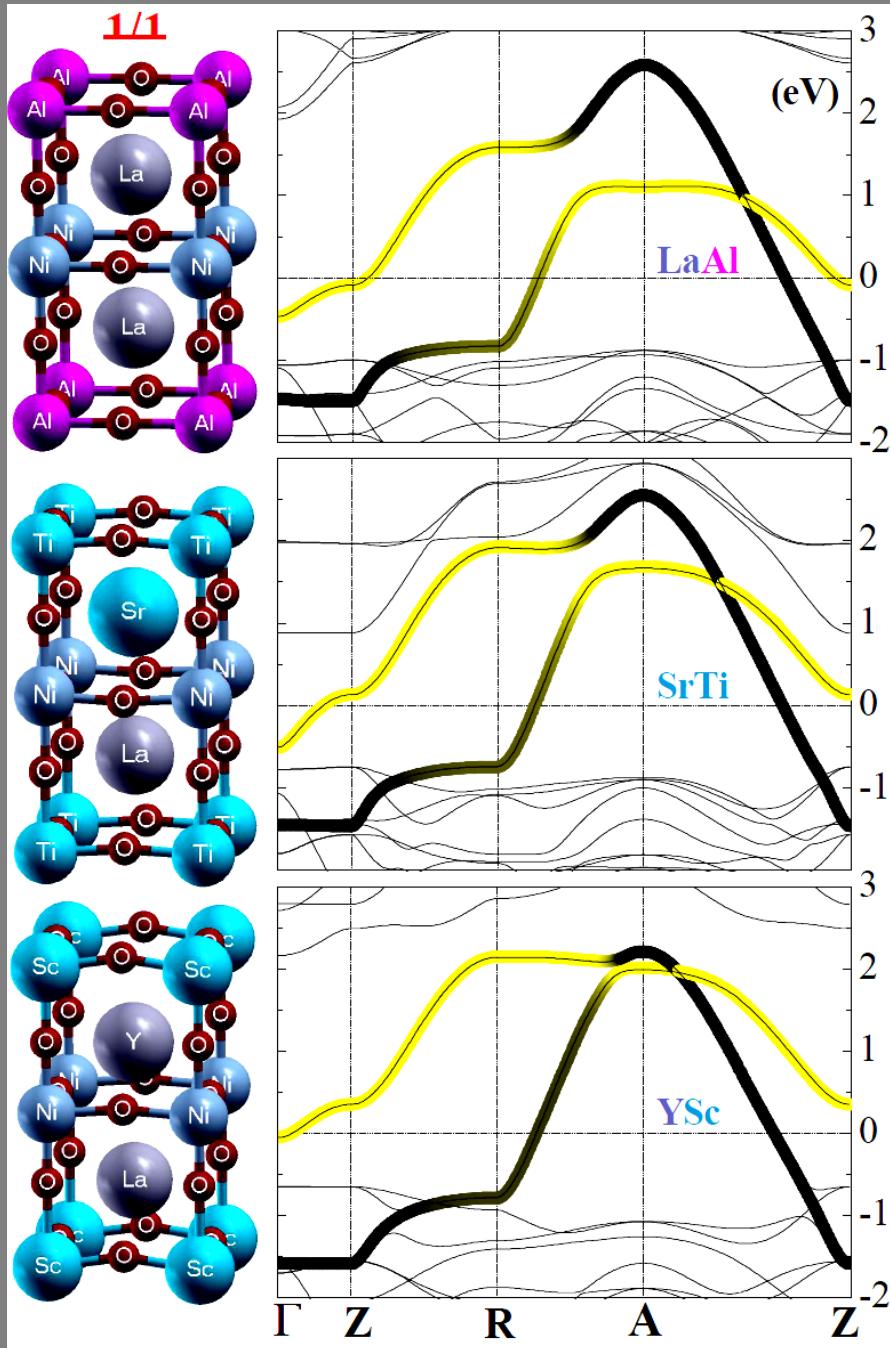


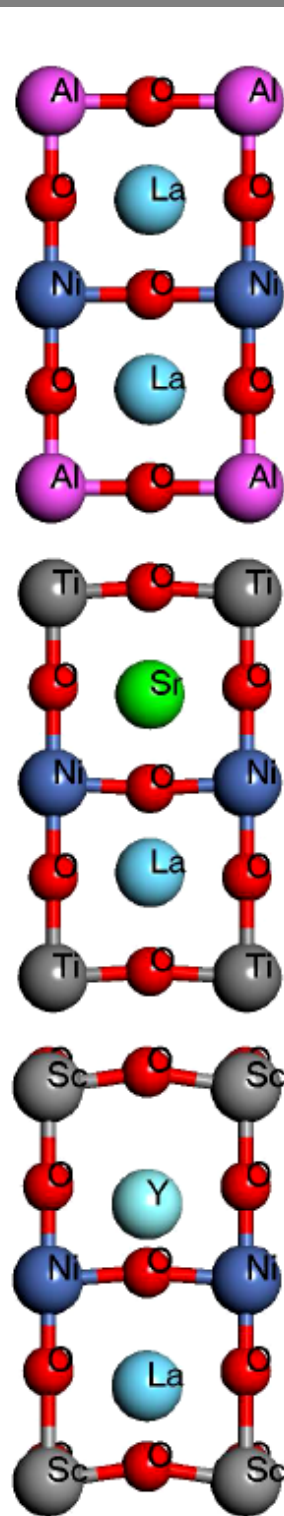
Charge ordering

FIG. 5. The phase diagram of transition temperatures vs bandwidth W^2 at room temperature. T_{IM} and T_N are taken from Refs. [23,25,29,30]. Lines inside the figure are guides to the eyes. Inset: definition of the angle ω used to obtain $W \sim \cos\omega / (\text{Ni-O})^{3.5}$.

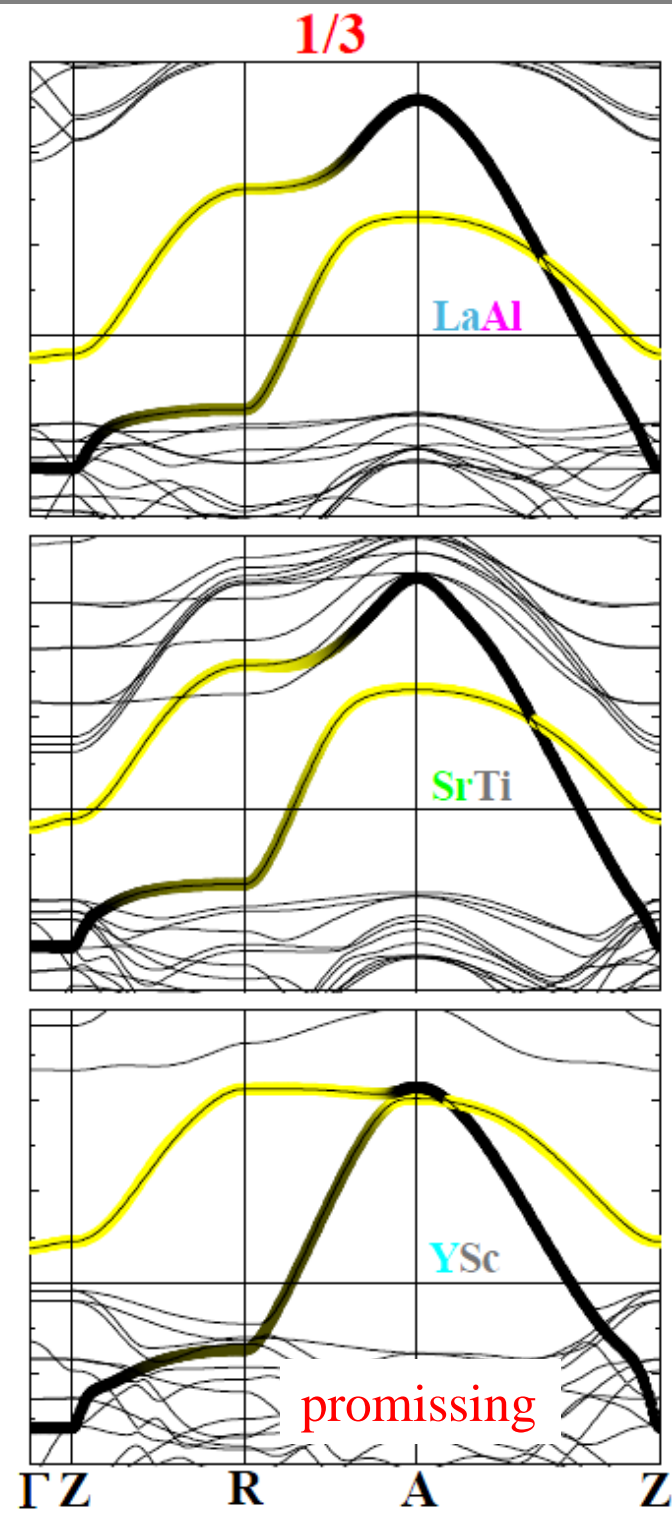
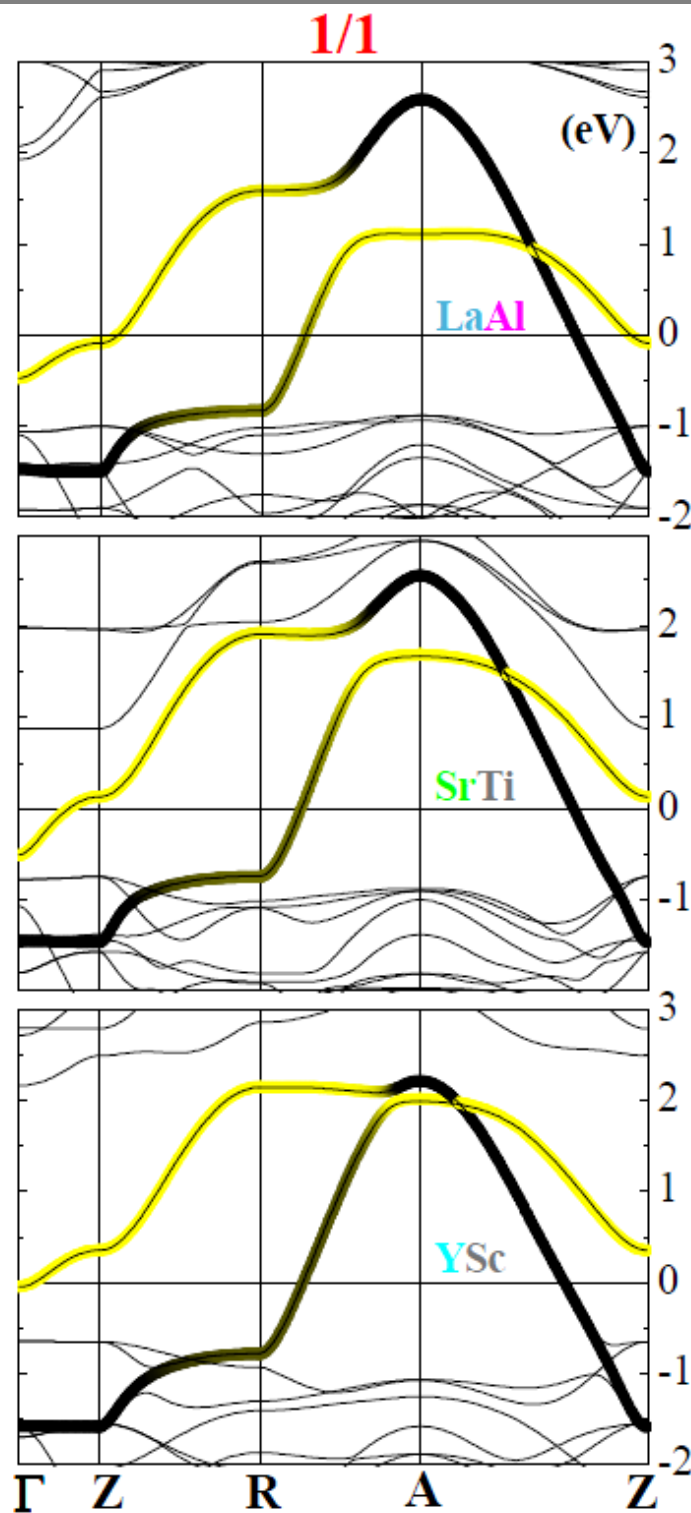
J.S. Zhou *et al.*, Phys. Rev. Lett. 95, 127204 (2005)

Chemical control by the A and B cations and the thickness of the insulating layer. This is also a tool for avoiding charge disproportionation.



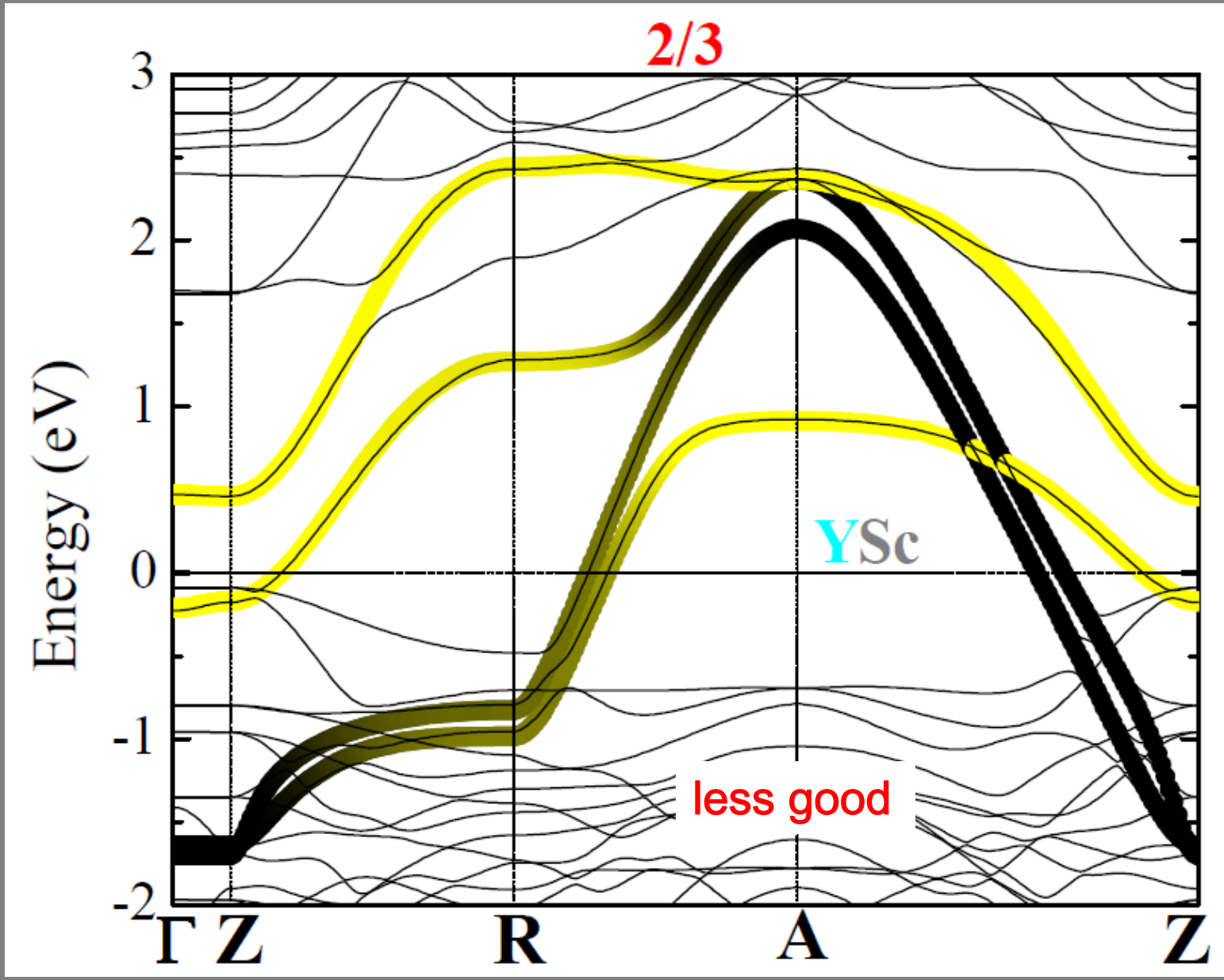


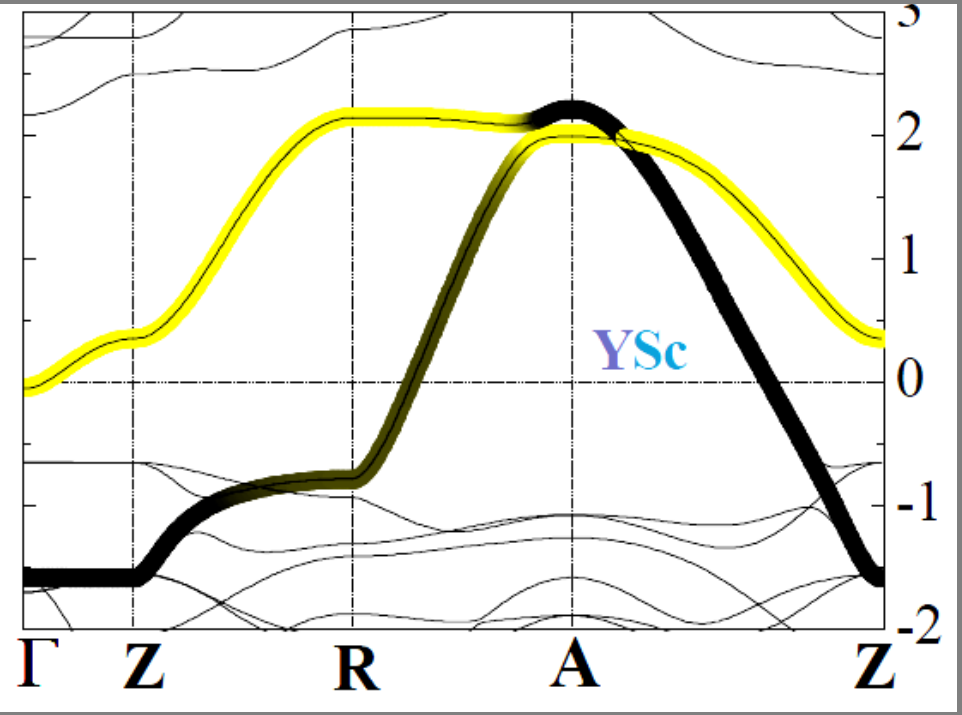
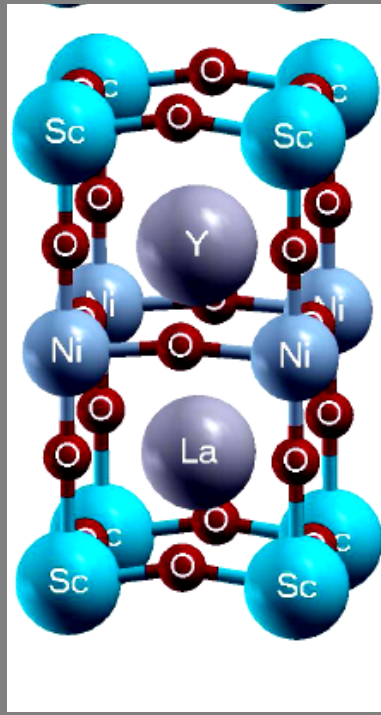
Adding insulating neighbor layers



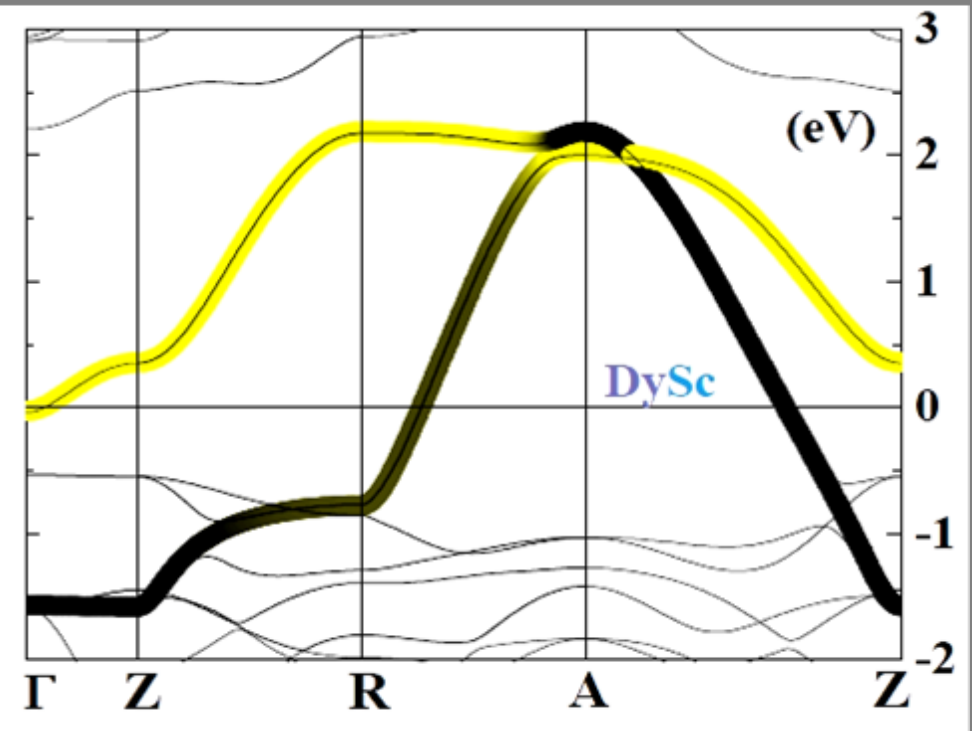
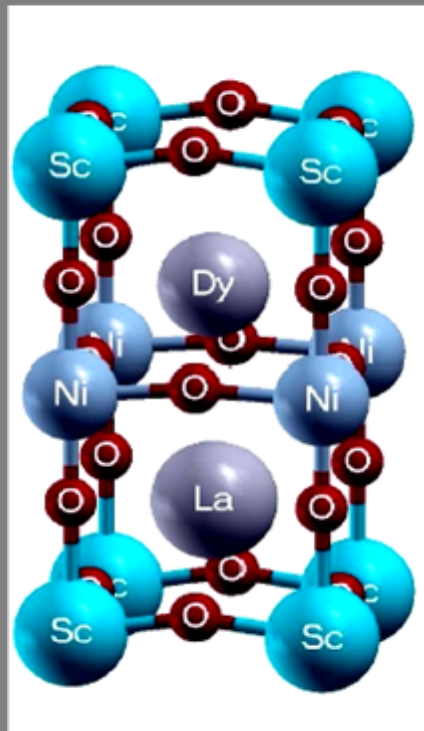


Adding a NiO_2 nearest-neighbor layer (bilayer)





On stock:
(H-U Habermeier)



Thank you for listening

and

**thank you to Nicola,
Claudia and Mac for
organizing this exciting
summer school**